8-9-2014

An Investigation of Mitochondrial Bioenergetics and the Turnover of Succinated Proteins in the Adipocyte during Diabetes

Ross Tanis
University of South Carolina - Columbia

An Investigation of Mitochondrial Bioenergetics and the Turnover of Succinated Proteins in the Adipocyte during Diabetes

By

Ross Tanis

Bachelor of Science
Michigan State University 2009

Submitted in Partial Fulfillment of the Requirements

For the Degree of Master of Science in

Biomedical Sciences

School of Medicine

University of South Carolina

2014

Accepted by:

Norma Frizzell, Director of Thesis

Edie Goldsmith, Reader

L. Britt Wilson, Reader

Lacy Ford, Vice Provost and Dean of Graduate Studies

Dedication

I would like to dedicate this thesis to my parent's Robert and Marie Tanis as well as my brother James Tanis. With their support I have always been given the opportunity to pursue my dreams and goals. My mentor Dr. Norma Frizzell has made all of this possible by allowing me the opportunity to pursue my Master's Degree in her laboratory, for which I will always be grateful.

Acknowledgements

I would like to thank my mentor, Dr. Norma Frizzell, first and foremost for making this opportunity possible and allowing me to pursue my Master's Degree in her laboratory. I would like to give a special thanks to Dr. Gerardo Piroli for his expertise and advice throughout my experience in this lab. I would also like to thank our current PhD student Allison Manuel and our former student Stani Day for teaching me new skills and assisting me throughout the course of my work. Also, I would like to thank Hannah Faile, our undergraduate student who I had a chance to mentor this past semester, for her dedication and assistance.

Abstract

We previously identified the chemical modification *S*-(2-succino)cysteine (2SC), which is formed when the Krebs cycle metabolite fumarate reacts with protein cysteine residues, also termed protein *succination*. Protein succination is increased in the adipose tissue of *ob/ob* and *db/db* mice *in vivo* and in 3T3-L1 adipocytes grown in high glucose *in vitro*. The increase in 2SC in the 3T3-L1 adipocyte occurs as a direct result of glucotoxicity and increased mitochondrial stress. We have shown that uncoupling agents, which lower mitochondrial stress, prevent the increase in succinated proteins.

In this study we examined the relationship between increased succination and mitochondrial bioenergetics in adipocytes matured in 30 mM (high) vs. 5 mM (normal) glucose. In addition we examined if sodium phenylbutyrate (PBA), which lowers protein succination, might be acting as an uncoupling agent in adipocytes cultured in high glucose. We observed that adipocytes matured in high glucose had a decreased spare respiratory capacity, increased proton leak across the inner membrane and increased non-mitochondrial respiration, consistent with increased mitochondrial stress. We also determined that PBA was not acting as an uncoupling agent but instead appeared to lower the mitochondrial respiratory protein content, thereby reducing respiration and protein succination.

The unfolded protein response (UPR) and endoplasmic reticulum (ER) stress have

previously been documented in the adipose tissue during diabetes and during adipocyte maturation in high glucose. We assessed the development of ER stress in adipocytes matured in 5 mM vs. 30 mM glucose and observed that although most ER stress markers were unchanged with glucose concentration, the terminal ER stress marker CHOP was consistently elevated in high glucose and this occurred in parallel with increased 2SC.

The use of PBA as a therapeutic agent for the treatment of T2DM is currently being investigated in human subjects as it has been shown to reduce ER stress in the adipose tissue of animal models of T2DM. We examined the effects of PBA administration for 8 weeks in *db/db* mice. We observed reduced serum glucose and reduced triglyceride (TG) levels after PBA treatment; however, there was no effect of PBA on 2SC or ER stress markers in the adipose tissue of *db/db* mice. Unexpectedly, PBA treatment increased ER stress and TG deposition in the liver of *db/db* mice.

Considering that 2SC is an irreversible and stable protein modification we wanted to determine if succinated proteins could be degraded intracellularly. We demonstrated that succinated proteins are degraded by the lysosome and are released from the cell as a free amino acid (2SC) and bound in a peptide.

Overall, these studies have further extended our knowledge of the relationship between mitochondrial stress, protein succination and ER stress. In addition, we have determined the mechanism of turnover of succinated proteins in the adipocyte *in vitro*.

Table of Contents

List of Figures

List of Abbreviations

ATF .....Activating Transcription Factor

Atg .....Autophagy-Related Proteins

BAT .....Brown Adipose Tissue

BW .....Body Weight

CCCP ..... Carbonyl Cyanide 3-Chlorophenylhydrazone

CHOP ..... CCAAT/Enhancer Binding Protein (C/EBP) Homologous Protein

D .....Differentiation

DEXA..... Dual X-Ray Absorptiometry

DMEM .....Dulbecco's Modified Eagles medium

DNP 2,4-Dinitrophenol

eIF2a..... Eukaryotic Initiation Factor Alpha

ER .....Endoplasmic Reticulum

Ero1-Lα.....Endoplasmic Reticulum Oxidoreductin-1-Like Protein

FBG .....Fasting Blood Glucose

FCCP ..... Carbonyl Cyanide 4-(Trifluoromethoxy) Phenylhydrazone

FFA..... Free Fatty Acid

GADD34.....Growth Arrest and DNA Damage-Inducible Protein

GC/MS .....Gas Chromatography/Mass Spectrometry

GRP78/BiP .....Glucose-Related Protein/Immunoglobulin Binding Protein

IRE1 ..... Inositol-Requiring Enzyme 1

IRS.....Insulin Receptor Substrate

JNK..... c-Jun Terminal-Kinase

kDa .....Kilo Dalton

M ..... Maturation

MCP1 ..... Monocyte Chemoattractant Protein-1

MEF ..... Mouse Embryonic Fibroblasts

mTORC2 .....Mammalian Target of Rapamycin Complex 2

NMR ..... Non-Mitochindrial Respiration

OCR..... Oxygen Consumption Rate

PBA ..... Sodium Phenylbutyrate

PDI .....Protein Disulfide Isomerase

PDK1 ..... Phosphoinositide-Dependent Kinase-1

PERK ..... RNA-dependent protein kinase-like ER kinase

PKB ..... Protein Kinase B

PPAR .....Peroxisome Proliferator-Activated Receptors

RIPA .....Radio Immunoprecipitation Assay Buffer

ROS .....Reactive Oxygen Species

SA .....Salicylic Acid

SRC .....Spare Respiratory Capacity

T2DM..... Type 2 Diabetes Mellitus

TG .....Triglyceride

TNFα.....Tumor Necrosis Factor Alpha

UPR..... Unfolded Protein Response

VEGF..... Vascular endothelial growth factor

WAT.....White Adipose Tissue

XBP-1 .....X-Box Binding Protein-1

XF.....Extracellular Flux

Chapter I

General Introduction

1.1. Epidemiology of Type 2 Diabetes Mellitus

Diabetes affects 25.8 million people, or 8.3% of the population, and is the seventh leading cause of death in the United States. There are 18.8 million diagnosed and 7.0 million undiagnosed people with diabetes. From 2005-2008, it was estimated that 79 million Americans had prediabetes, based on fasting blood glucose (FBG) and hemoglobin A1c levels. Diabetes predominantly affects those aged 20 to 65 and older but had an incidence rate of 0.26%, equivalent to 215,000 people, in 2010 for those under age 20. The estimated cost in 2012 of treating diagnosed cases of diabetes was $245 billion, with direct medical costs accounting for $176 billion. Further complications of the disease such as heart disease, kidney failure, stroke and amputations continue to exacerbate medial costs, accounting for approximately 10% of the costs associated with treating diabetes (1).

Obesity is frequently associated with the disease and 85.2% patients diagnosed with type 2 diabetes mellitus (T2DM) are either overweight or obese. From 2009-2010, it was reported that 69.2% of the population was overweight or obese and a striking 35.9% classified as obese (1). With over one third of the U.S. population suffering from obesity, it is paramount to address the economic, environmental and biological factors that contribute to T2DM. Although many risk factors have been attributed to T2DM

these vary widely among populations; with African Americans, Alaska Natives, American Indians, Hispanics/Latinos, Native Hawaiians, and Pacific Islander Americans being more susceptible than non-Hispanic whites (1). Despite evidence of some ethnic and genetic susceptibility, the evidence suggests physical inactivity and increased caloric intake are the greatest risk factors for developing T2DM (2).

1.2. Obesity, Hyperinsulinemia and Insulin Resistance

T2DM is the most prevalent form of diabetes, representing 90-95% of all adult cases of diabetes, and is a result of the body's insensitivity to insulin concomitant with hyperinsulinemia, hyperglycemia, and dyslipidemia (3). T2DM is commonly preceded by prediabetes, which is characterized by elevated FBG levels ranging between 100-125 mg/dL (5.6-6.9 mM). T2DM is characterized by fasting blood glucose levels above 126 mg/dL (7 mM) and hemoglobin A1c levels above 6.5% on two separate tests (4).

Insulin is produced by the pancreatic beta cells and is released in response to ingestion of a meal to facilitate the uptake of glucose into the peripheral tissues (5). In T2DM, there is a loss of insulin sensitivity in the peripheral tissues, despite hyperinsulinemia, resulting in sustained hyperglycemia (6). The insulin receptor and its signal transduction pathway have been extensively studied providing detailed insight into the intracellular mechanism of insulin signaling. Insulin binds to the insulin receptor, a tyrosine kinase receptor comprised of a dimer of αβ subunits. The alpha subunits reside on the outer leaflet of the lipid bilayer and contain the binding sites for insulin. The beta subunits are transmembrane helices with the carboxy termini residing in the cytosol (5). The alpha subunits inhibit the autophosphorylation of the beta

subunits in the absence of insulin. Upon binding of insulin, the inhibition is relieved and autophosphorylation activity of the beta subunits permits specific tyrosine residues to become phosphorylated. Insulin receptor substrate (IRS) proteins 1 and 2 have 20 potential phosphorylation sites that can be regulated and serve to propagate the cascade of events induced by insulin and other growth factors. Insulin signaling appears to be primarily mediated through IRS, which generates the second messenger phosphatidylinositol (3,4,5)-triphosphate by activating phosphoinositide 3-kinase leading to phosphoinositide-dependent kinase-1 (PDK1) and phosphoinositide-dependent kinase-2 /mammalian target of rapamycin complex 2 (mTORC2) activation. PDK1 and mTORC2 can phosphorylate Akt/protein kinase B (PKB) to promote cell growth and survival (7). Akt can also promote enhanced glucose uptake and storage and inhibit gluconeogenesis through suppression of forkhead transcription factor O1, or Foxo1. Alternatively, the activation of mammalian target of rapamycin complex 1 mTORC1 via Akt is responsive to amino acids and promotes protein synthesis, lipogenesis and inhibition of autophagy. Defects in the insulin signaling pathway can result from mutations, loss of function or over/under phosphorylation giving rise to insulin resistance (7).

As the body becomes less sensitive to insulin the pancreas continue to produce more insulin in an attempt to compensate for the reduction in glucose uptake. However, it has been shown that hyperinsulinemia can prevent glucose transporter type 4 (Glut4) trafficking to the membrane, further impairing glucose uptake (7). Additionally, the levels of IRS have been shown to be reduced, as activation of mTORC1 promotes their

ubiquitination and degradation. Activation of c-Jun N-Terminal kinase (JNK), a mitogen-activated protein kinase (MAPK) primarily activated by cytokines, can lead to p-IRS1 Ser^{307}, impairing insulin sensitivity and this can be mediated by both tumor necrosis factor alpha (TNFα) and hyperlipidemia (7, 8, 9, 10). Therefore the combined effects of dysregulated glucose metabolism, dyslipidemia and inflammation, in addition to individual risk, are key factors in determining the progression of the disease (11).

1.3. Symptoms and Treatment of Type 2 Diabetes Mellitus

A newly diagnosed T2DM patient will have a range of symptoms including frequent urination, increased thirst and fatigue; which can be attributed to the elevated FBG from impaired tissue glucose uptake. In these individuals, the initial treatment consists of monitoring blood glucose levels in response to a pharmacological agent, coupled with diet and exercise. Metformin is the pharmacological agent of choice that primarily controls blood glucose levels through regulation of hepatic gluconeogenesis (12). Thiazolidinediones and sulfonylureas are additionally used when metformin alone does not have the efficacy to reduce blood glucose levels. Thiazolidinediones act as peroxisome proliferator-activated receptors (PPAR) agonists, altering the expression of genes involved in glucose and lipid metabolism (13) while sulfonylureas stimulate the pancreas to release insulin (14). Although these drugs can help reduce hyperglycemia there is currently no cure for T2DM. The patient's quality of life with the disease depends on how well they manage their blood glucose levels, which can be enhanced through a healthy diet and regular physical activity. As the disease progresses complications in other organs such as the eyes, kidneys and nerves can arise (15). Many

of these tissues have non-insulin dependent glucose uptake and therefore their exposure to chronic hyperglycemia has been proposed to exacerbate cellular mitochondrial dysfunction. This results in increased superoxide production (oxidative stress) and intracellular damage in these tissues (16).

1.4 Adipocyte Metabolism in Type 2 Diabetes Mellitus

In healthy individuals the body responds to the ingestion of a meal by secreting insulin to facilitate glucose uptake into insulin sensitive tissues. In response to nutrient excess the adipose tissue can expand and store the surplus calories in the form of triglycerides (TGs). The storage capacity of the adipose tissue does not exceed its limit in healthy individuals and it contains a pool of preadipocytes that differentiate into adipocytes in response to nutrient excess. In the obese/diabetic individual, the hypertrophied adipocytes have lost their capacity to store excess fuel, resulting in the storage of fat in peripheral tissues such as liver and muscle (17).

Adipose tissue is considered an endocrine organ as it secretes a range of hormones known as adipokines. Increased or decreased production of several of these hormones is correlated with obesity and/or T2DM. Leptin was one of the first adipokines shown to be involved in nutrient regulation, functioning to decrease food intake and increase energy expenditure via the central nervous system (CNS) (17). However, despite the hyperleptinemina in obese subjects, the hormonal response in the CNS is reduced due to leptin resistance (8). Adiponectin is also secreted from the adipocyte and is known to act in an insulin sensitizing manner, increasing fatty acid oxidation in the muscle and suppressing gluconeogenesis in the liver. Increased plasma

levels of adiponectin are associated with a decreased risk for T2DM, while decreased levels are observed in patients with T2DM (8).

The energy stored in the form of adipocyte TGs are released as free fatty acids (FFAs) when required as fuel for peripheral tissues. Obesity occurs due to an imbalance in energy expenditure versus energy intake. In the obese state the white adipose tissue (WAT) takes on a markedly different phenotype. Adipose tissue is composed of a network of cells containing adipocytes and the stromal vascular fraction; comprised of macrophages, neutrophils, eosinophils, and endothelial cells (17). In the subcutaneous adipose tissue of humans with T2DM and the visceral adipose tissue of *ob/ob* and *db/db* mice, there is increased infiltration and proliferation of macrophages (18, 19). However, the immune response appears to be secondary to adipocyte dysfunction as hypertrophied adipocytes release more FFAs, which in turn leads to the recruitment of the immune cells (20). Increased circulating FFAs can also lead to deposition of FFAs in other organs such as the liver resulting in non-alcoholic fatty liver disease (21).

As the adipose tissue expands, angiogenesis does not keep pace with growth resulting in a hypoxic state that can lead to the induction of vascular endothelial growth factor (VEGF) and plasminogen activator inhibitor-1 (20). Both of these cytokines can modulate adiponectin gene expression, thereby compromising adiponectin mediated regulation of hepatic gluconeogenesis and fatty acid oxidation by the muscle (20). Further, in hypertrophied adipocytes, there is an increased secretion of the monocyte chemoattractant protein-1 (MCP- 1) that attracts immune cells and inflammatory cytokines, e.g. interleukin-6 (IL-6) and TNFα, which have been attributed to systemic

insulin resistance (8, 9, 20). Although adipose tissue is comprised of cell types including adipocytes and macrophages, recent evidence suggests that adipocyte dysfunction is an early player in the cascade of events that contributes to the development of T2DM (17).

1.5 Adipocyte Stress

Considering the burden of adipose tissue mass and the role of the adipocyte in energy metabolism, it is critical that we understand the mechanism of adipocyte dysfunction during the progression of diabetes. Increased metabolic flux in the adipocyte increases cellular oxygen consumption leading to increased production of reactive oxygen species (ROS) in T2DM (22). The production of ROS can lead to peroxidation of lipids forming the α,β-unsaturated aldehydes 4-hydroxy and 4-oxo *trans*-2,3 nonenal (23). These can react with cysteine, histidine and lysine residues to irreversibly modify proteins by carbonylation (23). In addition to mitochondrial derived oxidative stress, there is increased evidence of endoplasmic reticulum (ER) stress (ER stress) in the adipocyte in diabetes (24).

It has previously been shown that the differentiation of 3T3-L1 fibroblasts (an established cell culture model for the study of adipogenesis) into 3T3-L1 adipocytes occurs through the induction of the unfolded protein response (UPR) and ER stress (25, 26). During adipogenesis this response assists the differentiating endocrine cell through the up-regulation of chaperone proteins to help fold the newly synthesized proteins (25, 26). The UPR is a normal homeostatic response to the accumulation of misfolded proteins in the ER. Upon induction of the UPR, glucose-regulated protein 78/immunoglobulin-binding protein (Grp78/BiP) dissociates from the ER membrane to

help chaperone misfolded proteins. Oxidoreductase proteins such as protein disulfide isomerase (PDI) can then interact with the misfolded proteins in order to catalyze disulfide bond formation and correct folding, thereby relieving the pressure on the ER. When there is an accumulation of newly synthesized or misfolded proteins in the ER and chaperone mediated folding cannot keep pace and ER stress develops (25, 26).

There are three established pathways in the ER stress response (see Chapter 2, *Introduction* for more details). Briefly, in the absence of ER stress, Grp78/BiP is associated with 3 ER membrane spanning proteins: Inositol-requiring enzyme 1 (IRE1), which splices X-box binding protein 1 (XBP-1), activating transcription factor 6 (ATF6), and the RNA-dependent protein kinase-like ER kinase (PERK). However, during ER stress Grp78/BiP dissociates from these 3 membrane proteins and each of them initiates signal transduction pathways as part of the UPR. The net effect of this signaling is to cause up-regulation of chaperone proteins and transient attenuation of protein translation (Figure 1.1) (26, 27, 28).

1.6 Adipocyte Mitochondrial Stress

In parallel with oxidative and ER stress, mitochondrial stress has been documented in adipocytes matured in high glucose and in the adipose tissue of diabetic mice (29, 30, 31, 32). The reaction of fumarate, a Krebs cycle metabolite, with the thiol group on protein cysteine residues forms the chemical modification *S*-(2-succino)cysteine (2SC), also termed protein *succination* (Figure 1.2) (33). The levels of succinated proteins are increased in adipocytes matured in 30 mM glucose vs. 5 mM glucose and in the adipose tissue of diabetic mice (31, 32). Protein succination increases

due to mitochondrial stress in adipocytes matured in high glucose as a result of an increase in the ATP/ADP ratio. As a result of respiratory control, the electron transport chain is inhibited, which concomitantly increases the mitochondrial membrane potential ($\Delta\Psi_m$) and the NADH/NAD^+ ratio. Consequently the NAD^+ dependent enzymes of the Krebs cycle are inhibited resulting in increased fumarate and protein succination (30). The identity of ~40 succinated proteins in adipocytes has been confirmed (34) and further analysis of several of these has demonstrated that succination is associated with impaired structure or function (29, 35). For example, succination of adiponectin on cysteine 39 inhibits its polymerization into the biologically active high molecular weight form and thus it is not secreted but retained in the adipocyte. This provides a unique explanation for the impaired secretion and reduced circulating levels of this hormone in diabetes (29). Additionally we have shown that PDI, an ER chaperone protein, is succinated on an active site cysteine, thereby reducing its activity and potentially exacerbating ER stress in diabetes (unpublished results).

In this thesis I propose that protein succination, as a direct result of mitochondrial stress, is a unique contributor to ER stress by causing misfolded proteins to accumulate in the ER. I expect to observe increased ER stress in adipocytes matured in 30 mM glucose (high) vs. 5 mM (normal) glucose and I propose that chemical agents that reduce protein succination will lead to a decrease in ER stress. By demonstrating that reducing protein succination relieves ER stress, I hope to identify a new mechanism by which glucotoxicity contributes to adipocyte dysfunction.

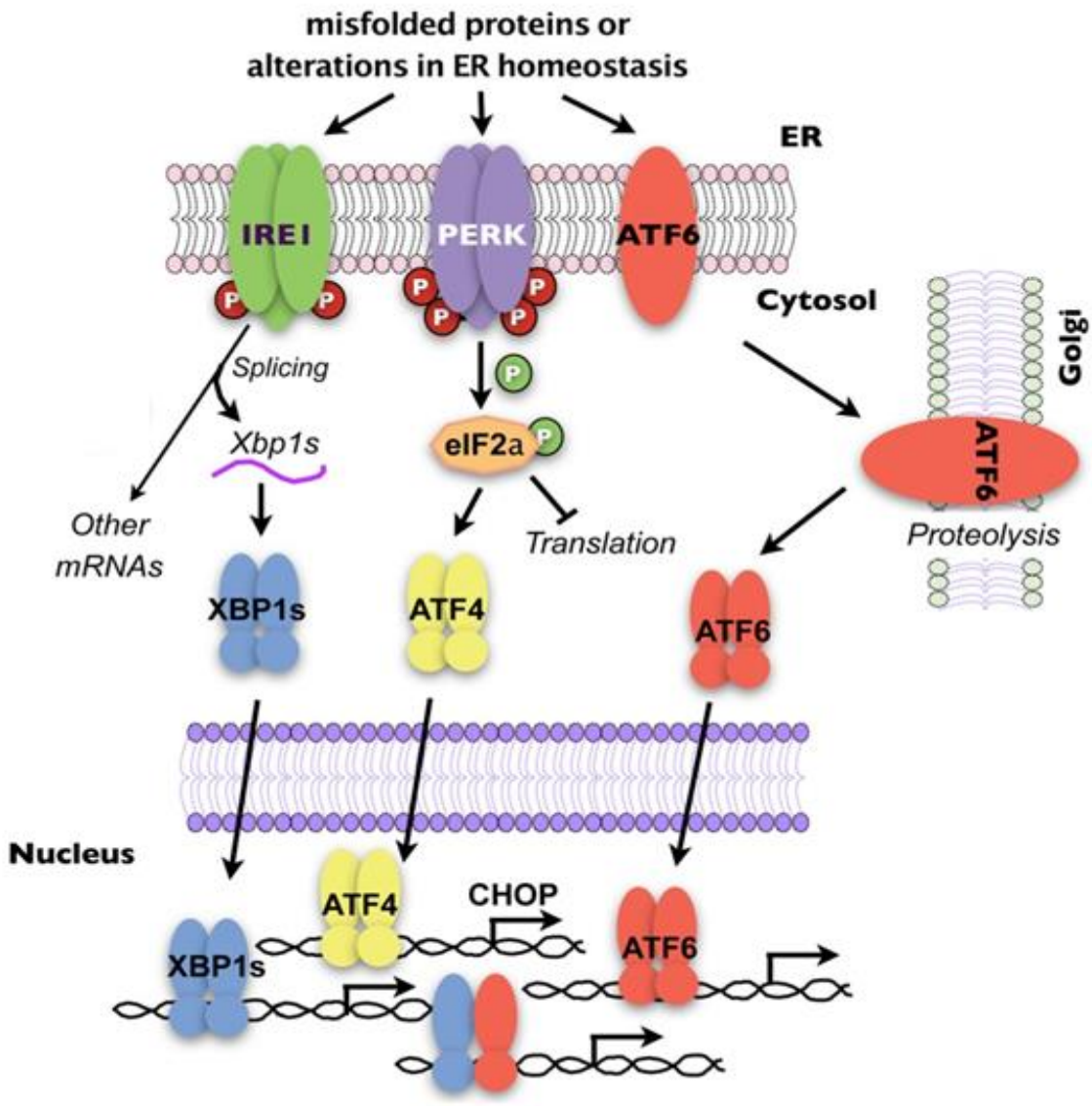

Figure 1.1: ER stress pathway. Protein misfolding in the ER induces the UPR. There are 3 signaling arms of the UPR that are activated upon increased protein misfolding: activation of (1) IRE1 leads to spliced (s) (XBP-1) and (2) ATF6 which leads to transcriptional up-regulation of chaperone proteins. The third arm involves PERK, which oversees the attenuation of nascent protein translation via phosphorylation of eukaryotic initiation factor 2 alpha (eIF2α). Further, activation of ATF4 leads to transcriptional up-regulation of CCAAT/enhancer binding protein (C/EBP) homologous protein (CHOP) (27), a terminal response to ER stress (28).

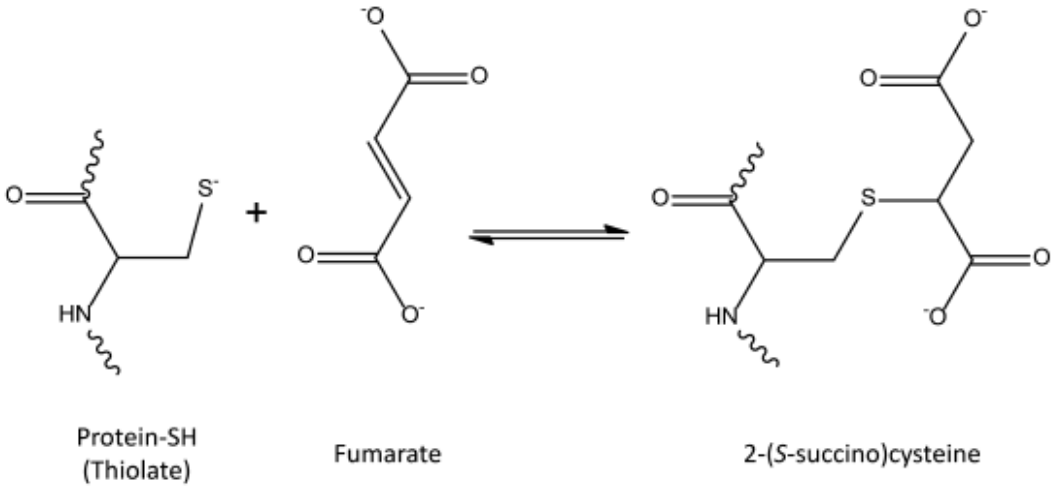

Figure 1.2: Formation of 2-(*S*-succino)cysteine (2SC). The reaction of fumarate with cysteine residues on proteins to form 2SC (33).

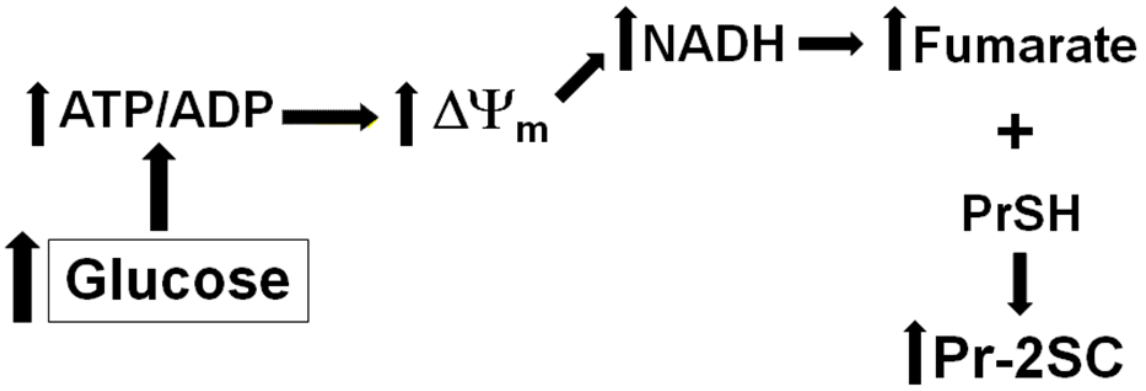

Figure 1.3: Glucotoxicity Driven Mitochondrial Stress increases Protein Succination.
Increased extracellular glucose concentrations contribute to mitochondrial stress as increased metabolism increases the ATP/ADP ratio. Accumulation of ATP inhibits the electron transport chain, increasing the mitochondrial membrane potential ($\Delta\Psi_m$) and the NADH/NAD^+ ratio, consequently inhibiting the NAD^+-dependent enzymes of the Krebs cycle. Inhibition of the Krebs cycle enzymes increases fumarate concentrations, allowing free protein thiol groups on cysteine residues (PrSH) to react with fumarate forming *succinated* proteins (Pr-2SC) (34).

Chapter II

Adipocyte Mitochondrial Metabolism and ER Stress

2.1. Introduction

The 3T3-L1 adipocyte model is a widely accepted model for the study of adipocyte function in obesity and diabetes (36). These studies are frequently conducted in the presence of high glucose concentrations (25-30 mM), as many cell lines are commonly maintained under these conditions. However, recent reports have documented that extracellular glucose concentrations have a significant impact on the measurement of mitochondrial bioenergetics (37), which is of importance for experimental conditions examining mitochondrial function in diabetes. While several studies have examined adipocytes cultured in both 5 mM (normal) and 25-30 mM (high) glucose (38, 39, 40) the majority of published studies appear to be conducted in high glucose medium. The Seahorse Extracellular Flux Analyzer (XF) 24 allows for the measurement of the oxygen consumption rate (OCR) in a respiring cell. In addition, the use of several chemical compounds that interfere with respiratory chain components allows assessment of several parameters of mitochondrial function. These include basal respiration, ATP synthesis coupled to oxygen consumption, proton leak (using oligomycin), spare respiratory capacity (SRC) (using an uncoupler e.g. carbonyl cyanide 4-(trifluoromethoxy) phenylhydrazone (FCCP)) and non-mitochondrial respiration (NMR)

(using rotenone/antimycin A) (Figure 2.1) (41). We hypothesized that adipocytes matured in 30 mM glucose versus 5 mM glucose would have an increased OCR and produce more ATP coupled to oxygen consumption. In addition, a recent report by Han *et al.* suggested that the majority of oxygen consumption in the cell was attributable to NMR (22). We wanted to investigate these claims as we have observed increased mitochondrial stress in the 3T3-L1 adipocyte (30, 31). Our overall aim was to compare the mitochondrial bioenergetic profile of adipocytes matured in 5 mM glucose (normal glucose) versus 30 mM glucose (high glucose).

The process of adipogenesis involves a change in phenotype from either a fibroblast (*in vitro*) or a preadipocyte (*in vivo*) into an adipocyte (17). When adipocytes are matured in high glucose, adipogenesis is accompanied by activation of the UPR as these cells change phenotype (25, 26). UPR driven increases in chaperone proteins can assist in the folding of newly synthesized proteins destined for secretion from the adipocyte. When the UPR is initiated, Grp78 dissociates from monomeric protein kinase RNA-like endoplasmic reticulum kinase (PERK), which is embedded in the ER membrane. This particular arm of the UPR has recently been confirmed as the most important signaling arm in adipocytes undergoing adipogenesis (25, 26). PERK then homodimerizes and is activated by autophosphorylation. Eukaryotic initiation factor α (eIF2α) is then phosphorylated by PERK at Ser-51 leading to an attenuation of protein translation. This response transiently relieves the cell from the burden of accumulating proteins (26). Downstream of p-eIF2α the activating transcription factor 4 (ATF4) translocates to the nucleus and up-regulates CCAAT/enhancer binding protein (C/EBP) homologous protein

(CHOP). The up-regulation of CHOP leads to the induction of growth arrest and DNA damage-inducible protein (GADD34), causing dephosphorylation eIF2α and restoration of cellular protein synthesis (Figure 1.1) (42). However, prolonged induction of CHOP is also associated with terminal ER stress and the induction of cellular apoptosis Figure 2.2) (27, 42-46).

Several studies have shown that the UPR and ER stress occur during adipogenesis in both high glucose (25 mM or 30 mM) and high insulin (25, 26). However, these conditions are not 'normal' and are instead comparable to diabetic conditions. Therefore, we hypothesized that activation of the UPR was only occurring as a result of the diabetic culture conditions and we predicted that cells matured in 5 mM (normal glucose) would not have an up-regulated UPR or ER stress response. To test the relationship between high glucose/insulin and UPR activation we compared adipocytes matured in 5 mM glucose/0.3 nM insulin (normal conditions) versus 30 mM glucose /3 nM insulin (diabetic conditions). We examined markers of adipocyte differentiation to ensure that the 3T3-L1 fibroblasts had undergone a phenotypic change into an adipocyte. We also assessed UPR/ER stress markers throughout the course of adipocyte maturation to compare the effects of the different glucose/insulin conditions.

2.2. **Results**

The respiratory profile of 3T3-L1 adipocytes matured in high glucose (30 mM) conditions has been described previously (23), however these conditions correspond to what could be considered a hyperglycemic, hyperinsulinemic environment and are not appropriate 'control' conditions for the study of normal adipocyte respiration. The

Seahorse XF24 was used to contrast the OCR of adipocytes after 2 days maturation (M2) in either 5 mM or 30 mM glucose. The glucose/insulin concentrations used were 5 mM/0.3 nM and 30 mM/3 nM to reflect concentrations similar to normal post-prandial conditions and a hyperglycemic/hyperinsulinemic state, respectively. A representative trace is shown in Figure 2.3A, illustrating the basal bioenergetic profile of adipocytes followed by ATP synthase inhibition (oligomycin), membrane depolarization with FCCP and complex I/complex II inhibition (rotenone/antimycin A), as denoted by the arrows. There was ~1.7-fold increase in the basal respiration and ~1.8-fold increase in ATP synthesis coupled to oxygen consumption in adipocytes grown in high glucose (gray bars) vs. normal glucose (black bars) ($^{***}p<0.001$, Figure 2.3B). Proton leak and NMR were also significantly increased in high glucose ($^{**}p<0.01$, Figure 2.3B). However, the SRC, a measure of the cellular capacity to increase mitochondrial respiration under stress, was ~2.4-fold lower in high glucose vs. normal glucose ($^{***}p<0.001$, Figure 2.3B). Several studies have described ER stress as a requirement for 3T3-L1 fibroblasts to undergo differentiation into 3T3-L1 adipocytes using high glucose and high insulin conditions (25, 26). To determine if only high glucose could induce ER stress we conducted adipocyte maturation in normal or high glucose/insulin and assessed several markers of both adipogenic differentiation and the UPR/ER stress. The production of adiponectin and PPARγ confirmed that the 3T3-L1 fibroblasts (F) had differentiated and matured into adipocytes in both 5 mM and 30 mM glucose during the 11 day time course (3 days differentiation (D) in 30 mM glucose followed by 8 days in 5 mM/0.3 nM or 30 mM/3 nM glucose/insulin maturation medium (M1-M8), Figure 2.4A). Notably,

adipocytes matured in 30 mM glucose had decreased total adiponectin levels vs. those cultured in 5 mM glucose towards the end of maturation (M7 and M8) (Figure 2.4A&B, lanes 16-23). Markers of the UPR and ER stress were upregulated in adipocytes as they begin maturation in either normal or high glucose. Grp78 increased throughout maturation in normal and high glucose, with a peak level occurring in 5 mM glucose at M5 (Figure 2.3C). PDI, endoplasmic reticulum oxidoreductin-1-like protein (Ero1-Lα) and p-eIF2α were most pronounced during days M1-5 of maturation in both normal and high glucose and declined thereafter until day M8 (M1-M8, Figure 2.4A, Lanes 4-23). Concomitant with a decrease in p-eIF2α levels there was a pronounced increase in CHOP levels in adipocytes, but notably this was only in the cells matured in 30 mM glucose (Figure 2.4A&E). Consistent with previous results (29, 31), the post-translational modification 2SC increased in adipocytes matured in 30 mM glucose for up to 8 days (M2-M8, lanes 8-23), and interestingly appeared to increase in parallel with CHOP levels (Figure 2.4A). In addition to the observed decrease in adiponectin detected in Figure 2.4, the adipocytes matured in 30 mM glucose secreted increased levels of pro-inflammatory cytokines, including TNFα, VEGF and MCP-1 (Figure 2.5A-C) versus those matured in 5 mM glucose. Taken together, these results confirm that increased protein succination occurs in parallel with increased ER stress (CHOP), decreased adiponectin production and elevated pro-inflammatory cytokine production when adipocytes are matured in high glucose conditions.

Recent work has suggested that insulin alone is sufficient to increase ER stress in adipocytes and adipose tissue (47, 48). Considering that our 5 mM glucose adipocytes

are cultured in 0.3 nM insulin and our 30 mM glucose adipocytes are cultured in 3 nM insulin, we investigated if the combined increases in 2SC and CHOP that we observed were due to either the glucotoxicity or the high insulin concentration. To do this we examined ER stress and protein succination in the absence/presence of 10 nM insulin with both 5 mM and 30 mM glucose. As observed in Figure 2.6, the addition of insulin leads to increased protein succination in adipocytes matured in 30 mM glucose (lanes 7-12) and has no effect on the levels of protein succination in adipocytes matured in 5 mM glucose (lanes 1-6), therefore it appears that combined glucotoxicity and elevated insulin are required to observe this biomarker of mitochondrial stress. Grp78 levels were measured to assess UPR activation and suggested that insulin leads to the induction of the UPR (lanes 1-3 vs. 4-6 or lanes 7-9 vs. 10-12), independent of glucose concentration. We then measured CHOP levels, and observed a pronounced increase in CHOP in 30 mM glucose with an added response in the presence of insulin. However, CHOP was unchanged in 5 mM glucose with or without insulin (Figure 2.6), indicating that both high insulin and glucotoxicity are necessary for the maximal induction of CHOP.

2.3. Discussion

The differentiation of 3T3-L1 fibroblasts into adipocytes has been extensively studied (36), with adipocyte maturation commonly occurring in 25 mM (~450 mg/dL) glucose and insulin concentrations ranging from 10-1700 nM (23, 48), well beyond the physiological range. In this study, we compared adipocytes matured in 5 mM glucose/0.3 nM insulin or 30 mM glucose/3 nM insulin to better reflect normal and

diabetic conditions, respectively. We examined the respiratory profile of adipocytes that had matured in 5 mM or 30 mM glucose for 2 days and observed that the adipocytes matured in 30 mM glucose had a ~1.7-fold increase in the basal respiration rate (Figure 2.3A&B). In contrast, the spare respiratory capacity, a measure of mitochondrial capacity to increase the rate of oxygen consumption, was ~2.4-fold lower in high glucose versus normal glucose. This data indicates that adipocytes matured in high glucose conditions are already respiring close to their maximal capacity and are not optimal for use as 'healthy' controls for normal adipocyte function. Recent reports have suggested that 3T3-L1 adipocytes predominantly consume oxygen in non-mitochondrial pathways (22). However, our OCR measurements allowed us to assess both mitochondrial and non-mitochondrial oxygen consumption as they included a final rotenone/antimycin A inhibition of Complex I/III, effectively inhibiting mitochondrial respiration. Our data demonstrate that non-mitochondrial respiration accounts for ~22% of the OCR (Figure 2.3B, NMR). This indicates that while non-mitochondrial respiration is significant, it is not the major source of oxygen consumption in the 3T3-L1 adipocyte model. ATP production coupled to oxygen consumption was increased in high glucose (Figure 2.3B, ATP) confirming our previous observations of an increased ATP/ADP ratio in adipocytes cultured in 30 mM glucose (30).

Recently, Valsecchi *et al*. highlighted the importance of glucose concentration for the study of mitochondrial (dys)function. They noted that primary cultures in the presence of high glucose do not show differences in ROS measurements that are observed when the same cells are cultured in normal glucose. Moreover, immortalized

cell lines that are frequently used to study mitochondrial function in high glucose have high glycolytic activity, rather than a dependence on mitochondrial metabolism (37). Additionally, increased proton leak in adipocytes matured in 30 mM glucose suggests there may be inner mitochondrial membrane damage or electron slippage (49). We have demonstrated that there are significant differences in the mitochondrial respiratory profile of adipocytes matured in 5 mM and 30 mM glucose. Adipocytes matured in high glucose are consuming more oxygen and therefore produce more ATP and have increased NMR and proton leak. This suggests that adipocytes matured in 30 mM glucose are not healthy controls as it appears their mitochondria are working closer to their maximal capacity and may have impaired electron transport chain complexes or integrity (49).

We investigated if UPR/ER stress during adipogenesis (25, 26) was unique to cells cultured in high glucose or if the UPR and ER stress were still increased when cells were cultured in 5 mM (normal) glucose. As shown in Figure 2.4A, both adipocytes cultured in normal or high glucose proceed through differentiation (D) and maturation (M) normally as indicated by the significant increase in PPARγ and adiponectin. Several markers of the UPR including Grp78, PDI and p-eIF2α were increased, confirming that UPR activation is actually a normal component of 3T3-L1 adipogenesis (25, 26), not only in 30 mM glucose but also in 5 mM glucose. Although there were subtle changes in UPR markers between 5 mM and 30 mM glucose at various time points, these changes were not significant (Figure 2.4A-D), but CHOP, a downstream marker of ER stress, was significantly increased as maturation progressed, most notably in 30 mM glucose (Figure

2.4A&E, M2-M8). Interestingly, as CHOP levels increased in 30 mM glucose this was associated with an increase in protein succination, a biomarker of mitochondrial stress (Figure 2.4A, anti-2SC). The increase in CHOP and succinated proteins corresponded to a decrease in total adiponectin levels at days M7 – M8 in 30 mM vs. 5 mM glucose (Figure 2.4A) and was also associated with an increase in the release of the pro-inflammatory markers TNF-α, MCP-1 and VEGF into the medium (Figure 2.5A-C). Han *et al*. have also demonstrated that adipocytes matured in 25 mM glucose have increased adipocyte-derived factors such as serum amyloid A and hyaluronan that facilitate monocyte recruitment and adhesion (40). This evidence suggests that glucose has intrinsic effects on the adipocyte that lead to metabolic stress and cellular dysfunction. Taken together, this data confirms that UPR activation is a normal aspect of 3T3-L1 adipogenesis and activation; however the sustained increase in CHOP is associated with mitochondrial stress, protein succination, and adipocyte inflammation and is unique to high glucose culture conditions (glucotoxicity).

Increased CHOP levels have classically been associated with the induction of apoptosis during ER stress (42, 43, 44, 45), however, our data suggests that CHOP may be increased independent of an apoptotic response, as there was no increase in cleaved caspase-3 at this stage of maturation (data not shown). Many recent reports have described alternative functions of CHOP unrelated to apoptosis, e.g. Han *et al*. have demonstrated that CHOP induction can inhibit adipogenesis in 3T3-L1 fibroblasts and mouse embryonic fibroblasts (MEFs) (26). Han *et al*. have also identified CHOP transcription binding sites in genes involved in protein synthesis such as tRNAs and

initiation factors. Interestingly, no apoptotic genes were found to be directly associated with transcriptional activation by CHOP (27). In C57BL/6J mice, CHOP was shown to suppress transcription of metabolic genes in the liver during ER stress (50), providing further evidence that CHOP is more promiscuous than once thought and its role is not limited to apoptotic events. This suggests that CHOP signaling is dependent on the nature of the stress signal and that the presence of CHOP in the cell is not necessarily indicative of an apoptotic response.

To determine whether the glucose or the insulin was the inducer of ER stress, we matured adipocytes in 5 mM or 30 mM with and without 10 nM insulin. We observed that insulin induced the UPR in both 5 mM and 30 mM glucose by upregulating Grp78 protein levels, but only high glucose and high insulin combined led to ER stress and mitochondrial stress as observed by CHOP and succinated protein levels, respectively (Figure 2.6). This confirms our earlier result indicating that adipocytes matured in high glucose are not healthy controls and are already under a state of stress, highlighting the importance of both glucose and insulin conditions for the study of mitochondrial bioenergetics and ER stress in the context of diabetes research.

Overall, the direct correlation between succination and CHOP levels raises the interesting possibility that mitochondrial stress and 2SC may have a role in sustained CHOP signaling. Kelch-like ECH-associated protein 1 (Keap1) has recently been described as a negative regulator of CHOP in adipocytes (51) and we have shown that Keap1 cysteines are succinated in fumarate hydratase deficient fibroblasts (52). We hypothesize that increased succination of Keap1 may promote CHOP stability to allow

sustained CHOP signaling, independent of ER stress, and this is the subject of ongoing investigations in our laboratory.

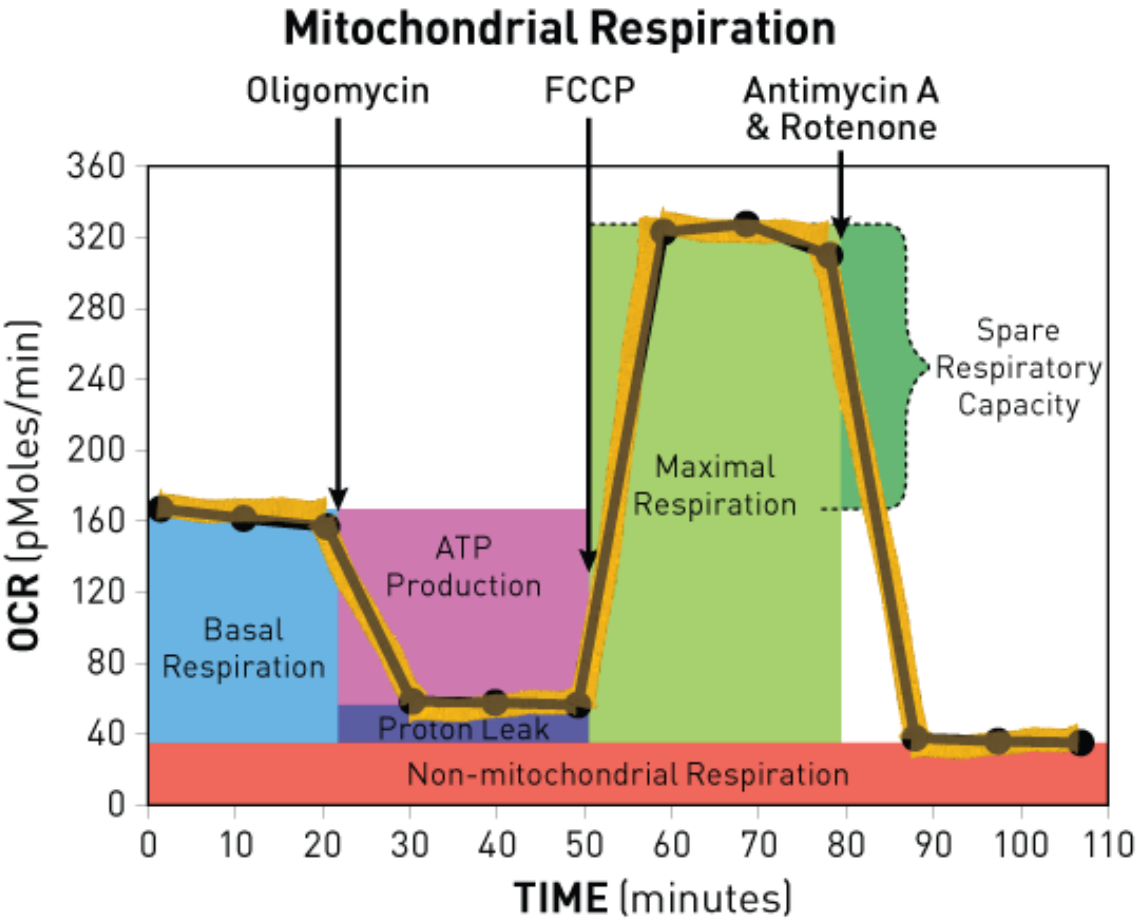

Figure 2.1. Schematic of bioenergetic profile generated from the Seahorse XF24. The bioenergetic profile of a respiring cell can be generated using the Seahrose XF24. The oxygen consumption rate (OCR) allows for the measurement of basal respiration, ATP production coupled to oxygen consumption, spare respiratory capacity (SRC), proton leak, and non-mitochondrial respiration (NMR) can be measured following the addition of specific chemical inhibitors as denoted by the arrows (41).

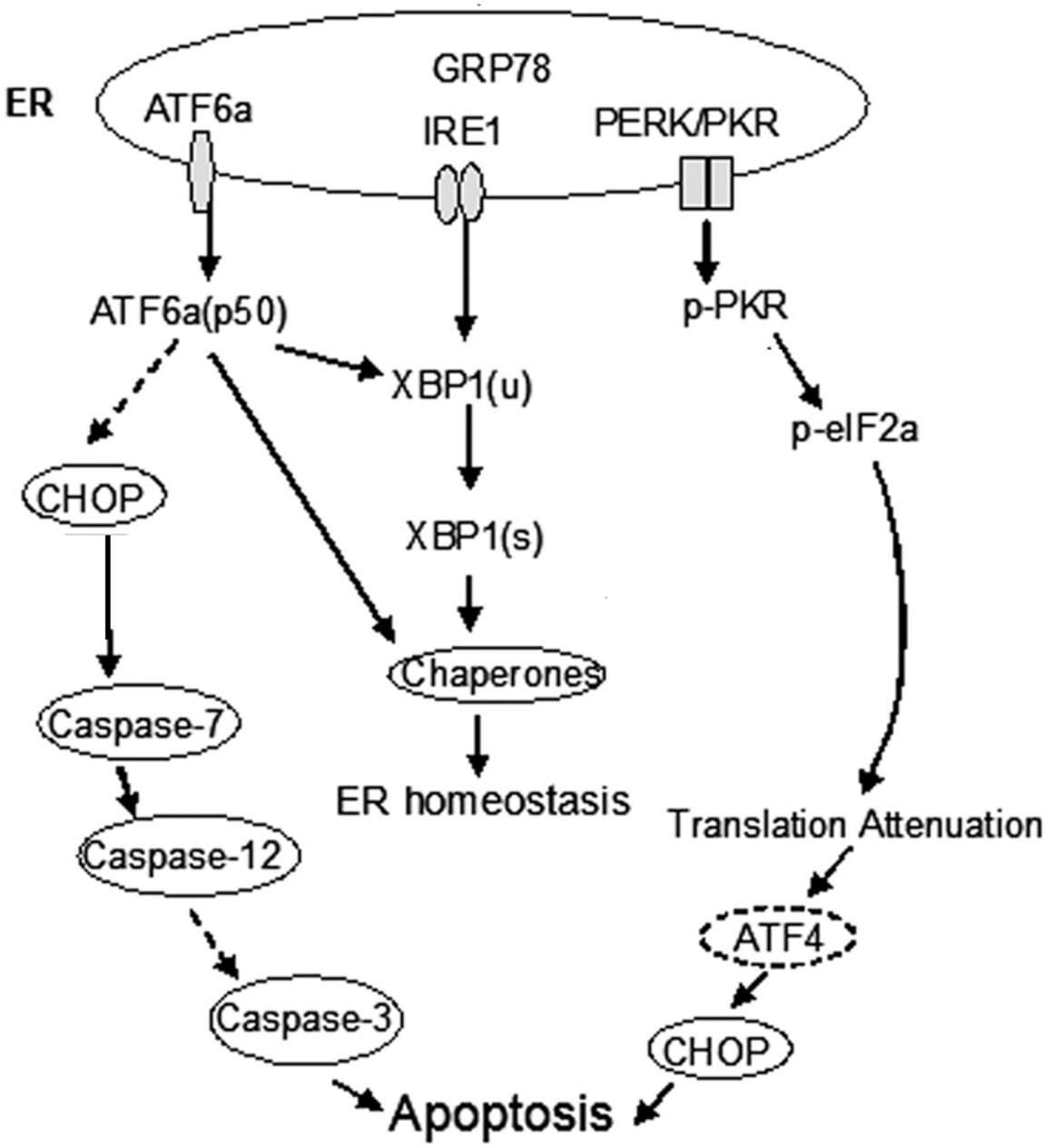

Figure 2.2 ER stress leads to apoptosis via upregulation of CHOP. ER stress leads to the induction of CHOP (See Figure 1.1 for more details) and cellular caspases ultimately leading to apoptosis (46).

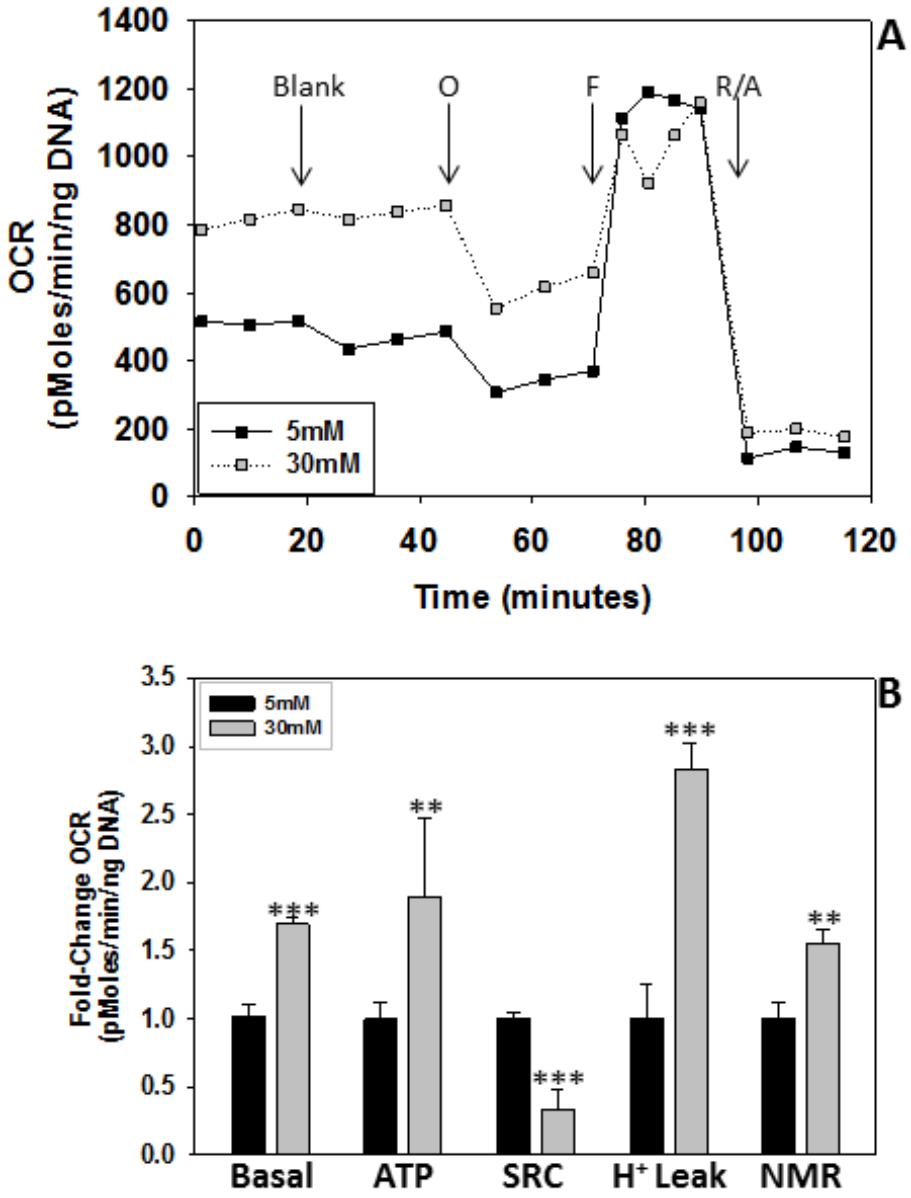

Figure 2.3 A & B: Bioenergetic profile of 3T3-L1 adipocytes in 5 mM and 30 mM glucose. (A) The respiratory profile of adipocytes cultured in 5 mM (black squares/black bars) or 30 mM glucose (gray squares/gray bars) was measured after 2 days maturation using the Seahorse XF24 Analyzer as described in the Materials and Methods. Drugs were added at the indicated arrows to assess mitochondrial function. (B) Basal, ATP production (ATP), spare respiratory capacity (SRC), proton leak (H^+ leak), and non-mitochondrial respiration (NMR) were measured following the addition of oligomycin (O), FCCP (F), and rotenone/antimycin A (R/A) respectively. Data are representative of n=4 measurements expressed as means ± S.D. Asterisks indicate statistical significance determined by an unpaired Student *t* test (**P<0.01 and ***P<0.001 for 30 mM glucose (gray bars) vs. 5 mM glucose (black bars). A Mann-Whitney Rank Sum Test was performed on data not normally distributed.

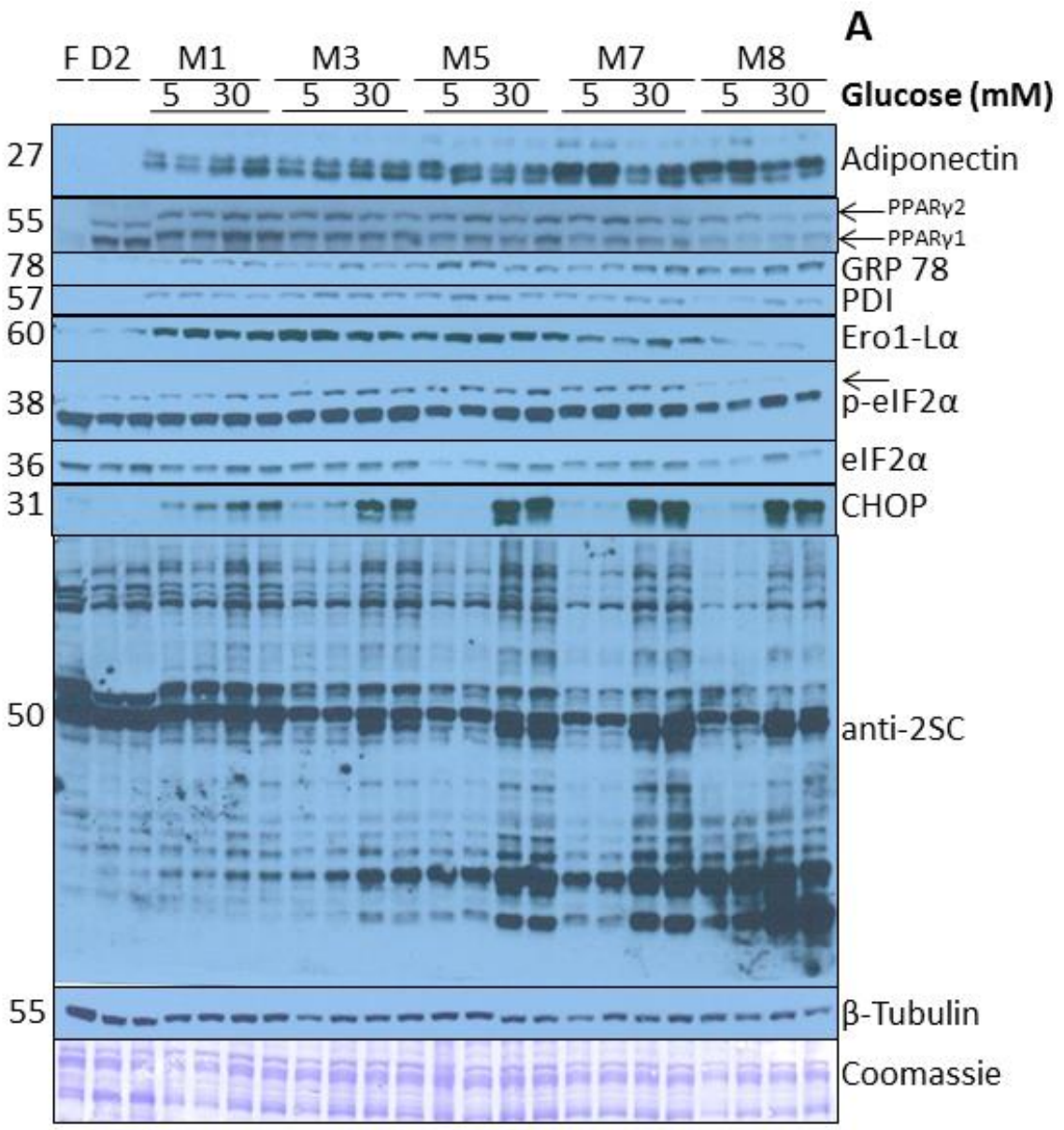

Figure 2.4 A: Adipogenesis proceeds via ER stress in normal or high glucose. (A) Time course detailing markers of adipogenic differentiation and UPR/ER stress in adipocytes cultured 5 mM (normal) or 30 mM (high) glucose. Total cell lysates (20 µg protein) from adipocytes harvested at the indicated time points were separated by 1-D PAGE. Adipogenic proteins and UPR/ER stress markers were detected as described in the Materials and Methods. **F** represents fibroblasts, **D** represent cells undergoing differentiation and **M** represents the maturation period in days in either 5 mM or 30 mM glucose. A representative Coomassie is shown as a loading control.

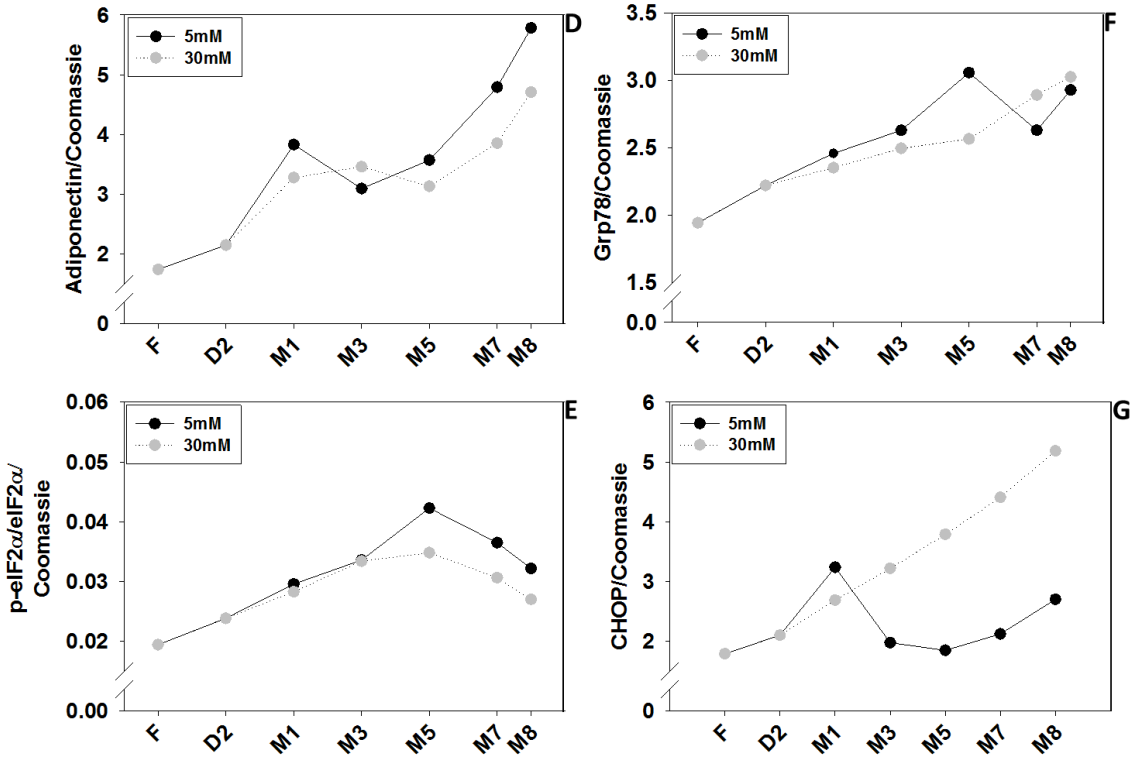

Figure 2.4 B-C: Adipogenesis proceeds via ER stress in normal or high glucose.
Quantification of band densitometry in Figure 2.3A for adipocytes matured in 5 mM (black circles) or 30 mM (gray circles) glucose. (B) Adiponectin. (C) p-eIF2α. (D) Grp78. (E) CHOP.

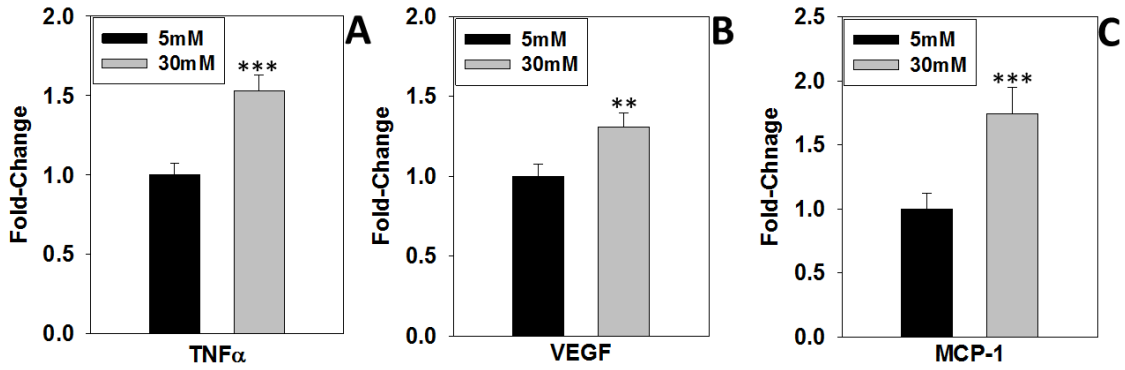

Figure 2.5: Increased secretion of inflammatory markers in high glucose. Secreted levels of pro-inflammatory cytokines as measure by mouse obesity ELISA as described in the Materials and Methods. (A) TNFα. (B) VEGF. (C) MCP-1. Data are representative of n=4 measurements expressed as means ± S.D. Asterisks indicate statistical significance determined by an unpaired Student *t* test (**P<0.01 and ***P<0.001 for 30 mM glucose (gray bars) vs. 5 mM glucose (black bars)).

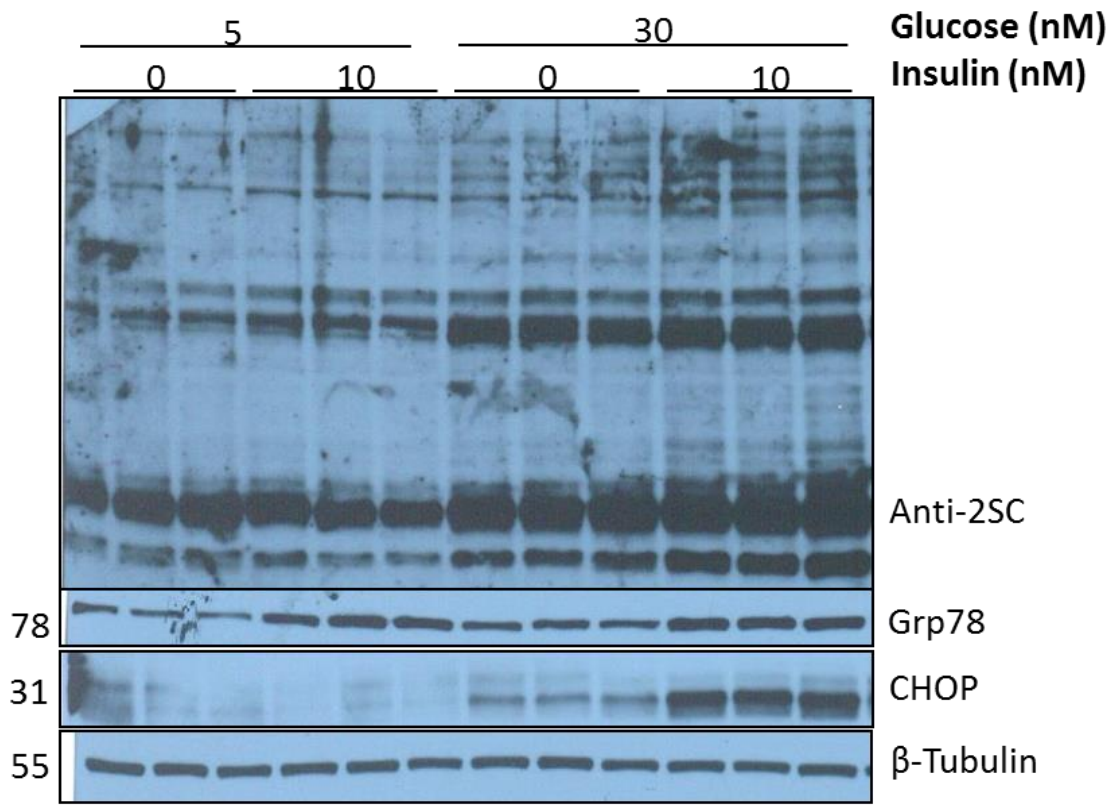

Figure 2.6: Insulin induces the UPR while added glucotoxicity activates the ER stress response. 3T3-L1 adipocytes were matured in either 5 mM or 30 mM glucose for 8 days in the absence/presence of 10 nM insulin. Protein, 20 µg, was separated by 1-D PAGE and 2SC, Grp78 (UPR) and CHOP (ER stress) were detected as described in Materials and Methods.

Chapter III

Is sodium phenylbutyrate a mitochondrial uncoupler?

3.1. Introduction

There are two types of adipose tissue found in mammals, white adipose tissue (WAT) and brown adipose tissue (BAT), both of which are responsive to insulin and can store TGs (53). WAT is the predominant form of AT in humans making up the bulk of fat, while BAT is a specialized tissue that plays a more prominent role in thermogenesis. BAT expresses uncoupling protein-1 (UCP-1) which is located in the mitochondria and can uncouple oxygen consumption from ATP synthesis, thereby dissipating the mitochondrial membrane potential and releasing energy in the form of heat (17). This effect of uncoupling AT has received attention as a possible therapeutic mechanism for weight loss, as it was first documented in the early 1900's that consumption of 2,4-dinitrophenol (DNP) led to weight loss. However, DNP is also known to be carcinogenic and is no longer clinically recommended for weight loss (54).

Using an *in vitro* model there are several chemicals that can be used as depolarization agents to study the effects of dissipating the $\Delta\Psi_m$. These include FCCP, carbonyl cyanide 3-chlorophenylhydrazone (CCCP) and DNP. These chemicals act as uncouplers by carrying a proton from the mitochondrial matrix across the inner membrane and consuming oxygen without producing ATP. Addition of an uncoupler to a

respiring cell will depolarize the $\Delta\Psi_m$, leading to an increase in the OCR as the protons are carried across the inner membrane without simultaneous production of ATP. We have previously shown that treatment of 3T3-L1 adipocytes with CCCP or salicylic acid (SA) (acting as a mild uncoupler) decreases the $\Delta\Psi_m$ (30). Therefore, we were interested in examining other agents that may also be acting as chemical uncouplers as we predicted that they would lead to a decrease in mitochondrial stress and consequently protein succination. We had observed that 3T3-L1 adipocytes treated with 1 mM sodium phenylbutyrate (PBA) for 8 days during maturation had reduced protein succination and a reduced $\Delta\Psi_m$. In other studies, PBA is currently being explored as a possible therapeutic agent for the treatment of ER stress in adipose tissue (55). However, considering that PBA and SA are similar in structure (Figure 3.1) and that SA has been shown to act as a mitochondrial uncoupler (56), we hypothesized that PBA may also be acting as a mitochondrial depolarization agent.

3.2. Results

PBA has been shown to lower ER stress in 3T3-L1 adipocytes matured in high glucose (25); therefore we examined the effect of PBA on mitochondrial stress and protein succination. As demonstrated in Figure 3.2A, adipocytes matured in high glucose have increased levels of 2SC compared to adipocytes matured in normal glucose for 8 days. When treated with 1 mM PBA for 8 days, the levels of 2SC in adipocytes matured in high glucose are significantly reduced and remain unchanged in normal glucose (Figure 3.2A). Next, we measured the $\Delta\Psi_m$ using a mitochondrial membrane permeable dye. CCCP was used as a positive control as this uncoupler has been shown to reduce

the levels of protein succination (30). In Figure 3.2B, CCCP reduced the $\Delta\Psi_m$ ($^{***}P<0.001$) as expected, however, PBA treatment also reduced $\Delta\Psi_m$ ~60% ($^{***}P<0.001$) compared to untreated 30 mM glucose adipocytes.

PBA has also been documented to inhibit adipogenesis *in vitro* (25). We also observed a significant reduction in PPARγ, the master regulator of adipogenesis, after treatment with 1 mM PBA (Figure 3.3A). Adipocyte triglyceride content was decreased in a dose dependent manner after 2 and 8 days of PBA treatment versus 30 mM glucose alone ($^{*}P<0.05$, Figure 3.3B&C). We next quantified the extracellular glucose concentrations in order to determine if PBA altered glucose uptake into the adipocyte. There was a significant amount of glucose remaining in the medium after 2 days of treatment with 1 mM PBA ($^{***}P<0.001$, Figure 3.3D) versus untreated cells.

Considering the reduction in $\Delta\Psi_m$ observed after PBA treatment (Figure 3.2A), we hypothesized that PBA may be acting as a mitochondrial depolarization agent. Using the Seahorse XF24, we compared the ability of PBA to decrease the $\Delta\Psi_m$ and subsequently increase the OCR versus FCCP or SA. FCCP uncoupled oxidative phosphorylation at previously titered micromolar concentrations, as demonstrated by the rapid increase in the OCR (Figure 3.4A, black/solid triangles, first arrow denotes addition of FCCP). We have previously shown that SA reduces both the $\Delta\Psi_m$ and the levels of 2SC-modified proteins in adipocytes matured in high glucose (30). Here, we confirmed that SA is acting as a mild uncoupler as increasing concentrations of SA depolarized the inner mitochondrial membrane leading to successive increases in the OCR (gray circles, Figure 3.4A, arrows denote addition of SA). In contrast, increasing

concentrations of 1 mM, 5 mM and 10 mM PBA (Figure 3.4A, black circles, arrows denote addition of PBA) did not appear to increase the OCR above the basal rate (Figure 3.4A), although the marginal increase was statistically significant with 10 mM PBA (***P<0.001, Figure 3.4B). As the affects after acute PBA treatment were minimal, we next examined the OCR after treatment with 1 mM or 5 mM PBA for 2 days. Interestingly, the basal OCR was significantly reduced in adipocytes matured in 30 mM glucose treated with 1 mM and 5 mM PBA (red circles vs. black triangles, red circles vs. green triangles Figure 3.4C, striped and checked bars vs. gray bars, basal respiration, ***P<0.001, Figure 3.4D). Other bioenergetic parameters such as oxygen-coupled ATP synthesis and NMR were significantly reduced with 5 mM PBA treatment compared to adipocytes matured in 30 mM glucose (*P<0.05, Figure 3.4D). Proton leak was significantly reduced with 1 mM and 5 mM PBA treatment compared to adipocytes matured in 30 mM glucose alone (***P<0.001, Figure 3.4D). Notably, 1 mM PBA preserved the ability of the adipocytes to respond to FCCP uncoupled respiration, whereas 5 mM PBA reduced the SRC (***P<0.001, Figure 3.4D). PBA treatment reduced both the adiponectin and the PPARγ content in the adipocytes, highlighting that PBA reduces markers of adipogenesis as early as 2 days (Figure 3.5A). As expected PBA treatment lowered the UPR as noted by reductions in calreticulin, PDI and p-eIF2α levels, particularly with 5 mM PBA. However, we observed that both CHOP cleaved caspase-3 levels were significantly increased in the presence of 5 mM PBA (Figure 3.5A), indicating that elevated PBA concentrations actually induce ER stress and lead to apoptosis. This was consistent with our observation that 5 mM PBA mildly reduced cell

viability (data not shown). Although PBA treatment did not reduce the mitochondrial DNA copy number (Figure 3.5B), there was a reduction in the protein levels of several mitochondrial proteins including succinate dehydrogenase (SDHA) and NADH dehydrogenase [ubiquinone] iron-sulfur protein 4 (NDUFS4, a component of mitochondrial complex I), versus the 30 mM glucose controls (Figure 3.5A), suggesting that PBA may selectively lower the levels of some mitochondrial proteins.

3.3. Discussion

Protein succination appears to be a biomarker of adipocyte dysfunction and increases as a consequence of mitochondrial stress. The increase in fumarate is associated with an increased ATP/ADP ratio, elevated $\Delta\Psi_m$ and increased NADH/NAD^+ (Figure 1.3) and this can be reduced after treatment with CCCP, a mitochondrial depolarization agent (30). To determine if mitochondrial stress and ER stress were linked, we treated adipocytes with 1 mM PBA and observed a significant reduction in succination and also the $\Delta\Psi_m$ (Figure 3.2A&B). We hypothesized that PBA may be acting as a depolarization agent, given that there was a reduction in the $\Delta\Psi_m$ upon treatment of adipocytes in 30 mM glucose with PBA (Figure 3.2B). Using the Seahorse XF 24 we added PBA to respiring adipocytes to determine if it had an acute effect on increasing the OCR. In contrast to known uncouplers such as FCCP and SA, we did not observe an appreciable increase in the OCR with 1 mM or 5 mM PBA (Figure 3.4A), confirming that PBA was not acting as an uncoupler at low doses. Although 10 mM PBA increased the basal OCR, it is not a tolerable dose as 5 mM PBA increased the levels of caspase-3 in adipocytes after 2 days treatment. Rather, when the adipocytes were treated with PBA

for 2 days we noted a decrease in the basal OCR and ATP production coupled to oxygen consumption (Figure 3.4C&D), which is consistent with the decrease in the $\Delta\Psi_m$. After further investigation we observed a reduction in the mitochondrial protein content, as noted by a decrease in SDHA and NDUFS4, but there was no change in the mitochondrial copy number (Figure 3.5A&B). Despite the reduction in the mitochondrial protein content with 1 mM PBA, the mitochondria still had the ability to increase the SRC when challenged with an uncoupler (Figure 3.4D, SRC). Additionally, basal respiration was decreased with 1 mM PBA treatment but ATP synthesis coupled to oxygen consumption remained unchanged, which may be attributed to decreased proton leak and enhanced membrane integrity (49). We also observed that PBA reduced glucose uptake by the adipocyte (Figure 3.3D), suggesting that the OCR may be reduced in part due to reduced metabolic flux (Figure 3.4D), providing further explanation for the decrease in mitochondrial protein content without a decrease in the SRC when 30 mM glucose is present. This is in contrast to *in vivo* studies using *ob/ob* mice where PBA was shown to reduce blood glucose levels after just 4 days of treatment, suggesting that it facilitates glucose uptake in an animal model of obesity (57). However, another report indicated that PBA had no effect on blood glucose in other models of diabetes such as the alloxan-induced diabetic mice or the Goto-Kakizaki rat (58). Therefore, it will be necessary to determine if PBA alters hyperglycemia in diabetic humans as cellular and animal models do not appear to show consistent effects.

PBA has been described as a chemical chaperone that can alleviate ER stress in the liver of *ob/ob* mice and the adipose tissue of *ob/ob* and high fat diet fed mice (25,

57). Basseri *et al*. further characterized PBA as an agent that can inhibit adipogenesis *in vitro* (25). In keeping with these results, we observed a decrease in PPARγ and adiponectin when adipocytes were treated with PBA (Figure 3.3A and 3.5A). Consistent with inhibition of adipogenesis, there is a dose dependent reduction in TG levels when adipocytes are treated with PBA during days 0-2 of maturation (Figure 3.3B&C). The UPR was also reduced by PBA as noted by the decrease in calreticulin and p-eIF2α (Figure 3.5A) but interestingly CHOP levels increased with PBA treatment.

ER stress induced production of CHOP has previously been linked with the induction of apoptosis (42-45) but recent reports have demonstrated CHOP also regulates adipogenesis (25) and it up-regulates genes involved in the UPR (27). More importantly, this study demonstrated that CHOP does not bind to promoter regions of genes involved in apoptosis, but instead found that CHOP bound to promoter regions of genes involved in protein synthesis, such as tRNAs and initiation factors. However, through forced production of CHOP, they demonstrated that premature restoration of protein synthesis could lead to cell death through the production of ROS and ATP depletion, suggesting that there is a delicate balance between the pro and anti-apoptotic CHOP actions within the cell (27). This is also supported by the increased levels of CHOP and cleaved caspase-3, a marker of cellular apoptosis, that we observed with 5 mM but not 1 mM PBA (Figure 3.5A). Taken together, our data indicate that PBA may inhibit adipogenesis *in vitro* through the forced production of CHOP, but that higher concentrations of PBA (>1 mM) further increase CHOP levels and may lead to cell death if ER stress is relieved before cellular homeostasis is restored.

Overall, while *in vitro* data suggest that there may be a therapeutic window for PBA, careful consideration must be taken when treating cells with PBA as ER stress is ultimately a protective response and premature relief from ER stress can initiate apoptotic events. In addition, enabling adipose expansion and the recruitment preadipocytes is a plausible therapeutic strategy for T2DM. However, our *in vitro* data suggest PBA might not be beneficial as it reduced the protein levels of PPARα and adiponectin leading to impaired adipogenesis.

Sodium salicylate

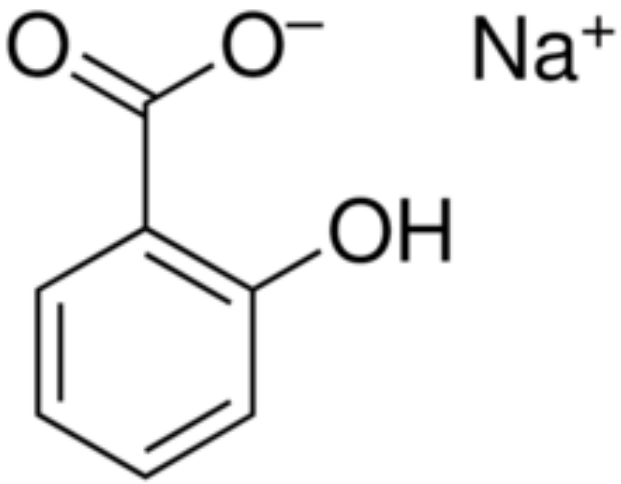

Sodium phenylbutyrate

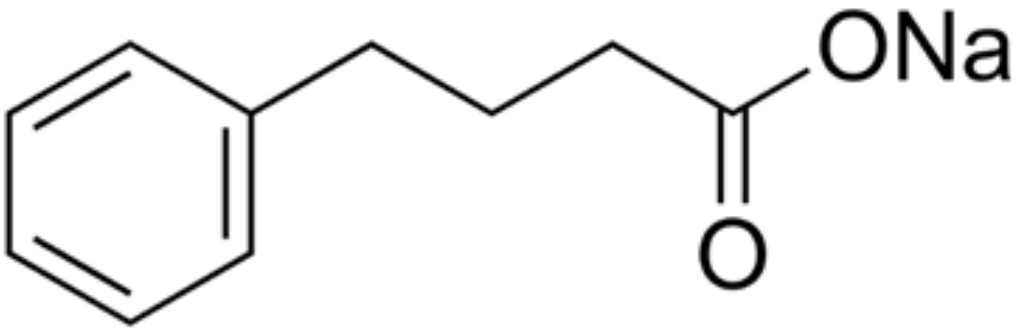

Figure 3.1 Chemical structure of sodium salicylate (SA) and sodium phenylbutyrate (PBA).

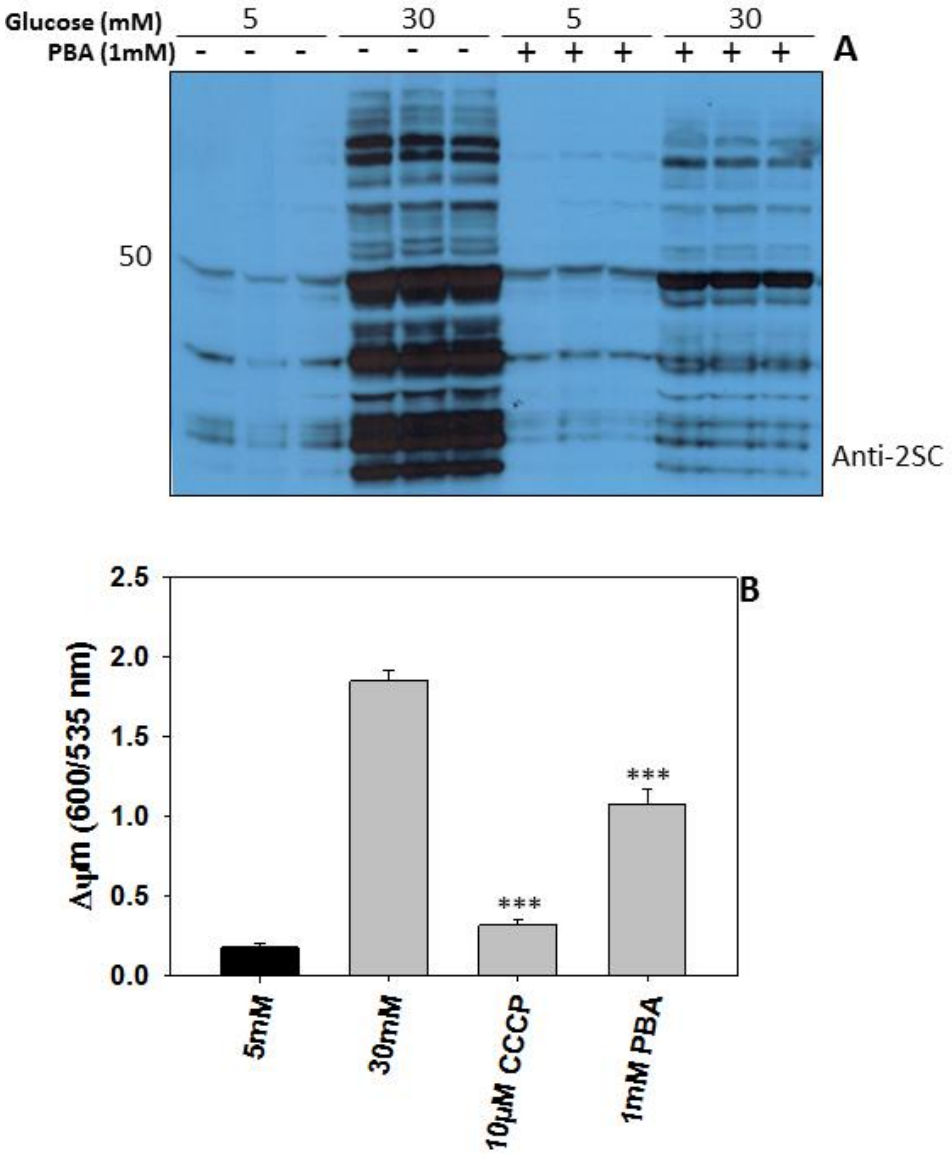

Figure 3.2: PBA reduces mitochondrial stress and 2SC levels. (A). Adipocytes were matured in 5 mM or 30 mM glucose with or without 1 mM PBA for 8 days. Total protein was harvested and 30 µg of protein was separated by 1-D PAGE and probed with anti-2SC polyclonal antibody to detect protein succination. (B) Adipocytes cultured in 5 mM glucose, 30 mM glucose or 30 mM glucose + 10 µM CCCP or 1 mM PBA for 2 days were loaded with the dye JC-1 to measure the $\Delta\Psi_m$. After 20 min the cells were washed and fluorescence was measured at Ex/Em 550/600 nm and Ex/Em 485/535 nm, as described in Materials and Methods. The $\Delta\Psi_m$ is expressed as a ratio of fluorescence at 600/535 nm. Data are representative of n=4 measurements expressed as means ± S.D. Asterisks indicate statistical significance determined by a one way ANOVA using Tukey's post hoc test (***P<0.001 for 30 mM glucose vs. 30 mM + CCCP or PBA).

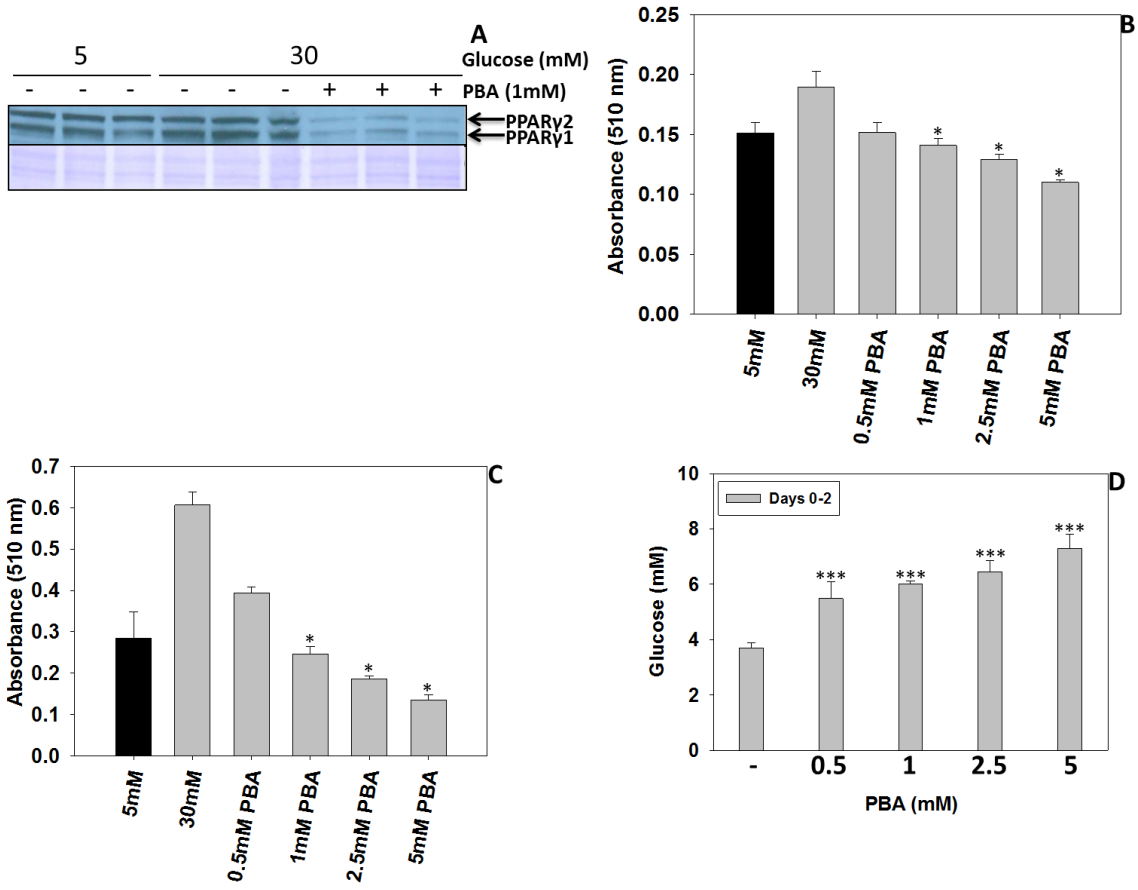

Figure 3.3: PBA reduces lipid content in adipocytes over the time course of maturation. (A) Adipocytes were matured in 5 mM or 30 mM glucose with or without 1 mM PBA. Total protein was harvested and 30 µg protein separated by 1-D PAGE and probed with anti-PPARγ. (B) Adipocytes were treated with PBA on days 0-2 (C) and days 0-8 of maturation. The triglyceride content was measured as described in the Materials and Methods. (D) The medium was collected after 2 days maturation and glucose content was measured as described in the Materials and Methods. The results are expressed as mean ± SD, n=4. Asterisks indicate statistical significance determined a One Way ANOVA ($^{***}p<0.001$, $^{**}p<0.01$ and $^{*}p<0.05$ for 30 mM glucose vs. 30 mM glucose + PBA). A Kruskal-Wallis One Way Analysis of Variance on Ranks using Dunn's method for data not normally distributed.

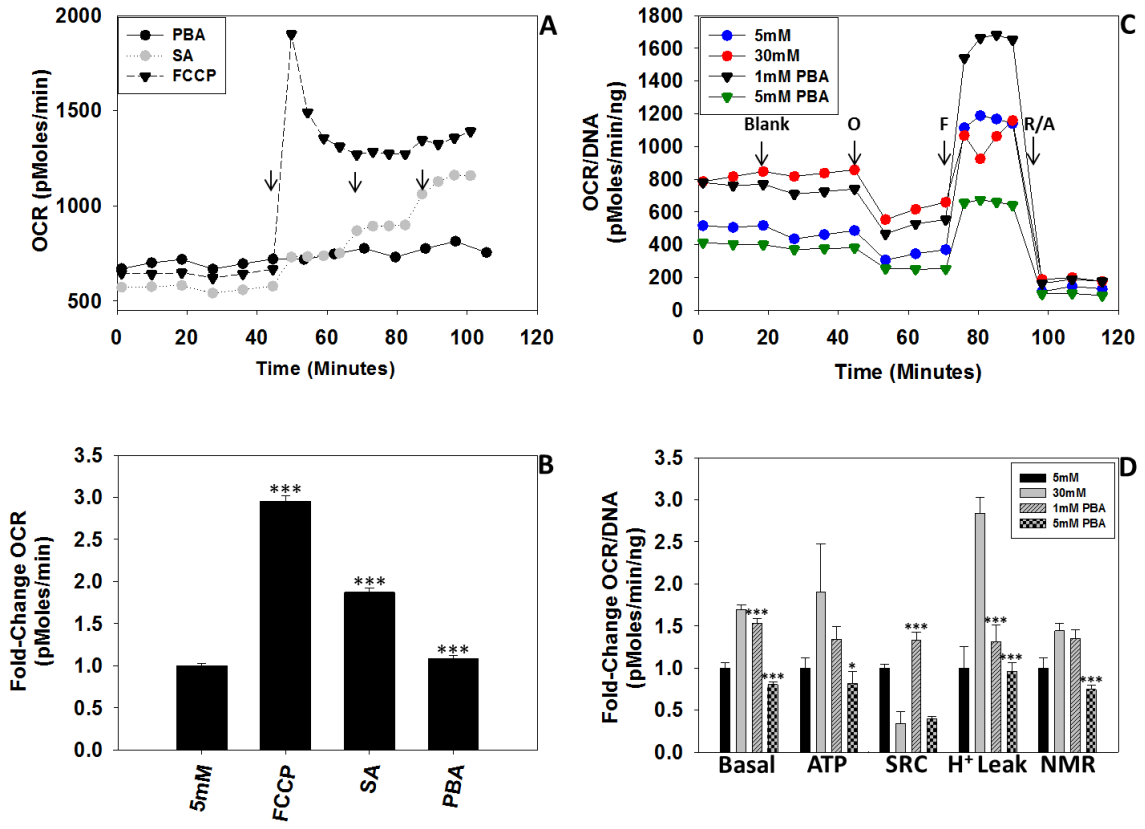

Figure 3.4: PBA reduces mitochondrial respiration in 30mM glucose. (A) To test whether or not PBA acted as a mitochondrial uncoupler, the Seahorse Extracellular Flux Analyzer (XF) 24 was used to measure effects on respiration when PBA is added acutely during the assay. FCCP (1.25 µM) served as a positive control and was only injected once (first arrow). PBA was injected into the wells on 3 occasions indicated by the arrows (black circles), at concentrations 1 mM, 5 mM and 10 mM PBA. SA was added to demonstrate the effects of a mild-uncoupler (gray circles) and was injected into the wells on 3 occasions indicated by the arrows at concentrations of 1 mM, 2 mM and 5 mM. (B) Fold-change increase of the basal oxygen consumption rate after the drugs were added, ***P<0.001 for 5 mM glucose vs. FCCP and SA, n=5. (C) The respiratory profile of adipocytes cultured in 5 mM (blue circles) and 30 mM (red circles) glucose or 30 mM with 1 mM (black triangles) or 5 mM (green triangles) PBA treatment on days 0-2 of maturation was measured using the Seahorse XF24 as described in the Materials and Methods. Drugs were added at the indicated arrows to assess mitochondrial function. (D) Fold-change in basal respiration, ATP production, SRC, proton leak, and non-mitochondrial respiration (NMR) were measured following the addition of oligomycin, FCCP and rotenone/antimycin A respectively. The results are expressed as a mean ± SD, n=5. Asterisks indicate statistical significance determined by a One Way ANOVA with a Tukey's post-hoc test (***P<0.001 and *P<0.05 for 30 mM glucose vs. 30 mM glucose + 1 mM or 5 mM PBA). A Kruskal-Wallis One Way Analysis of Variance on Ranks was performed when the data were not normally distributed.

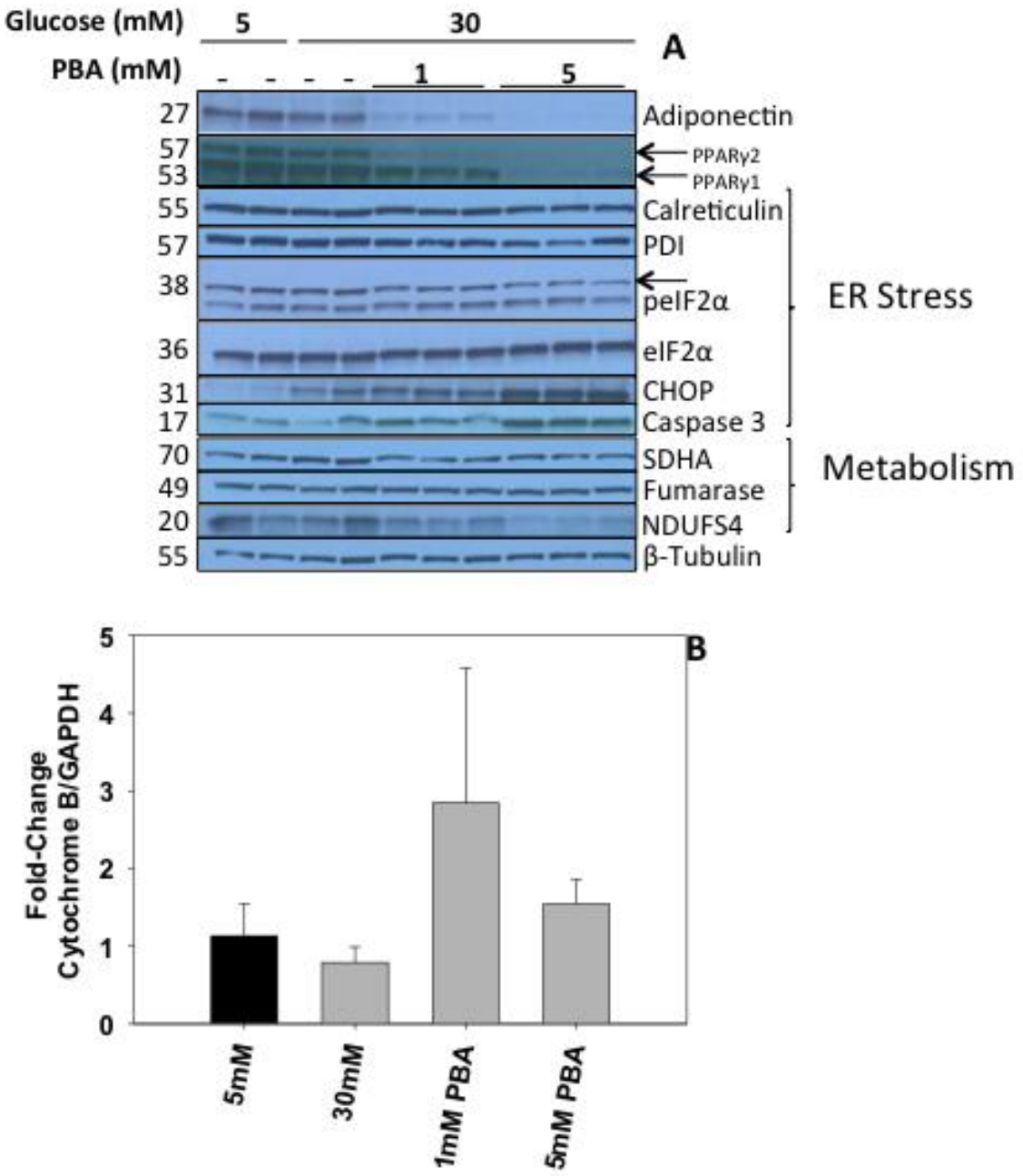

Figure 3.5: PBA reduces ER stress and inhibits adipogenesis. (A) 3T3-L1 adipocytes matured in 5 mM glucose or 30 mM glucose +/- 1 mM or 5 mM PBA were harvested after 2 days of maturation. Protein (20 µg) was separated by 1-D PAGE and markers of adipogenesis, UPR/ER stress and mitochondrial metabolism were detected as described in the Materials and Methods. (B) DNA was isolated and mitochondrial content was measured as described in the Materials and Methods, n=6. A One Way ANOVA using a Tukey's post-hoc test and a Kruskal-Wallis One Way Analysis of Variance on Ranks for data not normally distributed.

Chapter IV

Sodium Phenylbutyrate Treatment in *db/db* Mice

4.1. Introduction

The *db/db* mouse is a widely used model to study obesity and T2DM. There is a point mutation in the gene encoding the leptin receptor, rendering the receptor ineffective at binding its substrate hormone, leptin. *Db/db* mice have increased body weight at birth compared to heterozygotes, display hyperinsulinemia starting at 10-14 days after birth and hyperglycemia by 4-8 weeks (59). We have previously used this mouse model to examine protein succination in diabetes and have demonstrated that *db/db* mice have increased levels of 2SC in the adipose tissue compared to control animals (29, 32).

Previous experiments examining the effects of PBA in diabetic mice were conducted in the *ob/ob* mouse model and high-fat diet fed mice (25, 57). As we have previously used the *db/db* mouse, we were interested in determining whether or not PBA could reduce mitochondrial stress and protein succination in the adipose tissue of this model. We have shown that PDI is succinated on an active site residue and has reduced activity (unpublished results) which could promote ER stress by causing misfolded proteins to accumulate. Additionally, adiponectin is succinated on cysteine 39, preventing the normal incorporation of the monomer into trimers and higher

molecular weight species that can be secreted from the cell (29). Therefore, we hypothesized that if PBA could reduce mitochondrial stress and succination in *db/db* mice, this may ultimately lower ER stress by preventing the succination of chaperone and/or ER processed proteins. Considering that insulin resistant and obese humans are known to have increased adipose tissue ER stress (48), we anticipated that our studies might demonstrate the therapeutic effects of PBA as a potential T2DM treatment.

4.2. **Results**

We administered PBA to 7 week old *db/db* mice for 8 weeks to assess whether or not the drug could limit adipose tissue dysfunction and reduce 2SC accumulation. The drug was administered in the drinking water of at a dosage of 1 mg/g body weight (BW)/day for the first 4 weeks and reduced to 0.5 mg/g BW/day for the remaining 4 weeks.

As expected, Figure 4.1A demonstrates that *db/db* mice had significantly higher fasting blood glucose levels throughout the 8 weeks of the study compared to control mice ($^{\#\#}P<0.01$ $^{\#\#\#}P<0.001$, Figure 4.1A). PBA had no effect on the FBG levels of control mice receiving PBA treatment (Figure 4.1A). In *db/db* mice, there was a trend for PBA treatment to lower FBG but this was only statistically significant at weeks 2 through 6 ($^{*}P<0.05$, $^{**}P<0.01$, $^{***}P<0.001$ n=6, Figure 4.1A) due to the variability in FBG. Throughout the 8 week course of the study, *db/db* mice had a significantly higher body weight than control mice ($^{\#\#\#}p<0.001$, Figure 4.1B). PBA had no effect on the body weight of *db/db* mice whereas control mice receiving PBA treatment had a significantly higher body weight only after 7 weeks of treatment ($^{\$}p<0.05$, Figure 4.1A).

A regular chow diet was given *ad libido*. The amount of food consumed by the *db/db* mice was greater than the amount consumed by control mice, Figure 4.2A; although statistical analyses are not available as we housed 3 mice per cage. The *db/db* mice receiving PBA treatment tended to consume less food during the early weeks 1-5, ~7 g/day when compared to the untreated *db/db* mice who consumed ~9 g/day (Figure 4.2A). Food consumption was not different for any of the control mice throughout the study, with both groups consuming ~4-5 g/day. Water consumption was similar between control mice, ~0.2-0.3 mL/day/BW. The *db/db* (-)PBA mice consumed ~0.4-0.6 mL/day/BW (Figure 4.2B) whereas the *db/db* (+)PBA mice consumed ~0.2-0.3 mL/day/BW , similar to control mice (Figure 4.2B). The dosage of PBA in the water was reduced by 50% after 4 weeks treatment to ensure that the *db/db* (+)PBA mice were not drinking less water due to a dislike or ill effect of the drug.

We assessed whole body composition of the mice at 14 weeks of age (after 7 weeks of PBA treatment) using a Dual Energy X-ray Absorptiometry (DEXA) scan. *Db/db* mice had greater total lean mass, fat mass and % fat compared to control mice ($^{###}p<0.001$, Figure 4.3A). There were no differences in lean mass, fat mass or % fat with or without PBA treatment in the *db/db* groups (Figure 4.3A). Interestingly, we documented decreased lean mass and increased % fat in the control mice that received PBA treatment compared to the untreated control mice ($^{*}p<0.05$, Figure 4.3A). Upon sacrifice, we removed the epididymal fat pads from the animals and observed a significant increase in the mass of the fat pad from the *db/db* mice compared to control

mice ($^{###}$p<0.001, Figure 4.3B), but no change was observed between *db/db* (-)PBA and *db/*db (+)PBA mice (Figure 4.3B).

To assess insulin sensitivity, we performed an insulin tolerance test after 7 weeks of PBA treatment. Insulin was injected intraperitoneally and blood glucose was measured over the course of 120 minutes. There was no difference in the response to insulin observed in the control mice with or without PBA treatment (Figure 4.4). There was a slight but significant reduction in the blood glucose levels of the *db/db* (+)PBA after 120 minutes compared to *db/db* (-)PBA (*p<0.05, Figure 4.4).

As PBA has been shown to reduce TG levels in *ob/ob* mice (57) we measured TG content in the serum of overnight fasted mice. TG levels ranged from 50-90 mg/dL in control mice and were elevated in *db/db* (-)PBA mice to ~150 mg/dL beginning at 9 weeks of age (Figure 4.5A). *Db/db* (+)PBA mice had significantly reduced TG levels, ~50-75 mg/dL, compared to *db/db* (-)PBA mice (*P<0.05, **P<0.01 and ***P<0.001, *db/db* (+)PBA vs. *db/db* (-)PBA, Figure 4.5A) throughout the course of PBA treatment. We then examined the TG content in the liver and observed ~5-fold increase in *db/db* (-)PBA versus control mice ($^{###}$P<0.001 *db/db*, Figure 4.5B). Surprisingly, there was ~1.6-fold increase in TG levels in *db/db* (+)PBA compared to *db/db* (-)PBA mice (*P<0.05, Figure 4.5B).

We have previously shown that PBA can reduce the levels of protein succination in 3T3-L1 adipocytes (Figure 3.2A). There is increased succination in epididymal adipose tissue of in *db/db* (-)PBA and *db/db* (+)PBA vs. control mice at 15 weeks of age (8 weeks post treatment) (Figure 4.6, anti-2SC). We did not observe a reduction in the levels of

succinated proteins in the *db/db* (+)PBA compared to the *db/db* (-)PBA mice (Figure 4.6). The adipogenic marker PPARγ was increased in *db/db* (-)PBA and *db/db*/+)PBA mice versus control and was unaltered by PBA treatment. PDI is moderately increased and there is a pronounced increase in CHOP protein levels in *db/db* mice versus control. This was unchanged by PBA treatment (Figure 4.6). Grp78 was decreased in *db/db* (-)PBA mice compared to control, and was increased *db/db* (+)PBA mice. Overall, PBA did not appear to have any significant effects on protein succination or the UPR/ER stress proteins in the epididymal adipose tissue of *db/db* mice.

Previous studies have shown that the liver has reduced TG levels, improved insulin signaling and decreased ER stress in *ob/ob* mice upon PBA treatment (57). In the liver tissue of the *db/db* (-)PBA and *db/db (*+)PBA mouse we detected increased PDI and CHOP levels but decreased Grp78 compared to control mice (Figure 4.7). Considering the significant increase in liver TG levels in *db/db* (+)PBA mice, we examined several proteins involved in fatty acid synthesis. The levels of phospho-acetyl-CoA carboxylase (p-ACC) were unchanged between control and *db/db* (-)PBA mice but the *db/db* (+)PBA mice had increased levels of p-ACC compared to both groups. Fatty acid synthase (FAS) was increased in *db/db* mice versus control (Figure 4.7) but no difference was observed in the protein levels with PBA treatment.

4.3. Discussion

PBA has been documented to reduce ER stress and blood glucose levels in several rodent models of obesity and diabetes (25, 57). We chose to study the effects of PBA in the *db/db* mouse model of diabetes as we have previously demonstrated

increased levels of protein succination in the suprarenal, subcutaneous and epididymal adipose tissue of these mice at 15 weeks age (32). In addition, activation of the UPR and ER stress have been documented in the liver and adipose tissue of *db/db* mice (60, 61). As we have shown that adiponectin (29) and PDI (unpublished results) are succinated in the adipose tissue of *db/db* mice, we hypothesized that PBA might reduce protein succination, thereby reducing ER stress and improving adipose homeostasis in *db/db* mice.

We observed a significant reduction in blood glucose levels in *db/db* (+)PBA mice after 2 weeks of PBA treatment, lasting until week 6 (Figure 4.1A). While there was a trend for FBG to be lower in the *db/db* (+)PBA mice for the duration of the study, we reduced the concentration of PBA from 1 mg/g/day to 0.5 mg/g/day after 4 weeks of treatment over concerns regarding water consumption volumes. This change in dose may have contributed to the lack of a significant effect in FBG by weeks 7 and 8 of treatment. There was a trend for mice treated with PBA to have increased body weight compared to untreated mice (Figure 4.1B) and this is a documented side effect of the drug in humans (62). There was a trend for less food to be consumed by *db/db* (+)PBA mice in the first 4 weeks of the study but the amount of food consumed/day after 8 weeks was similar between the two groups, indicating that any trend for increased weight gain cannot be attributed to an increase in food consumption (Figure 4.2A). Water intake was monitored to ensure that the mice were receiving the correct drug dosage. We observed a significant reduction in the amount of water consumed in *db/db* (+)PBA mice during the first 4 weeks of the study compared to *db/db* (-)PBA mice (Figure

4.2B), therefore, we reduced the dosage of the drug appropriately to eliminate the possibility that any differences we observed were due to the effects of dehydration. Surprisingly, *db/db* (+)PBA mice consumed ~50% less water than *db/db* (-)PBA mice while control mice consumed the same amount of water throughout the 8 week treatment whether not PBA was present in their drinking water. As the drug concentration was adjusted weekly based on the body weight of the mice, by week 8 of treatment, the control (+)PBA mice were receiving a more concentrated solution of PBA water than the *db/db* (+)PBA mice. This suggests the reduced water consumption by the *db/db* (+)PBA mice was not related to taste, although PBA is known to have a bitter taste.

We assessed whole body composition at 14 weeks of age (7 weeks treatment) and did not observe any changes in lean mass, fat mass or % fat in *db/db* mice with or without PBA treatment. Surprisingly, control (+)PBA mice had significantly higher % fat and decreased lean mass compared to control (-)PBA (Figure 4.5A). As we did not observe any differences in FBG, serum TG levels or food/water consumption between control mice with or without PBA treatment, we did not initially examine the epididymal or liver tissue in the treated controls. However, we are planning to analyze these tissues in the future as PBA may be having select effects on control mice.

Non-alcoholic fatty liver disease is often associated with T2DM because increased serum TG levels and lipoprotein imbalances result in the uptake, synthesis and oxidation of free fatty acids by the liver (63). Although we observed a significant reduction in serum TG levels in *db/db* (+)PBA mice compared to *db/db* (-)PBA mice

(Figure 4.5A), there was an unexpected increase in TG levels in the liver tissue (Figure 4.5B). We next examined the lipogenic protein levels to determine if lipogenesis was more active after PBA treatment, explaining the increase in TGs. It was found that regulation of the first step of fatty acid synthesis by p-ACC was unchanged between control and *db/db* (-)PBA mice but FAS was increased in *db/db* (-)PBA mice (Figure 4.7), suggesting that the fatty liver in *db/db* mice at 15 weeks is associated with up-regulation of FAS (64). We also found that p-ACC levels were increased in *db/db* (+)PBA mice compared to *db/db* (-)PBA mice, which suggests that there would have been less TG deposition as ACC catalyzes the first step in fatty acid biosynthesis (Figure 4.7). Further examination of other components of the lipogenic pathway may be necessary to determine what is contributing to increased triglycerides in liver. Additionally the 15 week time point at which we looked at these enzymes may be too late and only offers limited insight into the regulation of TG accumulation which may have occurred at an earlier time point. (50).

Our *in vitro* data in 3T3-L1 adipocytes demonstrated that 1 mM PBA treatment for 8 days can reduce the levels of protein succination in adipocytes matured in 30 mM glucose (Figure 3.2A). As a result, we had hypothesized that PBA would reduce protein succination and thereby alleviate ER stress in *db/db* mice. Protein succination was unaffected in the epididymal adipose tissue after 8 weeks in *db/db* (+)PBA mice (Figure 4.6). We did not observe any difference in adipogenesis as noted by the master regulator of adipogenesis, PPARγ, in *db/db* (+)PBA. The protein levels of UPR or ER stress markers as indicated by PDI and CHOP were elevated in *db/db* mice but were

unchanged by PBA treatment (Figure 4.6). This is a surprising result as *db/db* mice have increased ER stress in the adipose tissue and that PBA was able to lower ER stress in and high fat diet fed mouse and *ob/ob* mouse (25, 57).

Overall, PBA reduced blood glucose levels and serum TGs in *db/db* mice, but increased the deposition of TGs in the liver – a negative metabolic outcome. The UPR and ER stress responses were unaffected by PBA treatment in the adipose tissue, which contrasts with the results of Ozcan *et al.* in *ob/ob* mice (57). However, this could be due to differences in the duration of the experiment, 8 weeks vs. 20 days, and/or age of mice at sacrifice, 15 weeks vs. 10-11 weeks (57). Our results thus far in the *db/db* model do not support the notion that PBA may be therapeutically useful in treating T2DM. Indeed our surprising finding that PBA increased deposition of TGs in the liver of *db/db* mice warrants further investigation of the negative effects of PBA.

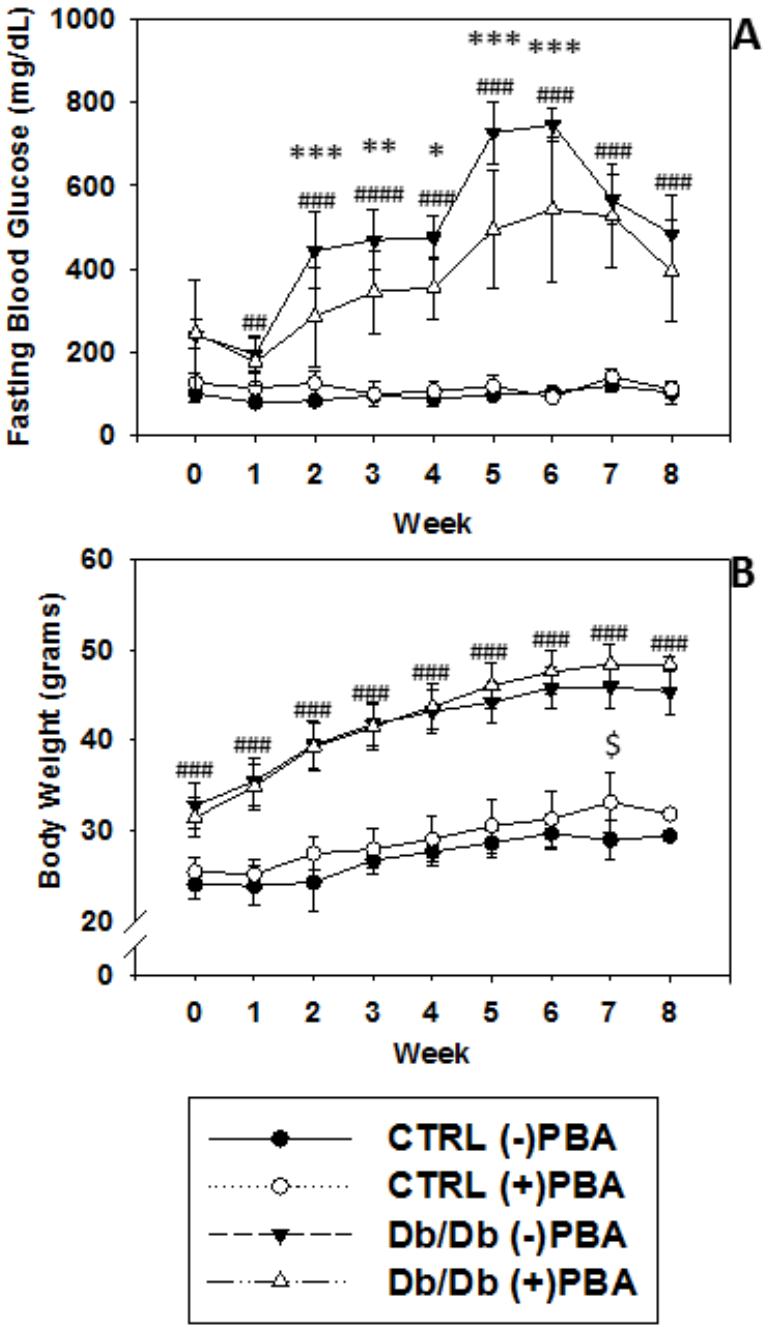

Figure 4.1: Effects of PBA treatment effects on fasting blood glucose and body weight. Control and *db/db* mice were treated with or without 1 mg/g BW/day for the first 4 weeks then reduced to 0.5 mg/g BW/day for the remaining 4 weeks of the study. (A) Fasting blood glucose was measured from the tail vein after an overnight fast. (B) Body weights were taken once per week in the morning after an overnight fast. Data are representative of n=5-6 mice expressed as means ± S.D. Data were subjected to a Two Way Repeated Measures ANOVA (One Factor Repetition) to test for significance ($^{\$}$P<0.05 for control (-)PBA vs. control (+)PBA and $^{\#\#\#}$P<0.001 for *Db/db* vs. control).

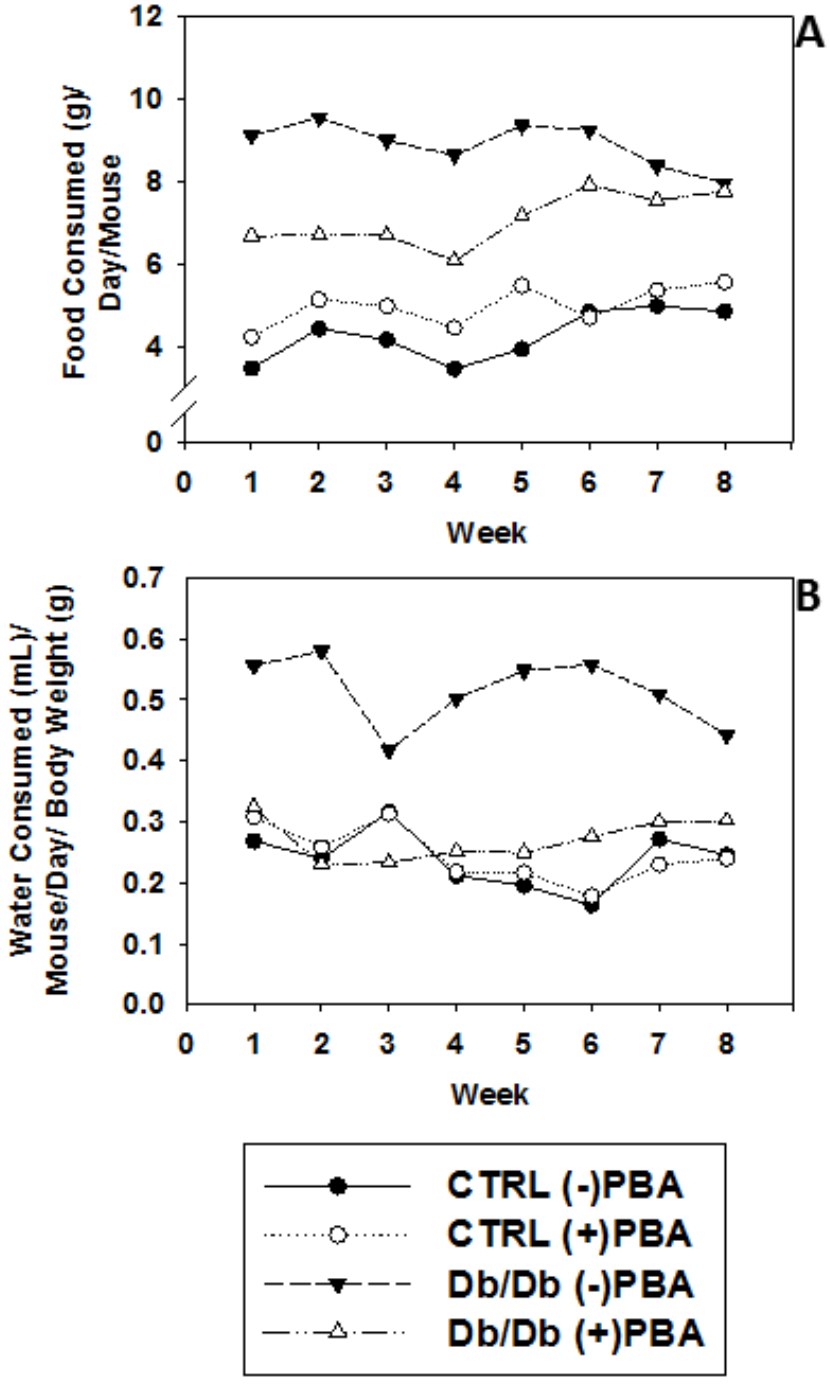

Figure 4.2: Effects of PBA treatment of food consumption and water intake. Food and water consumption were given *ad libido* to the mice. Control and *db/db* mice were treated with PBA in the drinking water at a dosage of 1 mg/g BW/day for the first 4 weeks then reduced to 0.5 mg/g BW/day for the remaining 4 weeks of the study. (A) Food consumption and (B) water intake were measured bi-weekly. Data are representative of n=2-3 mice per cage.

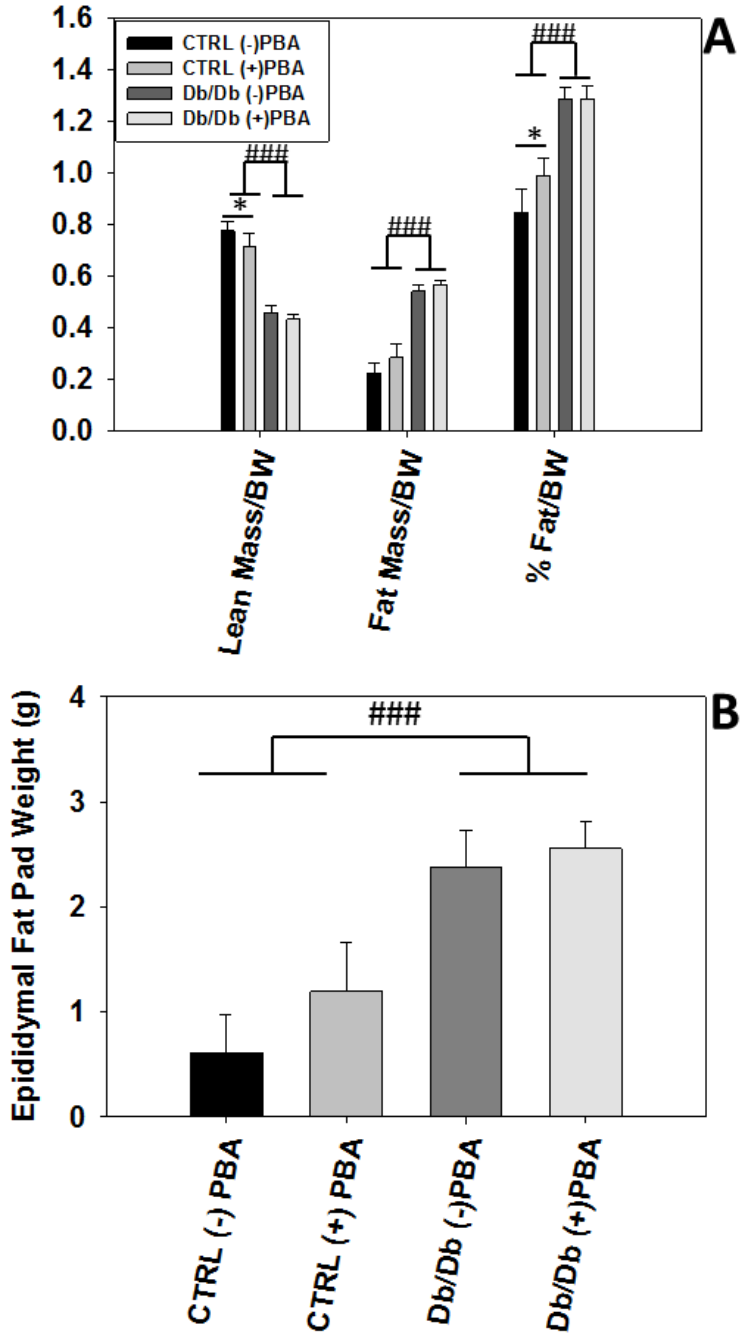

Figure 4.3: Effects of PBA treatment on body composition. (A) Mice were subjected to a DEXA scan at 14 weeks of age (7 weeks +/- PBA treatment) to assess fat and lean body mass. (B) At the time of sacrifice, epididymal fat pads were removed and weighed. Data are representative of n=5-6 mice expressed as means ± S.D. Data were subjected to a One-way ANOVA using Tukey's post hoc test to test for statistical significance ($^{###}$P<0.001 for *db/db* vs. control).

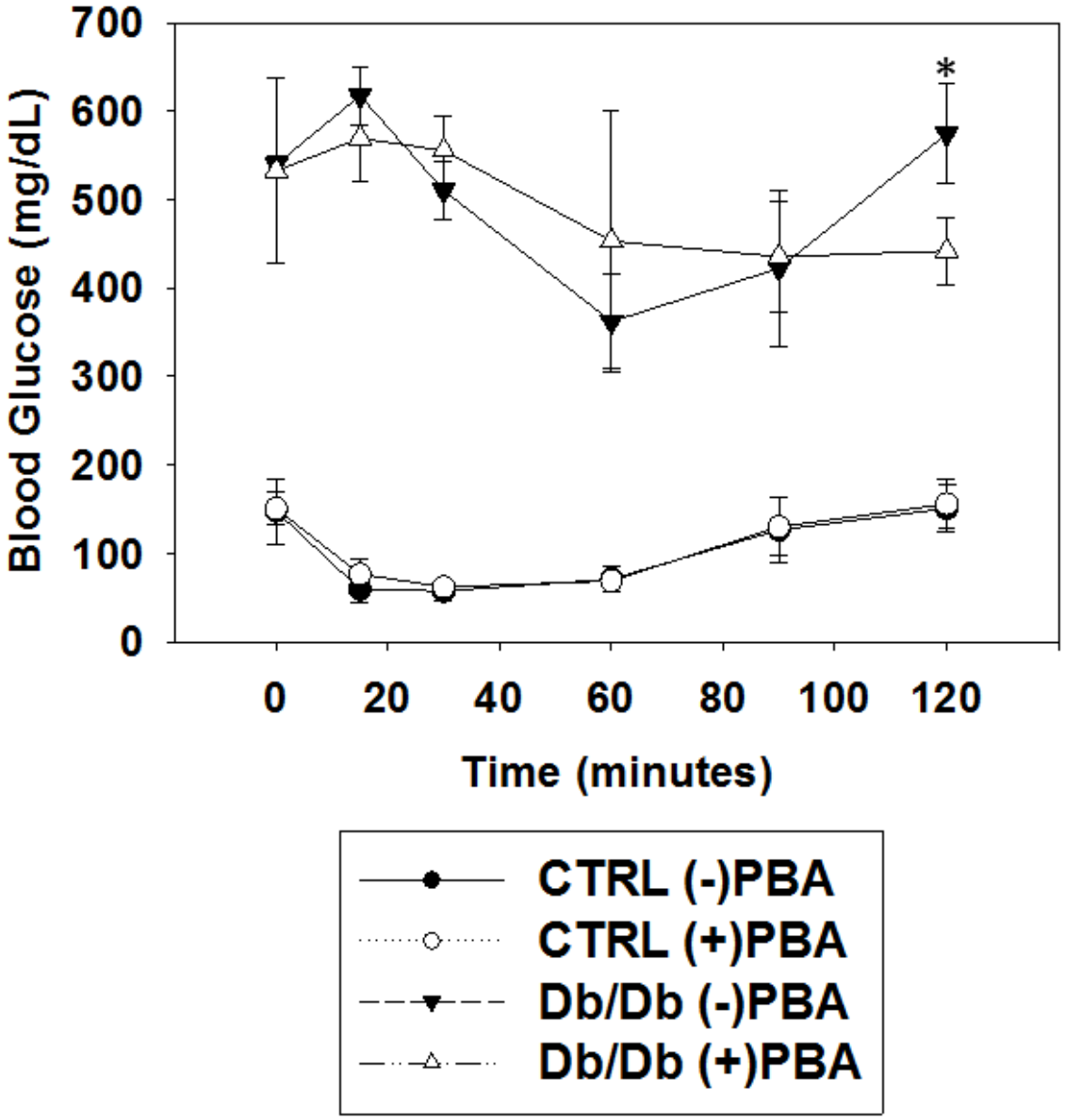

Figure 4.4: PBA Treatment improves insulin sensitivity. At 14 weeks of age (7 weeks -/+ PBA treatment) mice were fasted for 4 hours and then given an injection of 2U insulin intraperitoneally. Blood glucose was measured from tail vein bleeds over the course of 120 minutes. Data are representative of n=5-6 mice, expressed as means ± S.D. Data were subjected to Two Way Repeated Measures ANOVA (One Factor Repetition) to test for statistical significance ($^{*}P<0.05$ for *db/db* (-)PBA vs. *db/db* (+)PBA).

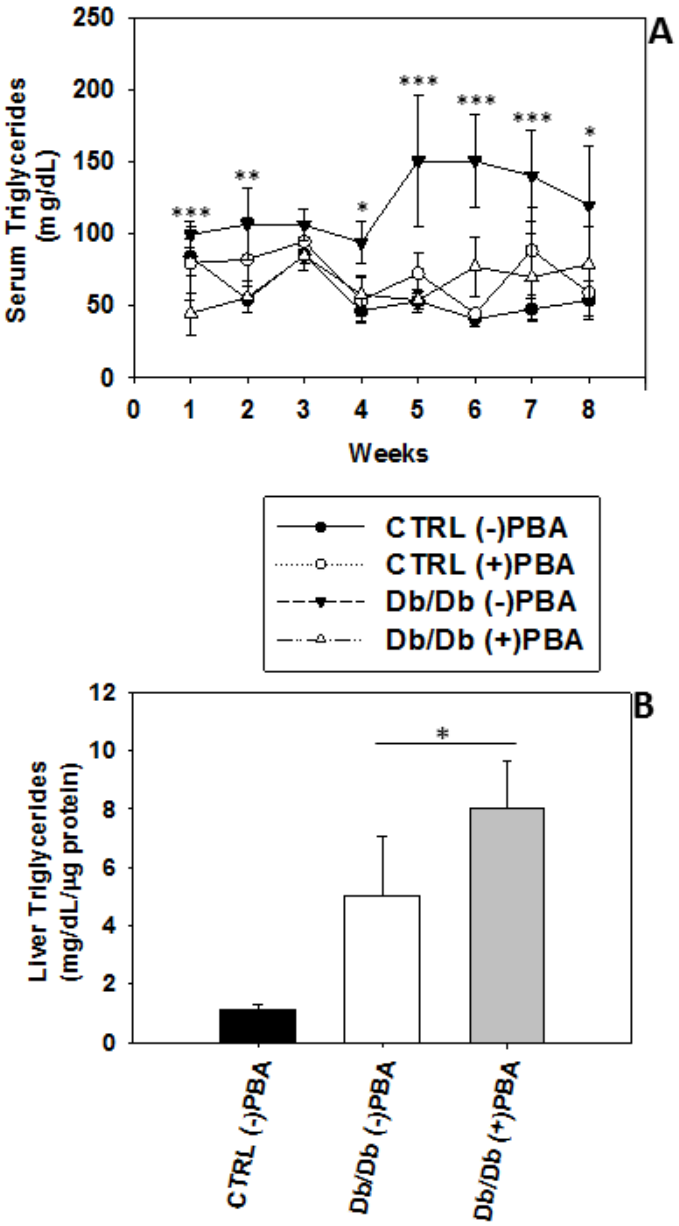

Figure 4.5 PBA reduces serum triglyceride levels but increases liver triglyceride levels. Mice were fasted weekly for 12-16 hours overnight and tail vein blood was collected. (A) Triglyceride levels in serum of overnight fasted mice. (B) A portion of the liver was used for triglyceride analysis and the results are expressed relative to the protein content. Data are representative of n=5-6 mice, expressed as means ± S.D. Asterisks indicate statistical significance as determined by a (A) Two Way repeated measure ANOVA and (B) a One Way Tukey's post hoc test (**P<0.01 and ***P<0.001 for *db/db* (-)PBA vs. *db/db* (+)PBA and $^{\#}$P<0.05, $^{\#\#}$P<0.01 and $^{\#\#\#}$P<0.001 for *db/db* (-)PBA vs. control).

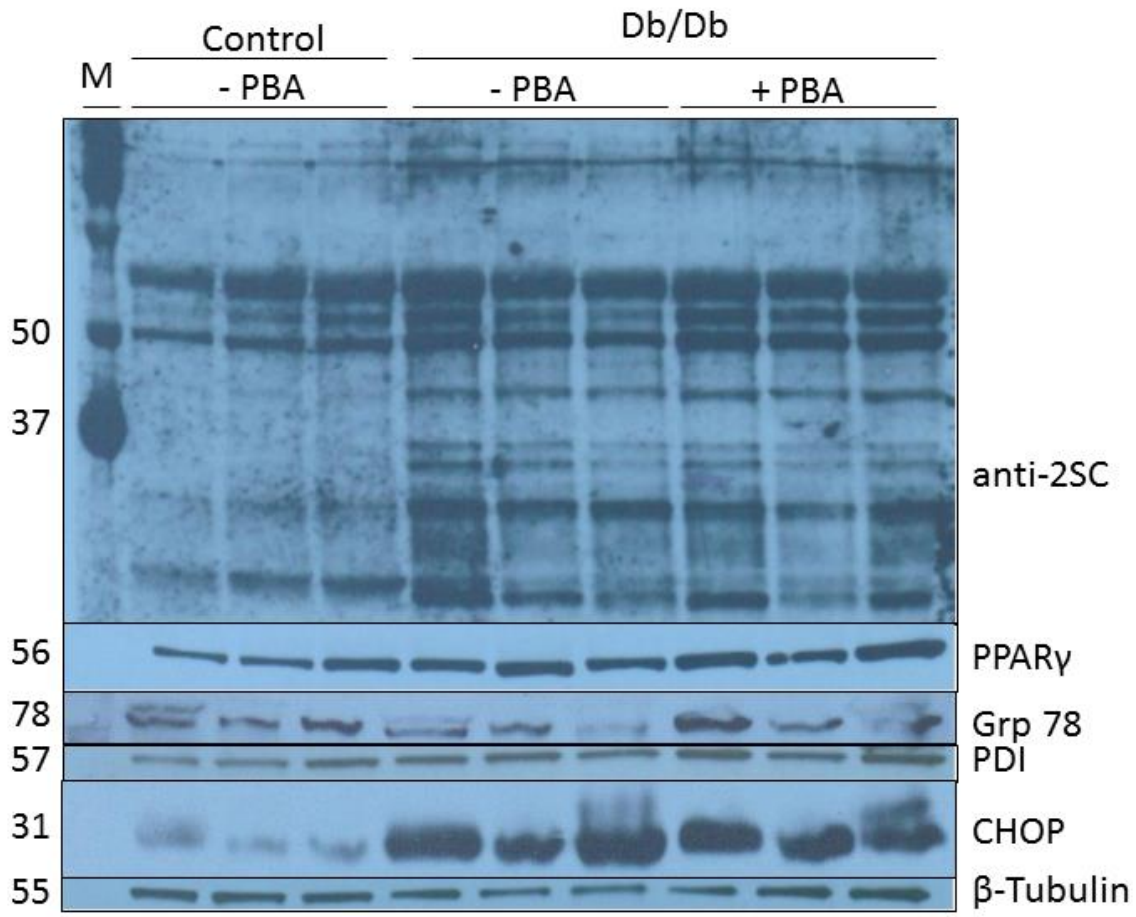

Figure 4.6 PBA does not reduce ER Stress in epididymal adipose tissue of *db/db* mice. Analysis of succinated proteins and ER stress markers in epididymal adipose tissue of control and *db/db* mice at 15 weeks of age (8 weeks +/- PBA treatment). Protein was separted by 1-D PAGE and 100 µg was used for the detection of 2SC using polyclonal anti-2SC antibody and 60 µg was used for the detection of Grp78, PDI (UPR) and CHOP (ER stress) proteins. Molecular weights are shown in kDa (left) and β-Tubulin is shown to demonstrate protein loading.

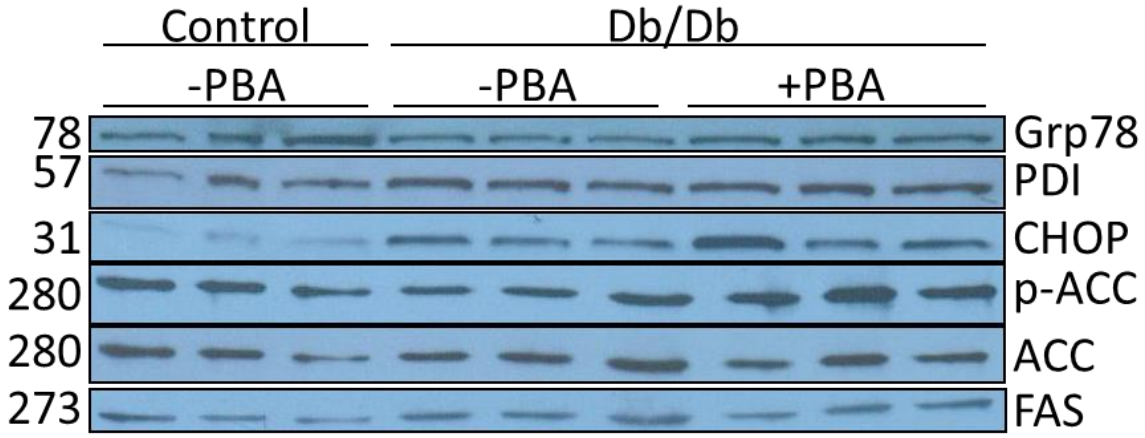

Figure 4.7 PBA does not alter the ER stress response but increases the inhibition of ACC. Analysis of UPR and ER stress proteins in control and *db/db* mice at 15 weeks of age Proteins, 40 μg, was separated by 1-D PAGE for the detection of Grp78, PDI (UPR) and CHOP (ER stress) and lipogenesis markers. Molecular weights are shown in kDa (left) and a Coomassie is shown to demonstrate protein loading.

Chapter V

The Turnover of Succinated Proteins

5.1. Introduction

In the cell there are two protein degradation pathways for the removal of damaged or unwanted proteins, the ubiquitin proteasome system (UPS) and the lysosomal degradation system (also referred to as autophagy) (Figures 5.1 & 5.2) (65, 66). Protein degradation is a regulated process that responds to remove damaged proteins and organelles or to provide amino acids in response to changes in the cellular nutrient status (67).

The UPS is primarily responsible for the degradation of cytosolic, ER, nuclear, and short-lived proteins. Turnover occurs in a sequential process by which an 8.5 kDa ubiquitin protein is attached to the protein to be degraded on a lysine residue (67). Subsequent ubiquitin molecules can be attached to internal residues on ubiquitin itself, forming an ubiquitin chain that signals the protein to be degraded by the proteasome (Figure 5.1) (65, 68). However, ubiquitin can also be a signal for certain proteins to be selectively degraded by autophagy, and it appears that the internal lysine residue of ubiquitin that serves as an anchor point for additional ubiquitin molecules is the key player in determining the proteins fate (67). The 26S proteasome is a large ~2.5 MDa ATP-dependent complex consisting of the 20s catalytic particle (CP) and the 19s

regulatory particle (RP). The CP is a barrel-shaped structure in which the proteolytic activity is sequestered and has limited access to proteins destined to be degraded as a result of gating by other residues. The proteolytic core contains three proteases with different specificities; acidic residues (caspase-like), basic residues (trypsin-like) and hydrophobic residues (chymotrypsin-like) (Figure 5.1) (68).

Autophagic degradation has a much broader proteolytic role than proteasomal degradation in that whole organelles such as mitochondria (mitophagy) or peroxisomes (pexophagy) can be degraded in addition to individual proteins (67). In the first step of autophagy a double-membraned structure known as a phagophore surrounds items to be degraded. As the phagophore is forming, more 'cargo' can be added and the membrane can continue to grow until it becomes an enclosed double-membrane structure known as an autophagosome, a process that is mediated by several autophagy-related proteins (Atgs) (Figure 5.2) (69). In the committed step of autophagy, microtubule-associated protein light chain 3 (LC3-I) is converted to LC3-II via lipidation with phosphatidylethanolamine and is attached to the autophagosome. The cargo-loaded vesicle can then fuse with the lysosome, which contains hydrolases capable of protein degradation (67). The primary hydrolases present in the lysosomes of adipocytes are cathepsin B (cysteine protease) and cathepsin D (aspartic protease) (70).

We have identified ~40 succinated proteins and the majority of these are cytosolic proteins (34). Additionally, we have previously demonstrated that 2SC is produced endogenously in rats and is excreted in the urine (31), suggesting that there is an intracellular mechanism that can facilitate the removal of succinated proteins. Due to

the stability of the thioether bond and that there are no known enzymes that can cleave the thioether bond, we hypothesized that succinated cytosolic proteins were predominantly being degraded in the adipocyte by the proteasome. We therefore investigated the turnover of succinated proteins in the 3T3-L1 adipocyte cultured in high glucose conditions versus normal glucose to determine if (1) succinated proteins were being turned over and (2) the mechanism of degradation of succinated proteins.

5.2. Results

The accumulation of succinated proteins in 3T3-L1 adipocytes in 30 mM glucose is significantly increased at days 4-6 of maturation in association with increased intracellular concentrations of fumarate (31). As noted in Figure 5.3A, there is an increase in the levels of 2SC in adipocytes matured in 30 mM glucose compared to 5 mM glucose for 8 days. The reaction of fumarate with cysteine is a non-enzymatic process, therefore, we next sought to determine if stable succinated proteins could be removed from within the cell. When adipocytes are matured in 30 mM glucose for 4 days and then switched to 5 mM glucose for the remaining 4 days of maturation, the levels of 2SC no longer accumulate and are similar to the levels observed in adipocytes that matured in 5 mM glucose for 8 days (Figure 5.3A). This indicated that there was intracellular turnover of the succinated proteins that had accumulated up until 4 days. We then sought to determine specifically when the levels of 2SC began to decline after removing the high glucose stimulus. As observed in Figure 5.3B, the levels of 2SC began to decline as early as 1 day after 30 mM glucose removal. In particular there is a greater reduction in band intensity for proteins with a mass ~30-37 kDa and ~75-100 kDa (Figure

5.3B). If the 30 mM glucose is replaced with 5 mM glucose for longer time periods, from 1 day up until 4 days, the extent of protein succination is further reduced (Figure 5.3B).

To determine the intracellular mechanism by which the succinated proteins were being degraded, we next inhibited either the proteasome or the lysosome. MG132 (a proteasome inhibitor) or chloroquine (a lysosomal inhibitor) were used to attenuate protein degradation. The adipocytes were matured for 4 days in 30 mM glucose and then switched to 5 mM glucose -/+ MG132 or chloroquine for the remaining 4 days of maturation. Figure 5.4A&B confirms that 2SC is increased in adipocytes matured for 8 days in 30 mM and that this is decreased when the high glucose stimulus is removed after 4 days and replaced with 5 mM glucose for the remaining 4 days (lanes 4-6 vs. 7-9). For the adipocytes that were switched from 30 mM to 5 mM glucose and simultaneously treated with 17.5 μM MG132 (lanes 10-12, Figure 5.4A), there was no accumulation of succinated proteins (Figure 5.4A), suggesting the proteasomal inhibition does not prevent the degradation of succinated proteins. However, in a parallel experiment where the adipocytes were switched from 30 mM to 5 mM glucose and treated with 25 μM chloroquine, succinated proteins did accumulate (lanes 10-12, Figure 5.4B). This indicated that the lysosome appears to be primarily responsible for the degradation of succinated proteins. Inhibition of the lysosome was confirmed by the pronounced increase in LC3-I and LC3-II in chloroquine treated adipocytes compared to the untreated adipocytes (Figure 5.4B).

Considering that we had established that succinated proteins were being degraded, we next sought to quantify the release of free 2SC from the adipocyte using

gas chromatography-mass spectrometry (GC/MS). We measured the basal levels of 2SC in the Dulbecco's Modified Eagles Medium (DMEM) and 10% fetal bovine serum (FBS) to ensure that the 2SC we detected was produced by the adipocyte (rather than measure any endogenous 2SC in the cell culture reagents). In DMEM, we detected ~0.03 mmol 2SC/mol lysine and in DMEM supplemented with 10% FBS we detected ~0.05 mmol 2SC/mol lysine (data not shown). It has previously been shown that the levels of fumarate in the cell culture medium increase throughout adipocyte maturation in 25 mM glucose (71). We determined the amount of 2SC present on FBS proteins (predominantly albumin) when adipocytes were matured in 5 mM or 30 mM glucose in order to ensure that any free 2SC detected in the maturation medium was being released from the cells and was not derived from the released fumarate modifying FBS proteins (Figure 5.5). In order to do this we separated the serum protein from the free amino acids/peptides released from the cell by trichloroacetic acid precipitation of the protein in the medium. When the serum protein was analyzed (after it was hydrolyzed to release free 2SC) there was no difference in the levels of 2SC in the maturation medium of adipocytes matured in 5 mM or 30 mM glucose on days 4-6, (Figure 5.5). This indicated that any changes in 2SC could not be attributed to fumarate reacting with serum proteins in the medium.

Next, we sought to quantify how much 2SC was being synthesized in and released from the adipocyte itself. Adipocytes were matured in 5 mM or 30 mM glucose for 8 days, or 30 mM glucose for 4 days then 5 mM glucose for the remaining 4 days -/+ chloroquine. As indicated in Figure 5.6A, there was an ~1.9-fold increase in 2SC in 30

mM glucose vs. 5 mM glucose in the cell lysate after 8 days of maturation ($^{***}p<0.001$, Figure 5.6A). In adipocytes that were switched to normal glucose after 4 days maturation, there was a significant reduction in 2SC in the cell lysate compared to adipocytes matured in 30 mM glucose for 8 days ($^{###}p<0.001$, Figure 5.6A). When the adipocytes were treated with chloroquine concomitant with the switch to 5 mM glucose the levels of 2SC were significantly elevated compared to 5 mM glucose ($^{***}p<0.001$, Figure 5.6A). We then examined when 2SC was being released from the cells into the culture medium. Analysis of the culture medium from early maturation days 2-4 revealed a ~1.5-fold increase in 2SC in the medium of adipocytes matured in 30 mM glucose vs. 5 mM glucose ($^{***}p<0.001$, Figure 5.6B). As before, on maturation day 4 a subset of adipocytes were switched from 30 mM to 5 mM glucose for the remainder of maturation and treated with or without chloroquine. The culture medium from days 4-6 contained ~1.5-fold more 2SC in 30 mM glucose than 5 mM glucose ($^{***}p<0.001$, Figure 5.6C). Surprisingly, there was no increase in the 2SC in the culture medium of adipocytes that had been switched from 30 mM to 5 mM glucose (Figure 5.6C), as might be expected if the 2SC was being degraded intracellularly and released from the cell. The levels of 2SC in the culture medium of adipocytes that had been treated with chloroquine were similar to 2SC levels observed in 5 mM glucose (Figure 5.6C), consistent with chloroquine preventing degradation and release. Culture medium from late maturation days 6-8 had a similar ~1.3-fold increase in 2SC in adipocytes matured in high glucose ($^{**}p<0.01$ and $^{***}p<0.001$ Figure 5.6D). 2SC did not increase in the culture medium of adipocytes that had undergone the switch from high to normal glucose on

days 6-8 (Figure 5.6D). Unexpectedly, the adipocytes that had been treated with chloroquine had a ~1.6-fold increase in 2SC in the culture medium on days 6-8 vs. adipocytes matured in normal glucose for 8 days ($^{***}p<0.001$, Figure 5.6D).

The above measurements demonstrated that free 2SC was detectable in the culture medium. However, the hydrolysis step in preparation for GC/MS analysis did not allow us to differentiate whether the 2SC was released as a free modified cysteine or as part of a small peptide incorporating the 2SC. We examined the culture medium of adipocytes matured in normal or high glucose on days 4-6. The samples were divided into two equal parts after removal of the serum proteins, one part being subjected to hydrolysis to determine the total amount of 2SC, and the other not hydrolyzed representing the amount of free 2SC released from the adipocyte. As observed in Figure 5.7, there was ~0.039 mmol 2SC/mol lysine total in the culture medium while there was 0.008 mmol 2SC/mol lysine detected as free 2SC in the culture medium in adipocytes matured in 5 mM glucose. In adipocytes matured in 30 mM glucose there was 0.09 mmol 2SC/mol lysine total in the culture medium while 0.04 mmol 2SC/mol lysine is liberated as free 2SC. The difference in the total 2SC and that detected as free 2SC (detected in the absence of peptide hydrolysis) represents the fraction that is peptide bound, demonstrating that 2SC is released both as a free amino acid and as part of a peptide.

5.3. Discussion

The formation of S-(2-Succino)cysteine (2SC) is an irreversible chemical modification as the reaction of fumarate with cysteine forms a thioether bond, which is

very stable, and there are no known enzymes that can cleave this bond. Protein succination is increased in 3T3-L1 adipocytes that have been matured 30 mM glucose vs. 5 mM glucose (Figure 5.3, 5.4 and 5.6) and in the adipose tissue of *ob/ob* and *db/db* mice (32). We were interested in determining if and how succinated proteins were being degraded in the adipocyte as we had previously shown that rats excreted 2SC in their urine (31), indicating turnover occurred *in vivo*. We observed that adipocytes matured in high glucose for 4 days that were then switched to normal glucose for the remaining 4 days of maturation had levels of succination similar to cells that had matured in normal glucose for 8 days, indicating that accumulated succinated proteins can be degraded intracelluarly (Figure 5.3A). We used the proteasomal inhibitor, MG132, and the lysosomal inhibitor, chloroquine, to determine which intracellular protein degradation pathway was responsible for the turnover of 2SC. In the presence of MG132, succinated proteins did not accumulate (Figure 5.4A) suggesting the proteasome was not involved. In contrast, when the adipocytes were switched to normal glucose in the presence of chloroquine, turnover of succinated proteins was prevented (Figure 5.2B), indicating that the lysosome was responsible for the degradation of succinated proteins. This conflicted with our original hypothesis, as we predicted the proteasome would be responsible for degrading succinated proteins considering that we had primarily identified succinated cytosolic and ER proteins (34). However, this data is interesting considering that autophagy is responsible for removal of damaged organelles such as mitochondria (mitophagy). It will be important in future studies to look at the turnover of specific organelle containing fractions by the lysosome.

The analysis of the 2SC content in the cell lysates and culture medium by GC/MS (Figure 5.6A-D) indicated that levels of succinated proteins in adipocytes matured in 30 mM glucose were always significantly increased compared to 5 mM glucose. We were able to detect 2SC in the culture medium at all time points from days 2-8 indicating the turnover of some fraction of succinated proteins appears to be a continuous process in adipocytes matured in both 30 mM and 5 mM glucose. We also demonstrated that 2SC is released from the adipocyte both as a free amino acid and as part of a peptide, as indicated by the differences in the levels of 2SC that were detected when the samples were prepared -/+ hydrolysis to release the 2SC (Figure 5.7).

When adipocytes are matured in high glucose and then switched to normal glucose, the levels of succinated proteins are significantly reduced compared to adipocytes that matured in high glucose for 8 days (Figure 5.6A). Analysis of the 2SC content in the culture medium of these adipocytes from days 4-6 and days 6-8 did not show an increase in the levels of 2SC released from the cell, which was unexpected as the intracellular levels of 2SC had been reduced close to normal levels. During the workup process of the cell lysate, the proteins are precipitated with 10% TCA and free amino acids and peptides remain the supernatant and this was not analyzed for the cell lysates. It is possible that the 'missing' 2SC had been degraded into peptides and amino acids, but had not yet been released into the medium by the cell and therefore was not detected.

In adipocytes that had been treated with chloroquine, the degradation of 2SC was prevented as indicated by the sustained levels of 2SC even when the high glucose

stimulus is removed (Figure 5.4B & 5.6A). The analysis of the culture medium on days 4-6 did not show a significant increase in the amount of 2SC compared to 5 mM glucose, indicating that the degradation of 2SC modified proteins had been prevented. However, the culture medium from days 6-8 indicated a significant increase in the levels of 2SC (Figure 5.6D) which was not expected when the lysosome is inhibited. We suspect that prolonged inhibition of the lysosome may alternatively up-regulate proteasomal activity, thereby degrading proteins that may not normally be degraded by that pathway and contributing to the detected increase in 2SC (72).

It is worth noting that although adipocytes matured in 5 mM glucose could produce more 2SC had they of been matured in 30 mM glucose (Figure 5.6A), there is still degradation of the basal levels of 2SC present in the adipocytes (Figure 5.6B-D), demonstrating that autophagy is constantly occurring in the adipocyte. We have preliminary data suggesting that autophagy is impaired in adipocytes matured in 30 mM glucose which may explain adipocyte dysfunction when in high glucose. Mitophagy has been shown to be an important process involved in the differentiation of 3T3-L1 fibroblasts into 3T3-L1 adipocytes as *atg5*$^{-/-}$ *and atg7*$^{-/-}$deficient MEFs have reduced adipogenesis efficiency as noted by defective lipid droplet formation and compromised TG synthesis (73). However, as our adipocytes proceed through differentiation normally in both 5 mM and 30 mM glucose (as indicated by the PPARγ and adiponectin production (Figure 2.3A)) autophagy is unlikely impaired at this stage. Interestingly, in 3T3-L1 adipocytes matured in high glucose, autophagy was suppressed and mRNA levels of pro-inflammatory cytokines were elevated (74) as were the levels of secreted

cytokines (Figure 2.4), suggesting that impaired autophagy is associated with adipocyte dysfunction.

In conclusion, we have shown that 2SC modified proteins are degraded through autophagy in the adipocyte. This is in contrast to our original hypothesis that the proteasome would be involved. We are currently studying the degradation of 2SC in different cellular compartments to examine if the location of succinated proteins within the cell determines the degradation pathway. In addition, we are interested in determining whether or not adipocytes matured in high glucose are undergoing autophagy at a different rate to adipocytes matured in 5 mM glucose. Therefore future studies will examine autophagic flux within the cell to determine the kinetics of succinated protein turnover.

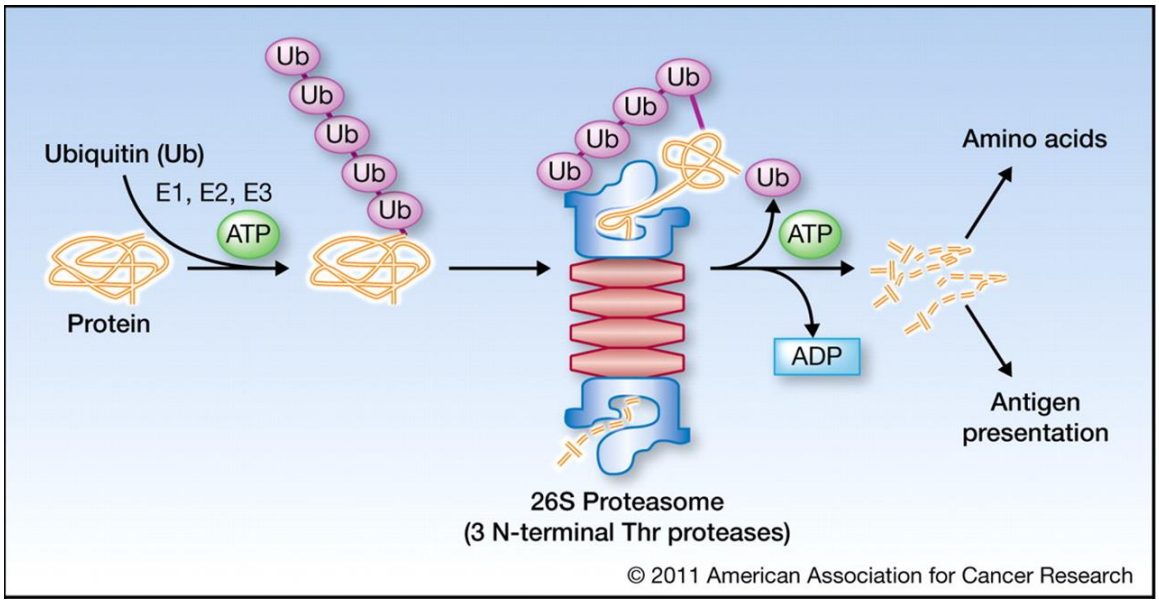

Figure 5.1. Schematic of protein degradation by the ubiquitin proteasome system. Misfolded or aggregated proteins are ubiquitinated in an ATP-dependent manner. The ubiquitinated protein is recognized by the proteasome which then degrades that protein into its constituent parts and recycles the ubuiquitin molecules for marking other proteins for degradation (65).

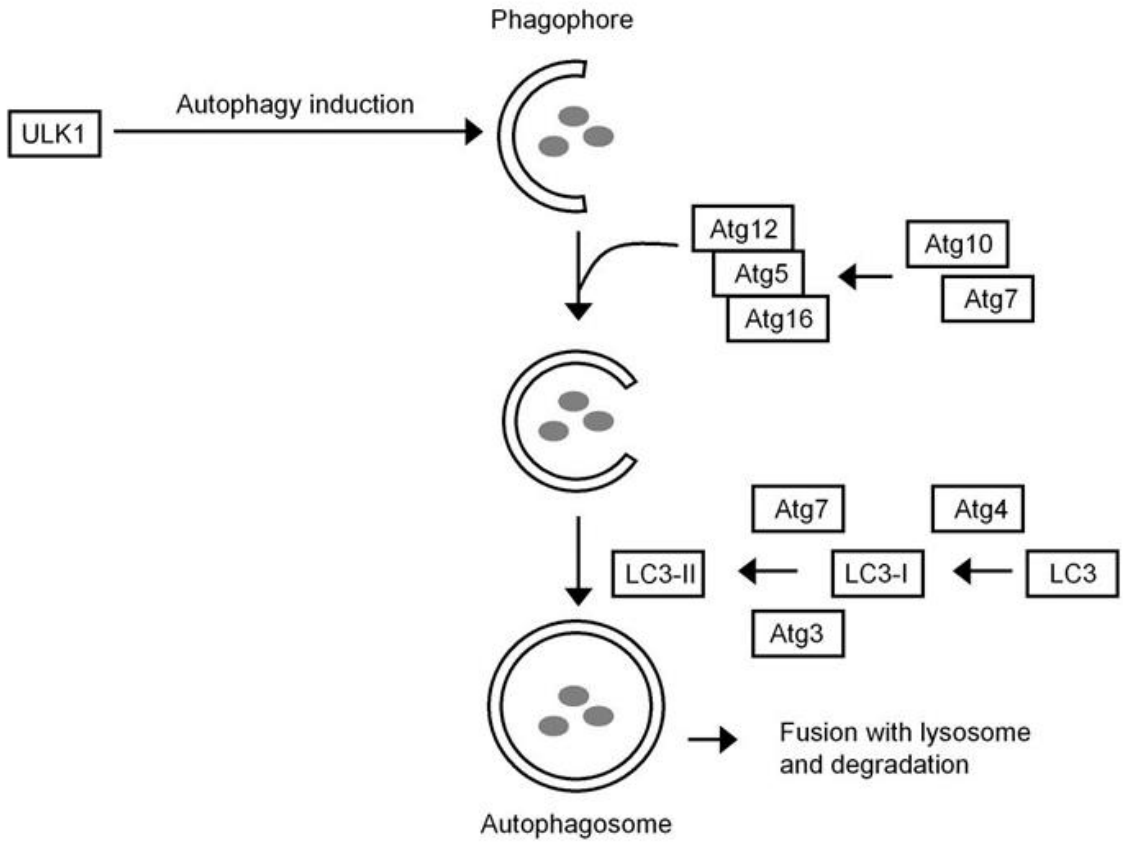

Figure 5.2 Induction of autophagy and lysosomal degradation. Schematic of autophagic degradation from phagophore formation to autophagolysosome formation. Atgs assist in the formation of the autophagic vesicle and Atg3 and Atg7 mediate lipidation of LC3-I, forming LC3-II which is incorporated in the autophagosomal membrane (66).

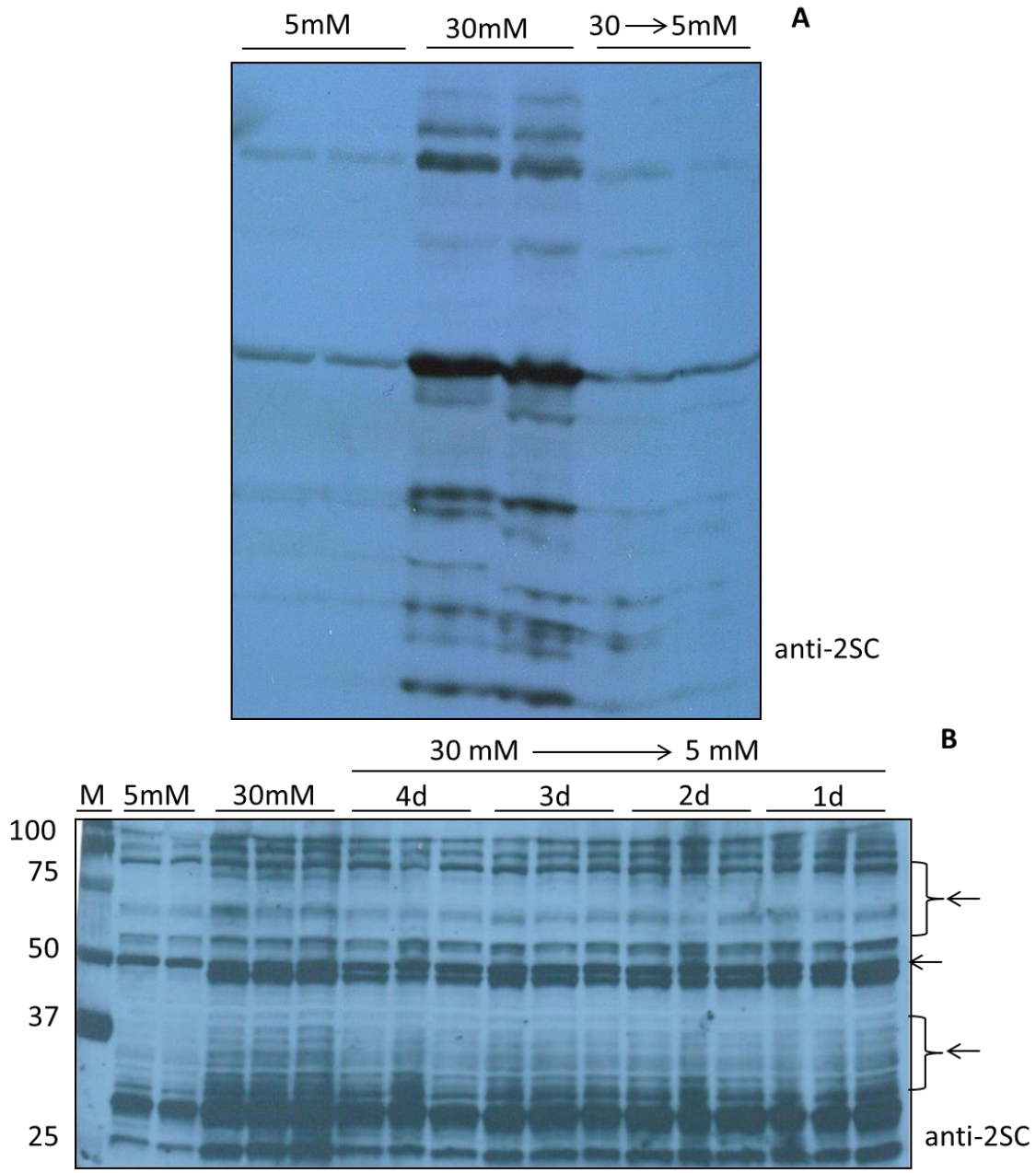

Figure 5.3. Time course of the turnover of succinated proteins. (A) Adipocytes were matured in 5 mM or 30 mM glucose for 8 days. A subset of adipocytes was matured in 30 mM glucose for 4 days then switched to 5 mM glucose for the remaining 4 days. Protein (40 µg) was separated by 1-D PAGE and succinated proteins were detected using a polyclonal anti-2SC antibody (B) Adipocytes were matured in 5 mM or 30 mM glucose for 8 days. A subset of adipocytes were switched from 30 mM glucose and replaced with 5 mM glucose for 4, 3, 2, or 1 remaining days of maturation (30→5). Protein (30 µg) was separated by 1-D PAGE and 2SC was detected using a polyclonal anti-2SC antibody to detect the presence of succinated proteins. Molecular weight (MW) markers (kDa) are shown as a reference for the range in MW of succinated proteins.

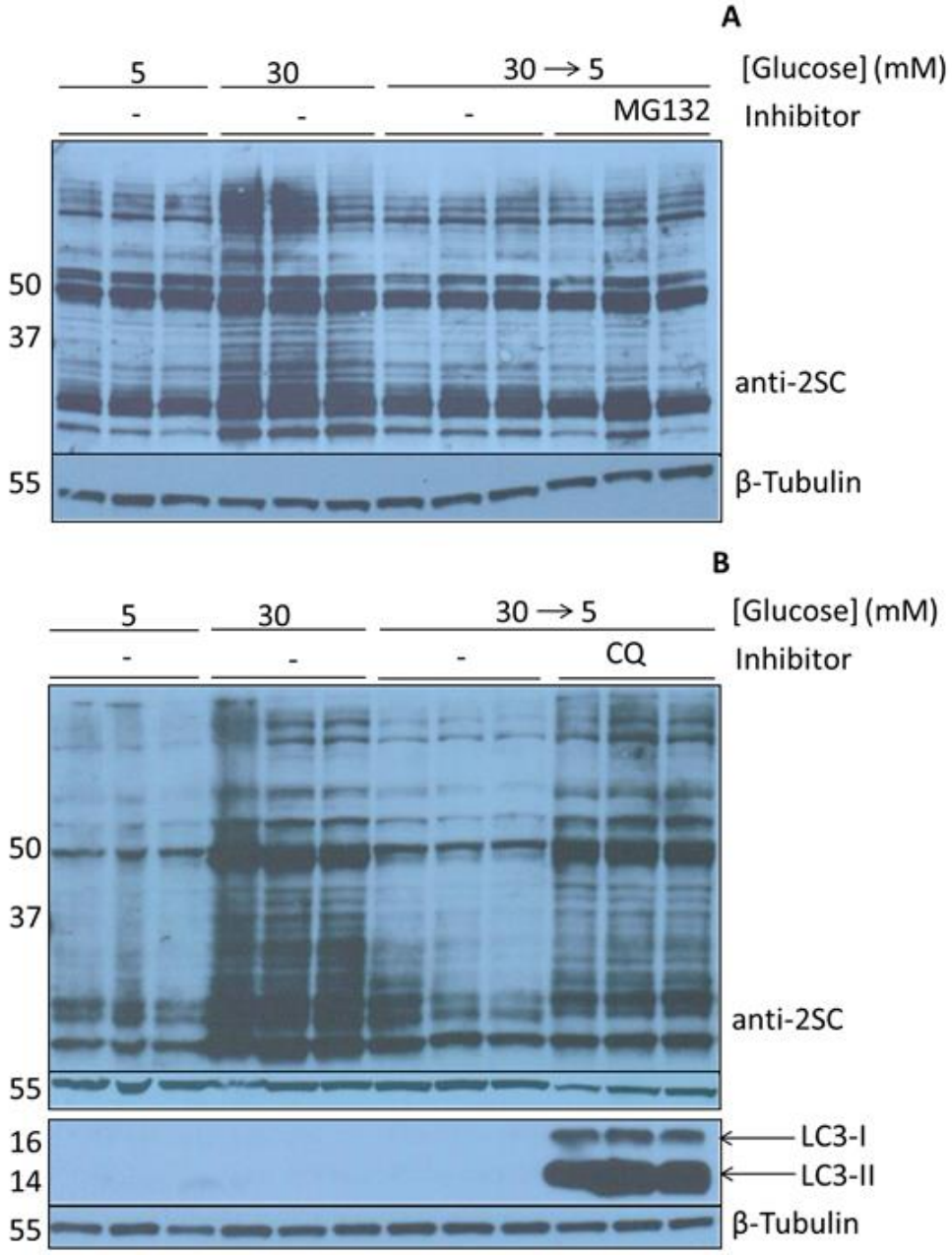

Figure 5.4. **Turnover of succinated proteins**. Adipocytes were matured in 5 mM or 30 mM glucose for 8 days. A subset of adipocytes were matured in 30 mM glucose for 4 days and then switched to 5 mM glucose for the remaining 4 days of maturation (30→5). They were then treated with or without (A) 17.5 µM MG132 or (B) 25 µM chloroquine. Protein (A) 30 µg and (B) 40 µg was separated by 1-D PAGE and detection of 2SC was performed using a polyclonal anti-2SC antibody. Western blotting for LC3 was assessed to confirm inhibition of lysosomal degradation. MW markers are shown in kDa and β-Tubulin is shown to demonstrate equal protein loading.

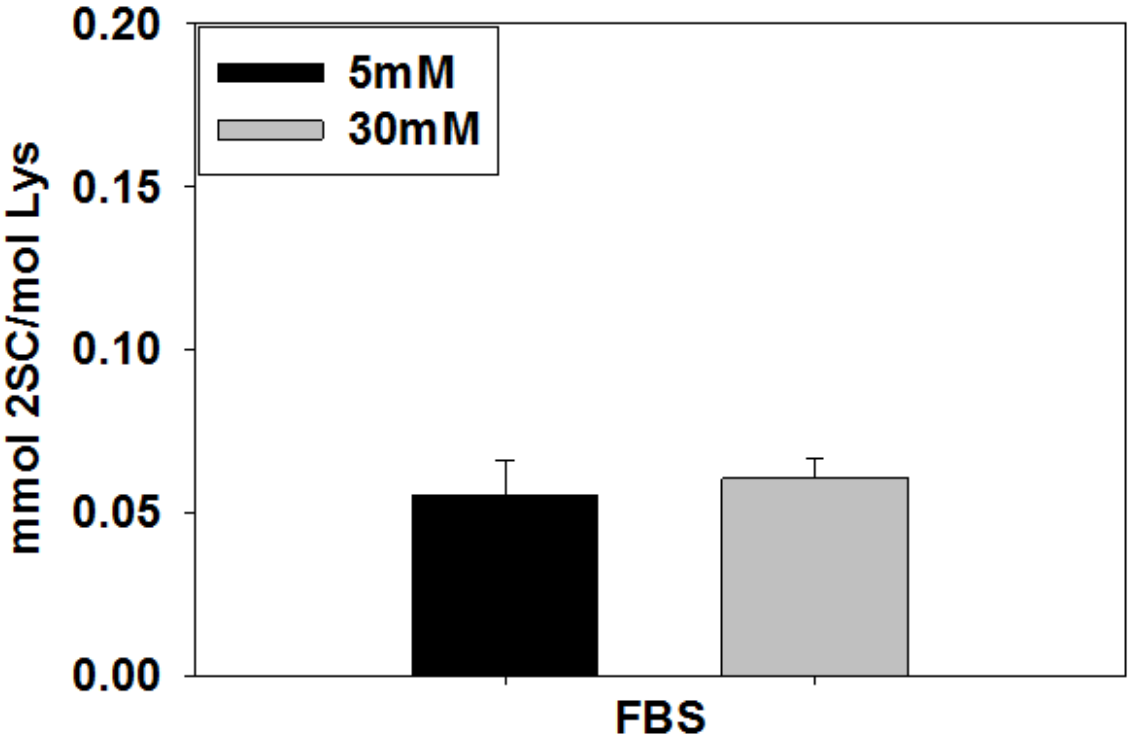

Figure 5.5. Modification of serum proteins by succination. 3T3-L1 adipocytes were matured in 5 mM or 30 mM glucose. The maturation medium was collected from the adipocytes on maturation days 4-6 and serum protein was TCA precipitated and analyzed by GC/MS for 2SC and lysine content. The 2SC content was normalized to the lysine content of the sample. Data are representative of n=4-5 measurements expressed as means ± S.D. Data were tested for statistical significance using an unpaired Student *t* test.

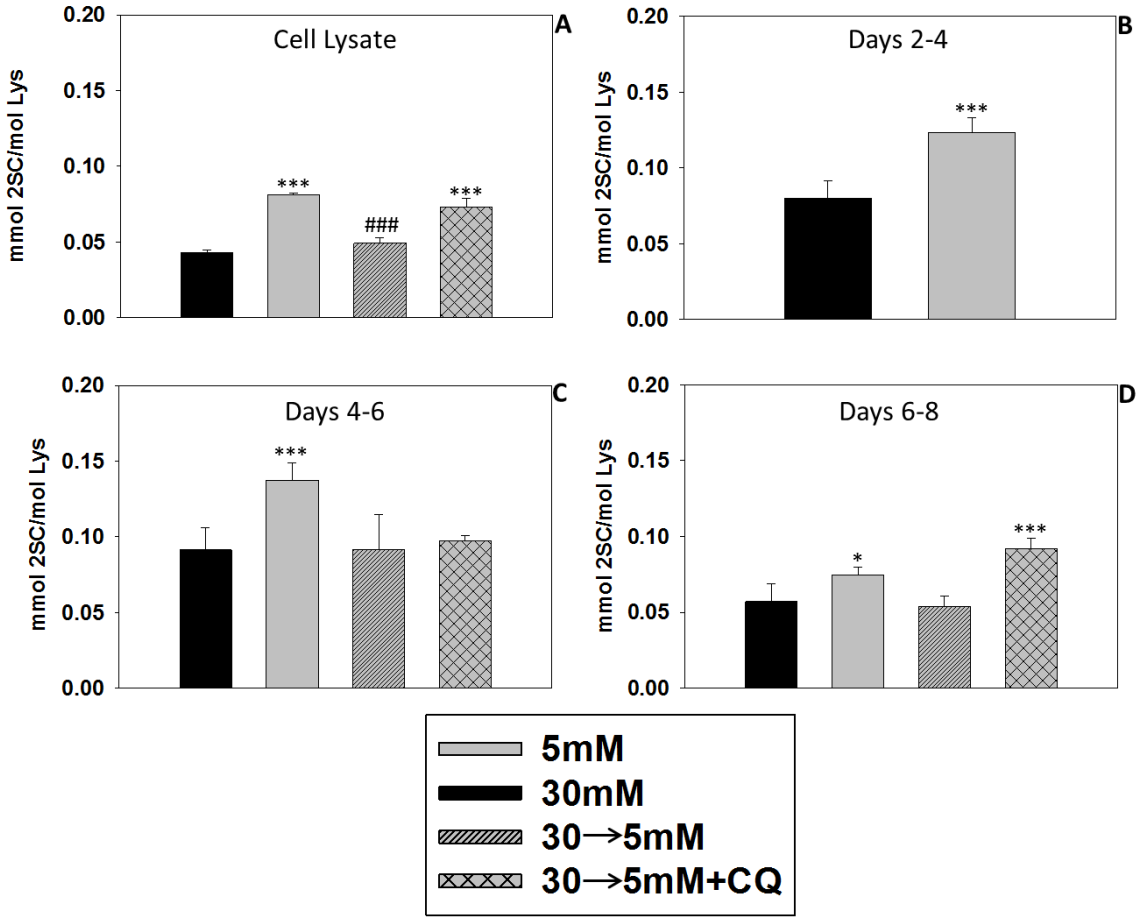

Figure 5.6. GC/MS analysis of 2SC content in adipocyte cell lysate and culture medium. Adipocytes were matured in 5 mM or 30 mM glucose for 8 days. A subset of adipocytes was matured in 30 mM glucose for 4 days and then switched to 5 mM glucose for the remaining 4 days (30→5) and treated with or without chloroquine (CQ). (A) On day 8, the cells were harvested and the levels of intracellular succinated proteins was determined in the cell lysate by GC/MS. Medium was collected from days (B) 2-4, (C) 4-6 and (D) 6- 8 of maturation and analyzed by GC/MS for 2SC content. Data are representative of n=5 measurements expressed as means ± S.D. Statistical significance was determined using a One Way ANOVA and Tukey's post hoc test (*P<0.05 **P<0.01 and ***P<0.001 for 30 mM glucose or 30 to 5mM ±CQ vs. 5 mM glucose and $^{###}$P<0.001 for 30 mM vs. 30 to 5 mM. Gray bars (5 mM), black bars (30 mM), striped bars (30 mM to 5 mM), and checkered bars (30 mM to 5 mM + CQ)).

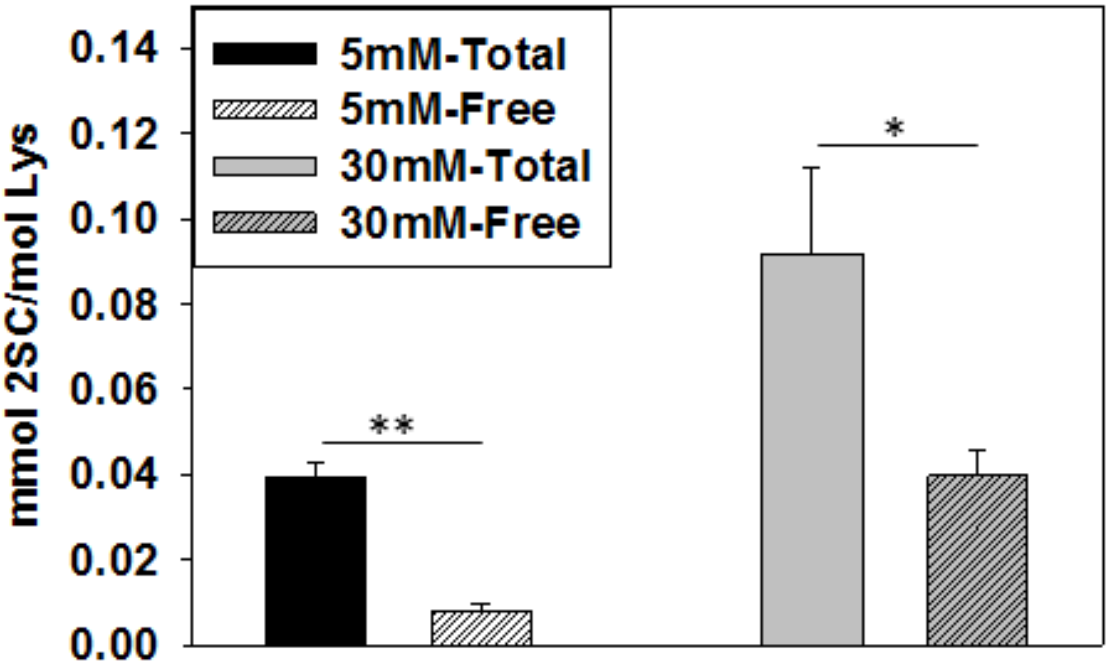

Figure 5.7: **Release of 2SC as an amino acid or in a peptide.** 3T3-L1 adipocytes were matured in 5 mM or 30 mM glucose. The medium from days 4-6 of maturation was analyzed for total and free 2SC content by GC/MS. Data are representative of n=3 measurements expressed as means ± S.D. Asterisks indicate statistical significance as determined by a paired Student *t* test (*P<0.05 and ***P<0.001. Black bars (total 2SC in 5 mM glucose), light gray striped (free 2SC in 5 mM glucose), gray bars (total 2SC in 30 mM glucose), and gray striped bars (free 2SC in 30 mM glucose)).

Chapter VI

Future Directions

We are interested in continuing our investigation into the role of ER stress in the development of T2DM and plan to examine human adipose tissue and determine if protein succination is increased in T2DM subjects. We are also interested in alternative chemical agents/uncouplers that may reduce protein succination as they may be therapeutically beneficial in treating T2DM.

Our results on the turnover of succinated proteins by autophagy were unexpected and intriguing. Consequently, we are interested in the role of autophagy in adipocyte pathology during T2DM. Our preliminary data suggests that autophagy may be dysfunctional in adipocytes matured in high glucose and interestingly, if the adipocytes are switched to normal glucose there is restoration of autophagic function. We have identified cathepsin B as a protein that is succinated at its active site, Cys-108 (34), so it will be of interest to determine if the activity of Cathepsin B is reduced and whether or not this affects lysosomal function in the adipocyte. We are also interested in another autophagy protein, Atg7, as the active site also contains a cysteine residue (75), and this may as also affect the rate of autophagy if succinated. Atg7 is one of the proteins that lipidates LC3-I, committing the autophagosome to fuse with the lysosome.

Lastly, as we have identified 2SC as a novel protein modification that is increased

in diabetes, were are interested in continuing to investigate the biochemical mechanism by which this leads to adipocyte dysfunction. We have identified over 40 succinated proteins (34) and we still have to examine the significance of many of these identified sites and to determine if and how the function of these 2SC modified proteins is affected in T2DM.

Chapter VII

Methods

Materials. Unless otherwise noted, all chemicals were purchased from Sigma Aldrich (St. Louis, MO). Preparation of 2SC antibody was prepared by Eurogentec (Fremont, CA) Sodium phenylbutyrate (PBA) was from Enzo Life Sciences (Farmingdale, NY) for *in vitro* studies and Scandinavian Formulas Inc. (Sellersville, PA) for *in vivo* studies. Polyvinylidene fluoride (PVDF) was purchased from GE Healthcare (Farifield, CT). L-glycine, sodium dodecyl sulfate (SDS), sodium salicylate (SA), and Tween-20 were purchased from Fisher Scientific (Waltham, MA). For *in vitro* studies insulin was purchased from Bio Ab Chem (Ladson, SC). For *in* vivo studies insulin was purchased from Sigma Aldrich (St. Louis, MO). For *in vitro* studies glucose oxidase was from Invitrogen (Grand Island, NY) and for *in* vivo studies glucose oxidase was from Raichem (San Marcos, CA). Criterion™TGX™ Precast Gels were from Bio-Rad (Hercules, CA). The CyQuant® assay was from Invitrogen (Grand Island, NY). All materials for the Seahorse XF24 were purchased from Seahorse Bioscience (North Billerica, MA) except pyruvate, glucose, insulin, and mitochondrial inhibitors.

Animal Models. Male C57BL/6 mice were purchased from Jackson Laboratories (Bar Harbor, ME). Mice were obtained at 5-6 weeks of age and allowed to acclimate 1-2 weeks with unrestricted access to food and water before experimental manipulations began.

PBA was administered in the drinking water at a dosage of 1 mg/g BW/day for the first 3 weeks and was reduced to 0.5 mg/g BW/day for the remaining 4 weeks of the study. Animals were sacrificed at 15 weeks of age. Blood glucose measurements were performed weekly after an overnight fast by collecting tail vain blood using a Bayer (Whippanny, NJ) Countour® blood glucose meter for control animals and the glucose oxidase assay for *db/db* mice.

Water and food consumption was measured biweekly. All animal handling and experiments were conducted according to the guidelines of the University of South Carolina Institutional Animal Care and Use Committee. Animals were sacrificed using CO_2 asphyxiation and epididymal adipose tissue was removed and rinsed in PBS with protease inhibitors and frozen on dry ice. Livers were removed and immediately frozen on dry ice.

Body Composition. Body composition was measured at 14 weeks using a Dual Energy X-ray Absorptiometry scan under isoflurane anesthesia, measuring fat and lean content.

Insulin Tolerance Test. Insulin tolerance tests were performed at 14 weeks of age on all mice. The mice were fasted starting the morning of the test for 4.5 hours. Insulin was injected intraperitoneally, 2 U. Blood was collected by tail vein at time 0, 15, 30, 60, 90, and 120 minutes after injection of insulin. Blood glucose was measured in control animals using a Bayer (Whippanny, NJ) Countour® blood glucose meter. In *db/db* mice, the glucose oxidase assay was used to measure serum blood glucose levels.

Protein Extraction from Adipose Tissue. Adipose tissue was added to 2.5 mL ice-cold radio immunoprecipitation assay buffer (RIPA) buffer and sonicated 3 times for 12-15

seconds each. The tissue sat on ice for 30 minutes and was then centrifuged at 2800 g for 10 minutes at 4 ^{o}C. A pellet, infranatant and supernatant were then visible. The infranatant, up to 1.5 mL was then collected using a needle and syringe. Acetone, 9X volume, was then added to the samples, vortexed, then let sit on ice for 10 min. The samples were then centrifuged at 2800 g for 10 minutes at 4^{o}C. The acetone was decanted and the samples let air dry for 10 min on ice. The samples were then resuspended in 0.5 – 1 mL of radio RIPA buffer and sonicated 3 times for 10 seconds each. The samples were then centrifuged at 15000 rpm for 10 min at 4 ^{o}C yielding an infranatant and a fat layer. The infranatant was collected and the protein concentration was determined using the Lowry assay.

Protein Extraction from Liver Tissue. Liver tissue was added to 2 mL ice-cold RIPA buffer and sonicated 2 times for 10-15 seconds each and was then centrifuged at 2800 g for 10 minutes at 4 ^{o}C. A pellet, infranatant and supernatant were then visible. The infranatant, up to 1.5 mL was then collected using a needle and syringe. Acetone, 9X volume, was then added to the samples, vortexed then let sit on ice for 10 min. The samples were then centrifuged at 2800 g for 10 minutes at 4^{o}C. The acetone was decanted and the samples let air dry for 10 min on ice. The samples were then resuspended in 1 mL of RIPA buffer and sonicated 3 times for 10 seconds each. The samples were then centrifuged at 15000 rpm for 10 min at 4 ^{o}C yielding an infranatant and a fat layer. The infranatant was collected and the protein concentration was determined using the Lowry assay.

Triglyceride Extraction from Liver Tissue. Liver tissue was added to ice-cold PBS with

protease inhibitors and sonicated 3 times for 10 seconds each. 300 µL of sample was then extracted using 8:4 chloroform:methanol. The samples were vortexed, then let sit on ice for 10 min followed by centrifugation at 2000 g for 10 min at 4 ^{o}C. Three layers formed with the protein interface dividing the infranatant and supernatant. The infranatant was collected and was dried under air. The samples were resuspended in 5% BSA and triglyceride concentration was determined using Infinity^{TM} Triglycerides assay kit (Thermo Fisher Scientific, Waltham, MA), according to the manufacturer's instructions.

Cell Culture. 3T3-L1 murine fibroblast were purchased from American Type Culture Collection (Manassas, VA) and maintained up to 8 passages in DMEM containing 5 mM glucose, 10% Bovine Calf Serum (Thermo Scientific), 1% penicillin/streptomycin (CellGro) at 37^{o}C with 5% CO_2 and 95% humidity. Medium was changed every 2 days. At 70-80% confluence cells were trypsinized (Thermo Scientific), neutralized with excess medium and collected by centrifugation at 1000 g for 5 min at 25^{o}C. The cells were then resuspended in medium for a new passage.

3T3-L1 fibroblasts were seeded at densities of 10,000, 50,000, and 100,000 cells/well for 24-well, 6-well plates and 10 cm^2 petri dishes respectively. 3T3-L1 fibroblasts were induced to differentiate when the fibroblast reached 24 hours post-confluence (~3-4 days) in DMEM with 10% Fetal Bovine Serum (Atlanta Biologicals), 1% penicillin/streptomycin, insulin (10 µg/mL), dexamethasone (0.3 µM), 3-isobutyl-1-methylxanthine (0.5 mM) and 30 mM glucose for 3 days. At day 0, differentiation medium was removed, cells were washed with PBS and maturation medium containing

5 mM/0.3 nM or 30 mM/3 nM glucose/insulin was applied. The medium was changed every 2 days and the adipocytes were matured for up to 8 days. Cells cultured in 5 mM glucose were supplemented with 5mM glucose daily and several hours prior to protein harvest to maintain glucose levels.

Measurement of triglycerides, glucose, and inflammatory markers in 3T3-L1 adipocytes. Triglyceride content was measured in 10 µl aliquots of cell lysates using the Infinity™ Triglycerides assay kit (Thermo Fisher Scientific, Waltham, MA), according to the manufacturer's instructions. Glucose concentration was measured in phenol red free medium using the Amplex® Red Glucose/Glucose Oxidase Assay kit (Invitrogen, Grand Island, NY). The media on 3T3-L1 adipocytes was replaced with serum-free DMEM for 18 hrs. Pro-inflammatory cytokines in the conditioned media were analyzed by ELISA according to the manufacturer's instructions (mouse Obesity ELISA, Signosis, Santa Clara, CA).

DNA isolation and mitochondrial content analysis. Cell lysates were collected in 500 µL PBS, centrifuged at 2000 rpm for 5 min to yield a pellet which was resuspended in 350 µL DNA lysis buffer (10 mM Tris-HCl, pH7 7.5, 400 mM NaCl, 2.5 mM EDTA , and 0.1% SDS), 50 µL of 50 mg/mL proteinase K and heated at 55°C overnight. The tubes were inverted to dissolve any remaining solid then extracted in a 1:1 ratio of lysis buffer:saturated phenol, pH 7.9. The samples were then centrifuged at 15000 rpm for 5 min, the supernatant was collected and extracted in a 1:1 ratio, supernatant:phenol/chloroform/isoamyl alcohol (25:24:1), pH 7.9 then centrifuged at 15000 rpm for 5 min. The supernatant was collected and the DNA was precipitated with

350 µL 100% ethanol and 35 µL of 3 M sodium acetate, pH 5.2, and collected by centrifugation at 15000 rpm for 2 min. The DNA pellet was washed with 70% ethanol, dried, then resuspended in 100 µL water. The samples were stored at -20°C until PCR.

Quantitative real-time PCR analysis was carried out in 25 µl reactions consisting of 2x SYBR green PCR buffer (AmpliTaq Gold DNA Polymerase, Buffer, dNTP mix, $MgCl_2$) (Applied Biosystems, Foster City, CA, USA), 0.150 µg DNA, DI water, and 60 nM of each primer. PCR was run with the DNA sample with Cytochrome B Forward, 5' - ATT CCT TCA TGT CGG ACG AG −3'; Cytochrome B Reverse, 5' - ACT GAG AAG CCC CCT CAA AT - 3', GAPDH Forward, 5' - TTG GGT TGT ACA TCC AAG CA - 3'; GAPDH Reverse, 5' - CAA GAA ACA GGG GAG CTG AG - 3'. Samples were analyzed on an ABI 7300 Sequence Detection System. Reactions were incubated for 2 minutes at 50°C and 10 minutes at 95°C, followed by 40 cycles consisting of a 15 sec denaturing step at 95°C and 1 min annealing/extending step at 60°C. Data were analyzed by ABI software (Applied Biosystems, Foster City, CA, USA) using the cycle threshold (C_T), which is the cycle number at which the fluorescence emission is midway between detection and saturation of the reaction. The $2^{-\Delta CT}$ method was used to determine changes in gene expression between Cytochrome B with GAPDH C_T as the correction factor.

Protein Extraction from Cells. All samples and reagents were kept on ice during protein harvest. The cells were washed 3 times with phosphate buffered saline (PBS). The cells were collected in RIPA buffer and pulse sonicated at 2 watts for 3 intervals of 3 seconds. Acetone was then added in 9 times the volume, the samples were vortexed then let precipitate on ice for 10 minutes. The protein was collected by centrifugation at 2000 g

for 10 minutes at 4^{o}C yielding a white to pale yellow protein pellet. The supernatant was decanted and the pellet let air dry for 10 minutes on ice. The protein was resuspended in RIPA buffer and pulse sonicated for 3 intervals of 3 seconds. The samples were stored at -70^{o}C until further analysis.

Western Immunoblotting. Samples were prepared using 25-40 μg for cell lysates and 40-100 μg for mice tissue with the addition of 5-7 μL 4X Laemmli loading buffer. The samples were then boiled at 95^{o}C, flash centrifuged then loaded on 7.5%, 12% or 18% gels and electrophoresed at 200 V for 60 min. The protein was transferred to a PVDF membrane in transfer buffer at 250 mA for 100 min or 40 mA at 4 ^{o}C. The membrane was ponceau stained then blocked in 5% non-fat milk or 5% bovine serum albumin (BSA) according to the manufacturer's instructions. Membranes were probed using primary polyclonal anti-2SC. Antibodies for ACC, p-ACC, calreticulin, cleaved caspase-3, eIF2α, p-eIF2α, Ero1-Lα, FAS, fumarase, LC3, and succinate dehydrogenase were from Cell Signaling. Adiponectin was from R&D Systems. CHOP was from Thermo Scientific. NDUSF4 was from AbCam. β-tubulin, Grp78 and PDI were from Santa Cruz. Pierce® ECL 2 Western Blotting Substrate or Amersham™ ECL™ Prime Western Blotting Detection Reagent (GE Healthcare) was used and followed by detection of chemiluminescence using photographic film (Denville Scientific, Metuchen, NJ). Image J software (NIH) was used to quantify band intensity by densitometry.

GC/MS Analysis of 2SC. 3T3-L1 adipocytes were matured as described in cell culture. The cell culture medium from adipocytes was collected on days 4, 6 and 8 of maturation and frozen at -70°C until further analysis. Adipocytes were harvested for protein after 8

days of maturation as described in protein harvest. DMEM and culture medium were extracted in an 8:4:3 chloroform/methanol/water ratio. The samples were vortexed and let precipitate on ice for 10 min followed by centrifugation at 2000 g for 10 min at 4^{o}C. Three layers formed, with the protein interface (albumin) separating the organic (bottom) and water/methanol (top) layer. The water/methanol layer was collected and the contents were dried overnight on a speedvac. The samples were resuspended in 600 µL water and sonicated, extraction was re-performed and the samples were dried overnight.

Cell lysates were extracted in a 1:1 ratio with 20% (w/v) trichloroacetic acid, vortexed, let precipitate on ice for 10 min then centrifuged at 2500 g for 5 min at 4^{o}C yielding a pellet and supernatant. The pellet was resuspended in 500 µL 10% (w/v) TCA and let precipitate on ice for 10 min then centrifuged at 2500 g for 5 min at 4^{o}C yielding a protein pellet.

To each sample 75 nmol D8-Lys, 0.375 nmol heavy labeled-2SC and 1 mL 12 N HCl was added, followed by overnight hydrolysis at 110^{o}C. The samples were then dried overnight on the speedvac. The samples were resuspended in 1 mL of 1% trifluoroacetic acid (TFA), sonicated, and passed over a C-18 SepPak column pre-wet with 2 mL methanol and 2 mL 1% TFA. The analyte was eluted with 20% methanol/1% TFA and dried overnight on the speedvac. To each sample was then added methanolic HCl, followed by vortexing, heating for 45 min at 65°C then dried under air. Trifluroacetic acid anhydride was then added, 1 mL, to each sample, and let sit for 1 hr at room temperature, then dried under air for ~15 min. Dichloromethane, 200 µL, was then

added to the samples before being centrifuged at 10,000 g for 5 min at 25^{o}C. The samples were then concentrated under air.

Samples were analyzed by multiple reaction monitoring GC-MS/MS on a TSQ 7000 (Thermo-Finnigan, Waltham, MA). The injection port was maintained at 200 °C, and the temperature program was 90 °C hold for 2 min, 10 °C/min from 90 to 140 °C, 3 °C/min to 220 °C, 15 °C/min to 300 °C, then hold at 300 °C for 5 min. The parent and daughter ion pairs monitored were: lysine m /z 180 > 69, d8 -lysine, m /z 188 > 69; 2SC, m /z 284 > 242, U-13 C3 ,15 N-2SC m /z 288 > 246. Quantification of analytes in protein samples was performed by isotope dilution mass spectrometry based on standard curves constructed from mixtures of known amounts of heavy labeled and natural abundance standard. The amounts of all analytes were normalized to the lysine content of the sample.

Seahorse Extracellular Flux Analyzer 24. 3T3-L1 murine fibroblast were seeded 10,000 cells/well in a 100 µL volume on XF24 V7 microculture plates coated with 0.2% gelatin (Sigma, porcine skin, Type A, Batch # 014K0077). The next day, 150 µL of medium was added to the cells. Fibroblasts grew for 3 days followed by differentiation and 2 days of maturation.

The night before the assay, an XF calibrant cartridge was hydrated overnight in XF calibrant, pH 7.4 at 37^{o}C with 0% CO_2. The day of the assay, the medium was removed, the adipocytes were washed with 1 mL of XF Assay Buffer, pH 7.4, followed by application of 600 µL XF Assay medium, pH 7.4, supplemented with 1% penicillin/streptomycin, 1 mM sodium pyruvate, 5 mM/0.3 nM or 30 mM/3 nM

glucose/insulin, and incubation for 60-90 min at 37^{o}C with 0% CO_2. Injections were added in a 1:9 volume in the following order: blank, oligomycin (5 µg/mL), carbonyl cyanide 4-(trifluoromethoxy)phenylhydrazone (FCCP) (1.25 µM), rotenone/antimycin A (3 µM/4 µM). Assay conditions involved a mixing (3 min), a wait (2 min), and a measure (3 min) after addition of the blank, oligomycin and rotenone/antimycin A (3 µM/4 µM) and PBA. For FCCP, the conditions were a mixing (2 min) followed by a measurement (2 min). For SA, the conditions were mixing (4 min), wait (2 min), followed by a measurement (2 min).

Following the assay the cells were washed with PBS and stored at -70^{o}C. The DNA content was quantified using the CyQuant® assay according to the manufacture's protocol.

Data Analysis. All graphs were generated in Sigmaplot 11. Statistical analyses of the data were performed on SigmaStat software (Sigmaplot 11, San Jose, CA). All data were plotted as means ± SD. An unpaired Student *t* test was used to test for statistical differences between two sets of data, except in Figure 5.7 where an unpaired *t* test was used. A One Way ANOVA using Tukey's post hoc test was used when comparing 3 or more sets of data. A Kruskal-Wallis One Way Analysis of Variance on Ranks was used for data not normally distributed. FBG and serum TGs were tested for statistical differences using a Two Way Repeated Measures ANOVA (One Factor Repetition). Differences were considered statistically significant at $^{*}p<0.05$, $^{**}p<0.01$ and $^{***}p<0.001$.

References

1 Centers for Disease Control and Prevention. National diabetes fact sheet: national estimates and general information on diabetes and prediabetes in the United States, 2013. Atlanta, GA: U.S. Department of Health and Human Services, Centers for Disease Control and Prevention, 2013.

2 http://diabetes.niddk.nih.gov/dm/pubs/statistics/

3 Tolman K, Fonseca V, Dalpiaz A, Tan M. Spectrum of liver disease in type 2 diabetes and management of patients with diabetes and liver disease. *Diabetes Care* 2007; 30(3):734-743

4 http://www.diabetes.org/diabetes-basics/diagnosis/?loc=db-slabnav

5 Lin Y and Sun Z. Current views on type 2 diabetes. *J Endocrinol* 2010; 204:1-11

6 www.diabetes.org

7 Guo S. Insulin signaling, resistance, and metabolic syndrome: insights from mouse models into disease mechanisms. *J Endocrinol* 2014; 220(2):T1-T23.

8 Cao, Haiming. Adipoctyokines in obesity and metabolic disease. *J Endocrinol* 2014; 220:T47-T59.

9 Saini, V. Molecular mechanisms of insulin resistance in type 2 diabetes. *World J of Diabetes* 2010; 168-75.

10 Weston C, Davis R. The JNK signal transduction pathway. *Curr Opin Cell Biol* 2007; 19:142-149.

11 http://diabetes.niddk.nih.gov/dm/pubs/riskfortype2/

12 Fullerton M, Galic S, Marcinko K, Sikkema S, Pulinilkunnil T, Chen Z, O'Neill H, Ford R, Palanivel R, O'Brien M, Hardie G, Macaulay S, Schertzer J, Dyck J, Denderen B, Kemp B, Steinberg G. Single phosphorylation sites in Acc1 and Acc2 regulate lipid homeostasis and the insulin-sensitizing effects of metformin. *Nat Med* 2013; 19(12):1649-1654.

13 Hauner, H. Diabetes/Metabolism research and reviews. *Diabetes Metab Res Rev* 2002; 18:S10-S15.

14 Thulé P, Umpierrez G. Sulfonylureas: a new look at old therapy. *Curr Diabetes Rep* 2014; 14:473.

15 http://www.cdc.gov/diabetes/pubs/estimates11.htm#footnotes

16 Brownlee M. The pathobiology of diabetic complications. *Diabetes* 2005; 54:1615-1625.

17 Rosen D, Spiegelman B. What we talk about when we talk about fat. *Cell* 2014; 156:20-44.

18 Haase J, Weyer U, Immig K, Klöting N, Blüher M, Eilers J, Bechmann I, Gericke M. Local Proliferation of macrophages in adipose tissue during obesity-induced inflammation. *Diabetologia* 2013; 57(3):562-571.

19 Amano S, Cohen J, Vangala P, Tencerova M, Nicoloro S, Yawe J, Shen Y, Czech M, Aouadi M. Local proliferation of macrophages contributes to obesity-associated adipose tissue inflammation. *Cell Metabolism* 2014; 19:162-171.

20 Hajer G, Haeften T, Visseren F. Adipose tissue dysfunction in obesity, diabetes, and vascular diseases. *Eur Heart J* 2008; 29:2959-2971.

21 Schwenger K, Allard J. Clinical approaches to non-alcoholic fatty liver disease. *World J Gastroenterol* 2014; 20(7):1712-1723.

22 Han C, Umemoto T, Omer M, Hartigh L, Chiba T, LeBoeuf R, Buller C, Sweet I, Pennathur S, Abel E, Chait A. NADPH oxidase-derived reactive oxygen species increases expression of monocyte chemotactic factor genes in cultured adipocytes. *J Biol Chem* 2012; 287:10379-10393.

23 Curtis J, Hahn W, Stone M, Inda J, Droullard D, Kuzmicic P, Donoghue M, Long E, Armien A, Lavandero S, Arriaga E, Griffin T, Bernlohr D. Protein carbonylation and adipocyte mitochondria function. *J Biol Chem* 2012; 287:32967-32980.

24 Gregor M, Hotamisligil G. Adipocyte stress: the endoplasmic reticulum and metabolic disease. *J Lipid Res* 2007; 48:1905-1914.

25 Basseri S, Lhoták Š, Sharma A, Austin RC. The chemical chaperone 4-phenylbutyrate inhibits adipogenesis by modulating the unfolded protein response. *J Lipid Res* 2009; 50:2486-2501.

26 Han J, Murthy R, Wood B, Song B, Wang S, Sun B, Malhi H, Kaufman RJ. ER stress signaling through eIF2α and CHOP, but not IRE1α, attenuates adipogenesis in mice. *Diabetologi*a 2013;56:911-924.

27 Han J, Back S, Hur J, Lin Y, Gildersleeve R, Shan J,, Yuan C, Krokowski D, Wang S, Hatzoglou M, Kilberg M, Sartor M, Kaufman R. ER-stress induced transcriptional regulation increases protein synthesis leading to cell death. *Nat Cell Biol* 2013; 15:481-490.

28 http://www.human.cornell.edu/dns/qilab/research.cfm

29 Frizzell N, Rajesh M, Jepson M, Nagai R, Carson J, Thorpe S, Baynes J. Succination of thiols in adipose tissue proteins in diabetes. *J Biol Chem* 2009; 284:25772-25781.

30 Frizzell N, Thomas S, Carson J, Baynes J. Mitochondrial stress causes increased succination of proteins in adipocytes in response to glucotoxicity. *Biochem J* 2012; 446:247-254.

31 Nagai R, Brock J, Blatnik M, Baatz J, Bethard J, Walla M, Thorpe S, Baynes J, Frizzell N. Succination of protein thiols during adipocyte maturation. *J Biol Chem* 2007; 282:34219-28.

32 Thomas S, Storey K, Baynes J, Frizzell N. Tissue distribution of S-(2-Succino)cysteine (2SC), a biomarker of mitochondrial stress in obesity and diabetes. *Obesity* 2012; 20:263-269.

33 Alderson N, Wang Y, Blatnik M, Frizzell N, Walla M, Lyons T, Alt N, Carson J, Nagai R, Thorpe S, Baynes J. S-(2-succinyl)cysteine: A novel chemical modification of tissue proteins by a Krebs cycle intermediate. *Arch of Biochem Phys* 2006; 450:1-8.

34 Merkley ED, Metz TO, Smith RD, Baynes JW, Frizzell N. The succinated proteome. *Mass Spectrom Rev* 2014; 33:98-109.

35 Piroli G, Manuel A, Walla M, Jepson M, Brock J, Rajesh M, Tanis R , Cotham W, and Frizzell N. Identification of Protein Succination as a Novel Modification of Tubulin. *Biochem J* 2014; [Epub ahead of print].

36 Rosen E, MacDougald O. Adipocyte differentiation from inside out. *Mol Cell Bio*. 2006; 7:885-896.

37 Valsecchi F, Grefte S, Roestenberg P, Joosten-Wagenaars J, Smeitink J, Willems P, Koopman W. Primary fibroblasts of NDUFS4$^{-/-}$ mice display increase ROS levels and aberrant mitochondrial morphology. *Mitochondrion* 2013; 13:436-443.

38 Gagnon A, Sorisky A. The effect of glucose concentration on insulin-induced 3T3-L1 adipose cell differentiation. *Obes Res* 1998; 6:157-63.

39 Lin, Y., Berg, A.H., Iyengar, P., Lam, T.K., Giacca, A., Combs, T.P., Rajala, M.W., Du, X., Rollman, B., Li, W., Hawkins, M., Barzilai, N., Rhodes, C.J., Fantus, I.G., Brownlee, M., Scherer, P.E. The hyperglycemia-induced inflammatory response in adipocytes *J Biol Chem.* 2005; 280:4617-4626.

40 Han C, Subramanian S, Chan C, Omer M,k Chiba T, Wight T, Chait A. Adipocyte-derived serum amyloid A3 and hyluronan play a role in monocyte recruitment and adhesion. *Diabetes* 2007; 56:2260-2273.

41 http://www.seahorsebio.com

42 Oyadomari S, Mori M. Roles of CHOP/GADD153 in endoplasmic reticulum stress. *Cell Death Differ* 2004; 11:381-389.

43 Song B, Scheuner D, Ron D, Pennathur S, Kaufman R. *CHOP* deletion reduced oxidative stress, improves β cell function, and promotes cell survival in multiple mouse models of diabetes. J*. of Clin Inves*. 2008; 118:3378-3389.

44 Oyadomari S, koizumi A, takeda K, Gotoh T, Akira S, Araki E, Mori M. targeted disruption of the *CHOP* gene delays endoplasmic reticulum stress-mediated diabetes. *J Clin Invest* 2002; 109:525-532.

45 Oyadomari, S, Takeda K, Takiguchi M, Gotoh T, Matsumoto M, Wada I, Akira S, Araki E, Mori M. Nitric oxide-induced apoptosis in pancreatic β cells is mediated by the endoplasmic reticulum pathway. *PNAS* 2001; 98(19):10845-10850.

46 Zhang, H, Ye X, Su Y, Yuan J, Liu Z, Stein D. Yang D. Coxsackievirus B3 infection activates the unfolded protein response and induces apoptosis through downregulation of p58^{IPK} and activation of CHOP and SREBP1. *J. of Virology*. 2010; 84(17):8446-8459.

47 Boden G, Duan X, Homko C, Molina EJ, Song W, Perez O, Cheung P, Merali S. Increase in endoplasmic reticulum stress-related proteins and genes in adipose tissue of obese, insulin-resistant individuals. *Diabetes* 2008. 57:2438-2444.

48 Boden G, Cheung P, Salehi S, Homko C, Loveland-Jones C, Jayarajan S, Stein T, Williams K, Liu M, Barrero C, Merali S. Insulin regulates the unfolded protein response (UPR) in human adipose tissue. *Diabetes* 2014; 63:912-922.

49 Hill B, Benavides G, Lancaster J, Ballinger S, Dell'Italia L, Zhang J, Darley-Usmar V. Integration of cellular bioenergetics with mitochondrial quality control and autophagy. *Biol Chem* 2012; 393:1485-1512.

50 Chikka M, McCabe D, Tyra H, Rutkowski D. C/EBP homologous protein (CHOP) contributes to suppression of metabolic genes during endoplasmic reticulum stress in the liver. *J Biol Chem 2013*; 288:4405-4415.

51 Huang X, Ordemann J, Müller J, Dubiel W. The COP9 signalosome, cullin 3 and Keap1 supercomplex regulates CHOP stability and adipogenesis. *Biology Open* 2012; 1:705-710.

52 Adam J, Hatipoglu E, O'Flaherty L, ternette N, Sahgal N, Lockstone H, Baban D, Nye E, Stamp G, Wolhuter K, Stevens M, Fischer R, Carmeliet P, Maxwell P, Pugh C, Frizzell N, Soga T, Kessler B, El-Bahrawy M, Ratcliffe P, Pollard P. Renal cyst formation in Fh1-deficient mice is independent of Hif/Phd pathway: roles for fumarate in KEAP1 succination and Nrf2 signaling. *Cancer Cell* 2011; 20:524-537.

53 Yehuda-Shnaidman E, Buehrer B, Jingbo P, Naresh K, Collins S. Acute Stimulation of White Adipocyte Respiration by PKA-Induced Lipolysis. *Diabetes* 2010; 59:2474-2483.

54 Grundlingh J, Dargan P, El-Zanfaly M, Wood D. 2,4-Dinitrophenol (DNP): A weight loss agent with significant acute toxicity and risk of death. *J Med Tox*icol 2011; 7(3):205-212.

55 http://clinicaltrials.gov/show/NCT00771901

56 Norma C, Howell K, Millar A, Whelan J, Day D. Salicylic acid is an uncoupler and inhibitor of mitochondrial electron transport. *Plant Physiol* 2004; 134:492-501.

57 Özcan U, Yilmaz E, Özcan L, Furuhashi M, Vaillancourt E, Smith R, Görgün C, Hotamisligil G. Chemical chaperones reduce ER stress and restore glucose homoeostasis in a mouse model of type 2 diabetes. *Science* 2006; 313:1137-1140.

58 Xu T, Chen R, Wang P, Zhang R, Ke S, Miao C. 4-Penylbutyric acid does not generally reduce glucose levels in rodent models of diabetes. *Clin Exp Pharmacol and Phys* 2010; 37:441-446.

59 http://jaxmice.jax.org/strain/000642.html

60 Han K, Choi J, Lee J, Song J, Joe M, Jung M, Hwang J. Therapeutic potential of peroxisome proliferators-activated receptor-α/γ dual agonist with alleviation of endoplasmic reticulum stress for the treatment of diabetes. *Diabetes* 2008; 57:737-745.

61 Han M, Chung K, Cheon H, Rhee S, Yoon C, Lee M, Kim K, Lee M. Imatinib mesylate reduces endoplasmic reticulum stress and induces remission of diabetes in db/db mice. *Diabetes* 2009; 58:329-336.

62 http://dailymed.nlm.nih.gov/dailymed/archives/fdaDrugInfo.cfm?archiveid=3849

63 Tolman K, Fonseca V, Dalpiaz A, Tan M. Spectrum of liver disease in type 2 diabetes and management of patients with diabetes and liver disease. *Diabetes Care* 2007; 30(3):734-743.

64 Li J, Chi Y, Wang C, Wu J, Yang H, Zhang D, Zhu Y, Wang N, Yang J, Guan Y. Pancreatic-derived factor promotes lipogenesis in the mouse liver; role of forkhead box 1 signaling pathway. *Hepatology*. 2011; 53(6):1906-1916.

65 Molineaux S. Molecular pathways: targeting proteasomal protein degradation in cancer. *Clin Cancer Res* 2011; 18(1):15-20

66 Eekels J, Sagnier S, Geerts D, Jeeninga R, Biard-Piechaczyk M, Berkhout B. Inhibition of HIV-1 replication with stable RNAi-mediated knockdown of autophagy factors. *Virol J* 2012; 9:69.

67 Wong E, Cuervo A. Integration of clearance mechanisms; the proteasome and autophagy. 2010; *Cold Spring Harb Perspect Biol* 2010; 2:a006734.

68 Voet D, Voet J. Biochemistry. Hoboken: John Wiley & Sons Inc, 2011. Print.

69 Zhang Y, Zeng X, Jin S. Autophagy in adipose tissue biology. *Pharmacological Res*. 2012; 66:505-512

70 Eguchi A, Feldstein A. Lysosomal Cathepsin D contributes to cell death during adipcoytes hypertrophy. *Adipocyte* 2013; 2(3):170175.

71 Lai R, Goldman P. Organic acid profiling in adipocyte differentiation of 3T3-F442A cells; increased production of Krebs cycle acid metabolites. *Metabolism* 1992; 41(5):545-547.

72 Nedelsky N, Todd P, Taylor J. Autophagy and the ubiquitin-proteasome system: collaborators of neuroprotection. *Biochim Biophys Acta* 2008; 12:691-699.

73 Zhang Y, Goldman S, Baerga R, Zhao Y, Komatsu M, Jin S. Adipose-specific deletion of *autophagy-related gene 7* (*atg7*) in mice reveals a role in adipogenesis. *PNAS* 2009; 106(47):19860-19865.

74 Yoshizaki T, Kusunoki C, Kondo M, Yasuda M, Kume S, Morino K, Sekine O, Ugi S, Uzu T, Nishio Y, Kashiwagi A, Maegawa H. Autophagy regulates inflammation in adipocytes. *Biochem Biophys Res Comm*un 2012; 417:352-357.

75 Kaiser S, Mao K, Taherbhoy A, Yu S, Olszewski J, Duda D, Kurinov I, Deng A, Fenn T, Klionsky D, Schulman B. Noncanonical E2 recruitment by the autophagy E1 revealed by Atg7-Atg3 and Atg7-Atg10 structures. *Nat Struct Mol Biol* 2012; 19(12):1242-1249.

Appendix A

Buffer Preparations

RIPA Buffer

The buffer was prepared in 200 mL stocks containing 50 mM Tris-HCl pH 8, 150 mM NaCl, 1% Triton-X, 0.5% sodium deoxycholate, 0.1% SDS, and 2 mM EDTA. On day of use, 2 mM sodium orthovanadate, 2 mM sodium fluoride and protease inhibitor (1:1000) was added to the buffer. The buffer was stored at 4^{o}C.

Running Buffer

One liter of 10x stock was prepared containing 250 mM Tris-HCl, 1920 mM glycine and 10% (SDS).

Transfer Buffer

One liter of 10X stock was prepared containing 250 mM Tris-HCl, 1920 mM glycine. Methanol was added at 20% for transfer process.

Wash Buffer

One liter of 10X stock was prepared containing 200 mM Tris-HCl, pH 7.4. Tween-20 was added at 0.05% to 1X was buffer.

Appendix B:

Lowry Assay

Pipette the specific amounts of reagents into the microplate in the order listed. All samples are prepared in duplicates.

Table B.1: Preparation of BSA standard curve for the Lowry assay.

Probe	BSA (µL)	H20 (µL)	Copper Reagent (µL)	Incubation	Folin-Ciocolateu (µL)	Incubation
Blank	0	20	20	20 minutes at 37°C	60	30 minutes at 37°C
1	1	19	20		60	
2	2	18	20		60	
3	3	17	20		60	
4	4	16	20		60	
5	8	12	20		60	
6	10	10	20		60	
7	20	0	20		60	
Sample	5	15	20		60	

Stock BSA
Dissolve 50 mg BSA (Bovine Serum Albumin) in 10 mL deionized water=5 mg/mL stock/working solution

Working Solutions: Dilute 400 µL of 5 mg/mL stock in 600 µL water=2 mg/mL solution

Table B.2: Preparation of copper reagent for Lowry assay.

Stock Solution	**Working Solution**
Copper Sulfate 1% (w:v)	100 µL
Sodium Tartrate 2% (w:v)	100 µL
Sodium Carbonate 10% (w:v) in 0.5 M NaOH	2 mL

Folin-Ciocolateu Phenol Reagent: Purchased as a 2 N stock solution. For working solution at 500 µL of stock solution to 5.5 mL of water
Read absorbance at 660nm.

Appendix C

Western Blotting

Gel Electrophoresis

1. After determining the protein content from the Lowry assay, 30-40 µg of protein was dissolved in water and 5 µL of Laemmli loading buffer was added.

2. Boil the samples for 15 min at 95°C then flash centrifuge.

3. Remove tape and comb from Bio-Rad pre cast Criterion gel and place in cassette.

4. Fill the cassette tank and gel with Tris/Glycine/SDS running buffer.

5. Load the samples into their individual lanes and 8 µL of marker into your lane of choice.

6. Run the gel at 200 V for 60 min.

Wet Transfer

1. Remove the gel from the pre-cast and cut to size

2. Soak the gel in Tris/Glycine/Methanol transfer buffer for 15 min.

3. Charge the PVDF membrane for ~30 sec in methanol. Soak the 2 pieces of blotting paper, 2 sponges, and the membrane in Tris/Glycine/methanol for 15 min.

4. Assemble the transfer apparatus, starting with the black side first. Keep all materials soaking in transfer buffer during the assembly.

5. Place the sponge flat on the black side, followed by a piece of blotting paper. Next, place the gel on top followed by the PVDF membrane. Roll out any air bubbles between the gel and membrane using a roller. Finally, put the remaining piece of blotting paper on top of the membrane and the sponge on top.

6. Assemble the apparatus and transfer at 250 mA for 100 min or 40 mA for at least 12 hrs.

7. Remove the membrane from the apparatus and wash 3 times with nanopure water. 8. Place the membrane in ponceau stain for 5 min then wash with nanopure water to visualize the bands. Inspect the membrane for equal loading and where bubbles formed during the transfer process. Wash the ponceau stain off the membrane with Tris-HCl wash buffer.

9. Block the membrane in 5% non-fat dry milk or 5% BSA for at least 1hr.

Immunostaining for 2SC

1. Prepare 1% milk by diluting the 5% milk 1:4 in Tris-HCl wash buffer.

2. Add 2SC antibody to the milk in a 1:5000 dilution. Incubate for at least 1 hr on the rocker.

3. Pour off the antibody and wash the membrane 3 times in wash buffer for 5 min each.

4. Add secondary antibody anti-rabbit to 1% milk, 1:15000 dilution and incubate for 1hr at room temperature.

5. Pour off the milk and was the membrane 3 times for 5 min each in wash buffer.

Developing

1. Prepare ECL solution by adding solution B to solution A and in a 1:40 dilution.

2. Add the ECL to the membrane and incubate for 5 min. Place the membrane in the cassette and cover with plastic wrap.

3. In the dark room, place a piece of X-ray film over the membrane then develop. Inspect the film after it has developed and adjust the exposure times accordingly.

Buffers

1. Stock Running Buffer: 10X SDS – 30.3 g Tris base, 144 g glycine and 10 g SDS dissolved to 1 L water
   - Working solution=100mL of 10X stock diluted to 1L water
2. Stock Transfer Buffer: 10X transfer – 30.3 g Tris base and 144 g glycine dissolved to 1 L water
   - Working solution=150 mL of 10X stock and 300 mL of methanol diluted to 1 L water

3. Stock Wash Buffer: 10X Wash – 24.4 g Tris base dissolved to 1 L water, pH 7.4
    - Working solution=100 mL of 10X stock and 500 µL Tween-20 diluted to 1 L water